UNIVERSIDADE FEDERAL DO PARANÁ

LUCAS FARIAS MACIEL RODRIGUES

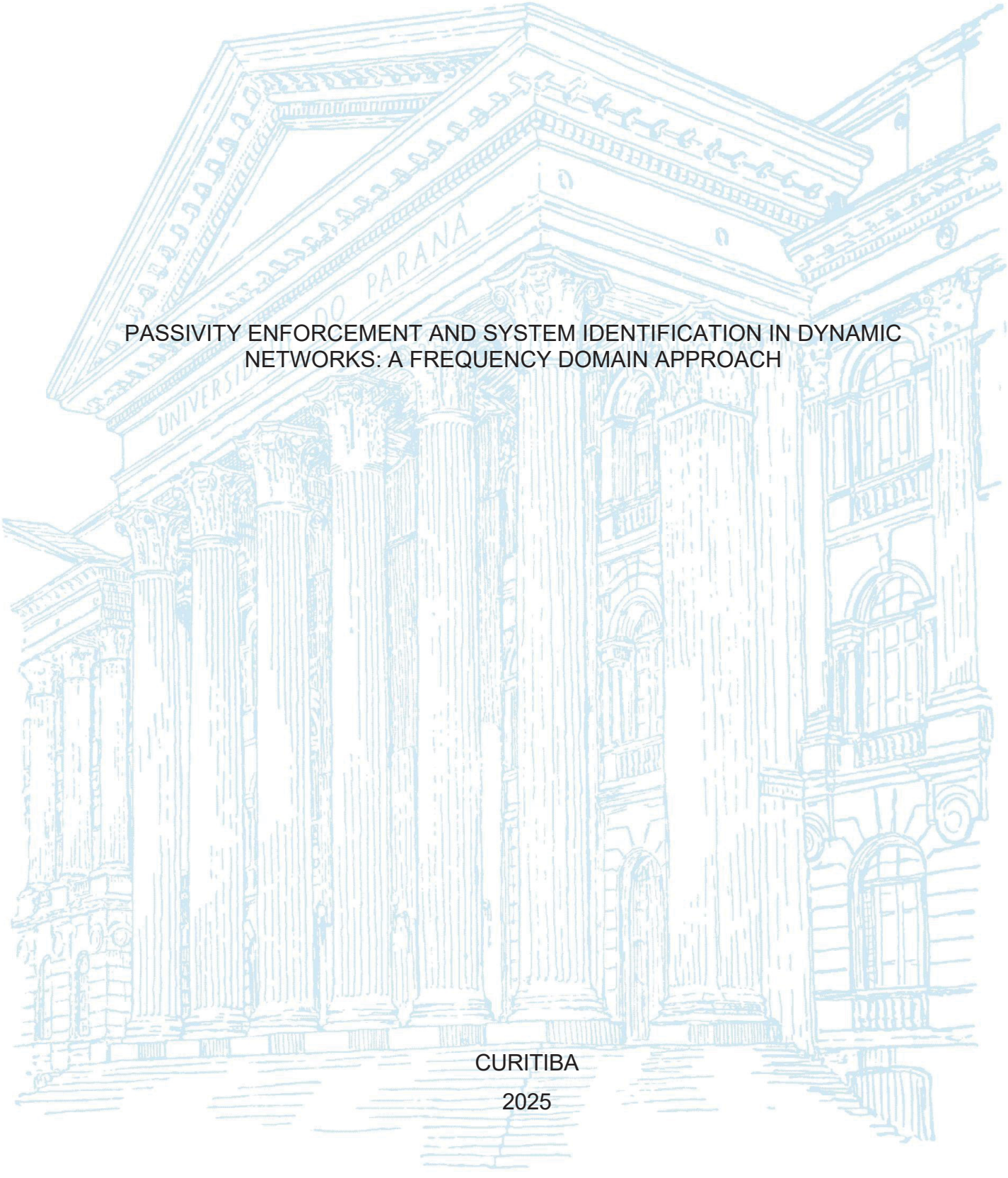

PASSIVITY ENFORCEMENT AND SYSTEM IDENTIFICATION IN DYNAMIC NETWORKS: A FREQUENCY DOMAIN APPROACH

CURITIBA

2025

LUCAS FARIAS MACIEL RODRIGUES

PASSIVITY ENFORCEMENT AND SYSTEM IDENTIFICATION IN DYNAMIC NETWORKS: A FREQUENCY DOMAIN APPROACH

Tese apresentada ao Programa de Pós-Graduação em Engenharia Elétrica, Setor de Tecnologia, Universidade Federal do Paraná, como requisito parcial à obtenção do título de Doutor em Engenharia Elétrica.

Orientador: Prof. Dr. Gustavo Henrique da Costa Oliveira

Coorientador: Prof. Dr. Lucas Pioli Rehbein Kurten Ihlenfeld

CURITIBA

2025

DADOS INTERNACIONAIS DE CATALOGAÇÃO NA PUBLICAÇÃO (CIP)
UNIVERSIDADE FEDERAL DO PARANÁ
SISTEMA DE BIBLIOTECAS – BIBLIOTECA DE CIÊNCIA E TECNOLOGIA

Rodrigues, Lucas Farias Maciel
Passivity enforcement and system identification in dynamic networks: a frequency domain approach / Lucas Farias Maciel Rodrigues. – Curitiba, 2025.
1 recurso on-line : PDF.

Tese (Doutorado) - Universidade Federal do Paraná, Setor de Tecnologia, Programa de Pós-Graduação em Engenharia Elétrica.

Orientador: Gustavo Henrique da Costa Oliveira
Coorientador: Lucas Pioli Rehbein Kurten Ihlenfeld

1. Redes inteligentes de energia. 2. Sistemas lineares. 3. Energia elétrica - Passividad. I. Universidade Federal do Paraná. II. Programa de Pós-Graduação em Engenharia Elétrica. III. Oliveira, Gustavo Henrique da Costa. IV. Ihlenfeld, Lucas Pioli Rehbein Kurten. V. Título.

Bibliotecário: Elias Barbosa da Silva CRB-9/1894

MINISTÉRIO DA EDUCAÇÃO
SETOR DE TECNOLOGIA
UNIVERSIDADE FEDERAL DO PARANÁ
PRÓ-REITORIA DE PÓS-GRADUAÇÃO
PROGRAMA DE PÓS-GRADUAÇÃO ENGENHARIA ELÉTRICA - 40001016043P4

TERMO DE APROVAÇÃO

Os membros da Banca Examinadora designada pelo Colegiado do Programa de Pós-Graduação ENGENHARIA ELÉTRICA da Universidade Federal do Paraná foram convocados para realizar a arguição da tese de Doutorado de **LUCAS FARIAS MACIEL RODRIGUES**, intitulada: **Passivity Enforcement and System Identification in Dynamic Networks: A Frequency Domain Approach**, sob orientação do Prof. Dr. GUSTAVO HENRIQUE DA COSTA OLIVEIRA, que após terem inquirido o aluno e realizada a avaliação do trabalho, são de parecer pela sua APROVAÇÃO no rito de defesa.

A outorga do título de doutor está sujeita à homologação pelo colegiado, ao atendimento de todas as indicações e correções solicitadas pela banca e ao pleno atendimento das demandas regimentais do Programa de Pós-Graduação.

Curitiba, 27 de Fevereiro de 2025.

Assinatura Eletrônica
10/03/2025 08:07:42.0
GUSTAVO HENRIQUE DA COSTA OLIVEIRA
Presidente da Banca Examinadora

Assinatura Eletrônica
21/03/2025 16:50:09.0
BRUNO OTÁVIO SOARES TEIXEIRA
Avaliador Externo (UNIVERSIDADE FEDERAL DE MINAS GERAIS)

Assinatura Eletrônica
06/03/2025 22:33:57.0
ROMAN KUIAVA
Avaliador Interno (UNIVERSIDADE FEDERAL DO PARANÁ)

Assinatura Eletrônica
09/03/2025 15:56:45.0
STÉPHANE VICTOR
Avaliador Externo (IMS/BORDEAUX)

Assinatura Eletrônica
21/03/2025 14:53:10.0
LUCIA VALÉRIA RAMOS DE ARRUDA
Avaliador Externo (UNIVERSIDADE TECNOLÓGICA FEDERAL DO PARANÁ)

Acknowledgments

This work marks the culmination of years of dedication, challenges, and learning. It would not have been possible without the support and contributions of several individuals and institutions, to whom I extend my deepest gratitude.

First and foremost, I would like to express my sincere appreciation to the Federal University of Paraná (UFPR) for providing the academic environment and resources necessary for the completion of this research.

I am grateful to my advisor, Prof. Dr. Gustavo Henrique da Costa Oliveira, and my co-advisor, Prof. Dr. Lucas Pioli Rehbein Kurten Ihlenfeld, for their invaluable guidance, patience, and encouragement throughout this process. Their insights and expertise have enriched this work, and their unwavering support has been essential in overcoming the many challenges encountered along the way.

I would also like to acknowledge CAPES, the Brazilian research funding agency, for its financial support, which allowed me to dedicate myself fully to this research.

A special thank you to Prof. Paul Van den Hof and the Eindhoven University of Technology (TU/e) for warmly welcoming me as a guest student in the Netherlands. The opportunity to collaborate in such a prestigious research environment has been an incredibly enriching experience, contributing to both my academic and personal development.

To all who have been part of this journey, directly or indirectly, my sincere thanks.

RESUMO

Sistemas de engenharia modernos estão cada vez mais interconectados, formando redes dinâmicas complexas. Garantir a passividade, uma propriedade essencial para a troca de energia, é um desafio na identificação e modelagem de tais sistemas. À medida que as redes se tornam mais complexas, as técnicas tradicionais de identificação frequentemente falham em preservar a passividade do sistema, levando a modelos que violam as condições de balanço de energia. Esta tese aborda o problema da identificação de módulos locais dentro de uma rede dinâmica, garantindo a passividade ao longo de todo o processo de identificação. A literatura existente ainda não apresentou um arcabouço capaz de identificar diretamente sistemas passivos inseridos em redes dinâmicas. Essa limitação motiva o desenvolvimento de um arcabouço de identificação consciente da passividade, que integra restrições de passividade desde a etapa inicial da estimação. O principal objetivo desta tese é desenvolver uma metodologia de identificação de sistemas no domínio da frequência para sistemas interconectados, assegurando a preservação da passividade ao longo do processo de estimação. Isso é alcançado por meio da incorporação de restrições de passividade dentro da estrutura de identificação de sistemas. A metodologia proposta neste trabalho segue uma abordagem em duas etapas: (i) uma estimação não paramétrica da Função de Resposta em Frequência (FRF) é obtida para fornecer uma caracterização inicial do sistema; e (ii) um método de identificação paramétrica refina essa estimação enquanto incorpora restrições de passividade As principais técnicas utilizadas neste estudo incluem um novo método de Ajuste Vetorial no Domínio da Frequência (FD-VF), que atua como a ferramenta principal para identificação paramétrica, e estratégias de imposição de passividade baseadas no Lema de Kalman-Yakubovich-Popov (KYP). A principal contribuição da abordagem baseada em otimização utilizada é sua capacidade de garantir que o modelo identificado permaneça passivo em cada iteração. A abordagem desenvolvida incorpora condições de passividade desde a etapa de geração dos dados. Os resultados demonstram que a metodologia desenvolvida identifica modelos passivos sem comprometer a precisão da estimação. Estudos de caso comparativos mostram que a imposição de passividade durante o processo de estimação leva à obtenção de modelos passivos a cada iteração da identificação paramétrica.

Palavras Chave: identificação do sistema; redes dinâmicas; passividade; domínio da frequência; sistemas lineares; passividade; Vector Fitting.

ABSTRACT

Modern engineering systems are increasingly interconnected, forming complex dynamic networks. Ensuring passivity, an essential property for energy exchange, is a challenge in system identification and modeling. As networks grow in complexity, traditional identification techniques often fail to preserve system passivity, leading to models that violate energy balance conditions. This thesis addresses the problem of identifying local modules within a dynamic network while guaranteeing passivity throughout the identification process. Existing literature has not yet presented a framework to directly identify passive systems embedded in dynamic networks. This limitation motivates the development of a passivity-aware identification framework that integrates passivity constraints from the initial estimation stage. The main objective of this thesis is to develop a frequency-domain system identification methodology for networked systems that ensures passivity preservation throughout the estimation process. This is achieved by integrating passivity constraints into the system identification framework. The methodology proposed in this work follows a two-stage approach: (i) a non-parametric estimation of the Frequency Response Function (FRF) is obtained to provide an initial system characterization; and (ii) a parametric identification method refines this estimation while incorporating passivity constraints. The core techniques used in this study include a novel Frequency Domain Vector Fitting (FD-VF), which serves as the primary tool for parametric identification, and passivity enforcement strategies based on the Kalman-Yakubovich-Popov (KYP) Lemma. The key contribution of the optimization-based approach used is its ability to ensure that the identified model remains passive at every iteration. The developed approach incorporates passivity conditions from the data generation stage onward. The results demonstrate that the developed methodology identifies passive models while maintaining the estimation accuracy. Comparative case studies illustrate that enforcing passivity during the estimation process leads to the estimation of passive models in each iteration of the parametric identification. This work contributes to the field of dynamic network identification by addressing the challenge of passivity enforcement in dynamic network identification.

Keywords: system identification; dynamic network; frequency-domain; linear systems; passivity; Vector Fitting.

LIST OF FIGURES

LIST OF TABLES

List of symbols

$\mathcal{G}$ *and* $\mathcal{H}$	are graphs.
$\mathbf{A}$	is an adjacency matrix.
V	is the number of vertexes in a graph.
$\mathbf{A}_d$	is a delay-adjacency matrix.
$\mathbf{M}$	is an incidence matrix.
w_k	is a node signal.
ω	refers to a frequency vector.
$\mathbf{G}$	refers to a network model matrix.
$\mathbf{I}$	refers to the identity matrix.
G_{ji}	is the estimated transfer function that relates node i to node j.
G_{ji}^0	denotes a transfer function of the data generating system.
$\widetilde{G}_{ji}$	denotes a frequency response function estimate.
$\breve{G}_{ji}$	denotes a passive state-space realization.
r_j	is an external probe added to node j.
R_j	is a proper transfer function.
r_j	is an external probe added to node j.
v_k	is a noise signal added to node k.
e_k	is a white process noise in node k.
$\mathcal{N}_j$	represents the index set of internal variables that are directly linked to w_j, meaning that an index k belongs to N_j if and only if $G_{jk} \neq 0$.

$\mathcal{N}_r$ denotes the set of indices of existing external signals in the network's nodes.

$\mathcal{T}_j$ denotes the set of indices of external variables that are correlated with a given node signal w_i.

L refers to the number of nodes in a dynamic network.

$\mathbf{T}(q)$ denotes the open-loop response of a dynamic network.

$A(q), B(q), C(q),\ and\ D(q)$ denote polynomials that compose rational transfer functions.

$n_a, n_b, n_c,$ and n_d refer to the order of the respective polynomial $A(q), B(q), C(q), D(q)$.

θ is the parameter vector.

$\hat{w}_t(t|t-1)$ is the one-step-ahead predictor.

ϵ is the predictor error.

N refers to the number of samples collected.

$H(q)$ refers to the filter of the process noise.

$\mathbf{R}_{w_i r_i}$ is the cross-correlation function.

ϕ_w is the spectral density of the signal w.

$\overline{\mathbb{E}}$ is the expectation operator.

$\bar{x}$ refers to the mean value of x.

δ_x is the variance of x.

b is the bias.

Φ is a supply function.

CONTENTS

1 Introduction

The rapid growth of interconnected systems in today's technology poses significant challenges for the analysis, modeling, and control of real-world systems. As these systems become larger and more complex, the field of dynamic systems research is now shifting from examining individual components to comprehensively understanding how systems interact with each other. This paradigm shift is essential to navigate the intricacies of modern interconnected systems. While significant strides have been made in enhancing model accuracy, particularly in discerning the dynamics of distinct subsystems within a network, a noticeable gap persists in ensuring the preservation of system's fundamental properties, including the passivity, in the resulting models. This thesis endeavors to address the following question: How to guarantee that the estimated model maintains the system's passivity property? The subsections of this introductory chapter build on the understanding of dynamic networks and their identifiable components.

1.1 Introduction

Increasing complexity and interconnectivity of systems is an evident trend in many domains. Autonomous driving systems and decentralized control systems serve as illustrative examples, which rely on a complex network of sensors, processors, and actuators that operate together to control and respond to changing conditions. These systems share a common characteristic: they are dynamic networks. Henceforth, dynamic networks can be aptly characterized as an assembly of internal variables dynamically interconnected within the network (DANKERS, 2014). Such networks entail structured interconnections of dynamic systems, all driven by external excitation and disturbance signals.

Dynamic networks are everywhere. Whether we consider devices connected via the internet, people in social media, automobiles in traffic, or many transportation applications, they are all based on connecting systems together. As it became common to interconnect

multiple subsystems, applications of dynamic networks are abundant in many fields. Molecular interactions, chemical reactions, and population dynamics in both humans and animals represent a mere subset of systems whose behavior can be effectively modeled and analyzed using dynamic network frameworks. Within these frameworks, information flows seamlessly between individual subsystems, undergoing continuous alterations as it traverses the network's intricate pathways.

Modern society exemplifies the ubiquity of dynamic networks. Consider the intricate web of connections in a smart power grid, where power sources, loads, and control units seamlessly interact to optimize energy distribution (ZHENG *et al.*, 2021). Similar dynamics govern the intricate flow of data and communication protocols in autonomous driving systems, where vehicle-to-vehicle and vehicle-to-infrastructure interactions ensure safe and efficient navigation (ZHENG *et al.*, 2015). Even fundamental building blocks like distributed control systems (RISTEVSKI; YUCELEN; MUSE, 2021) and the interconnected regions of the human brain, facilitating cognitive functions (TELESFORD *et al.*, 2011), operate as dynamic networks. The ever-volatile terrain of the stock market (ALAMEER *et al.*, 2020) and even a simple electronic circuit, with its discrete components, further highlight the universality of this concept.

Though many of these dynamic systems have been present for centuries, the pressing need for their formal treatment has only intensified in recent years. This urgency stems from the burgeoning complexity and scale of these systems, posing challenges in modeling and parameter estimation. Notably, the proliferation of low-cost remote communication devices within computer science (MICHAIL; SPIRAKIS, 2018) has further exacerbated this need. This confluence of factors has propelled a concerted effort to establish a comprehensive theory of dynamic networks, aiming to address the ever-growing demand for rigorous frameworks to understand and manage these intricate systems.

At its core, a *dynamic network* is a collection of interconnected elements, each representing a measurable aspect of a system. These elements, often called nodes, interact with each other in ways that can change over time. For instance, a traffic network: each car is a node, and the flow of traffic between them represents the interaction. These

interactions can be influenced by external factors, like a sudden downpour, or internal factors, like a car changing lanes.

In other words, dynamic networks consist of interconnected nodes, each representing an internal variable and exhibiting dynamic relationships with its neighbors. We assume these nodes' signals can be effectively measured using suitable devices. Previous research (WILLEMS, 2008a) categorizes the nature of these interconnections based on the variables they transmit. For example, thermal, electric, and mechanical interconnections represent the flow of temperature/heat, voltage/current, and force/position, respectively. Dynamic networks often contain disturbance sources, unmeasured but impactful on internal signal values. Additionally, external signals, serving as excitations, further influence node behavior.

The dynamic relationships between nodes are effectively captured by a network of interconnected systems, which we refer to as *modules* in this thesis. These modules act as individual dynamic systems, typically described by transfer functions or other models with a finite number of connection points. Notably, the nature of these interconnections cuts across diverse domains, encompassing financial transactions, transmission lines, and myriad other objects and systems. This breadth exemplifies the versatility of dynamic networks in modeling real-world scenarios (WILLEMS, 2008b).

This work focuses on networks with dynamic interactions among internal elements, aptly termed dynamic networks. Each internal variable exhibits dynamic relationships with other variables within the network. The complexity is further amplified by unmeasured disturbances, which influence the internal variable values through unobservable channels. Additionally, external variables, introduced as probing signals, can shape the network's behavior and dynamics.

To succinctly capture the network's structure and the conditional dependencies among its variables, graph theory comes into play. Specifically, directed graphs provide a convenient representation. A directed graph comprises directed edges connecting a pair of nodes, thus delineating a direction of influence or interaction (ETESAMI; KIYAVASH, 2014). For each dynamic network, it is possible to associate a directed graph, where the edges of this graph symbolize the modules within the dynamic network, and the vertices

represent the internal signals (ZHANG; MOORE; NEWMAN, 2016).

As dynamic networks grow in complexity, conventional approaches to model identification become impractical. While identifying an isolated subsystem may appear straightforward, doing so for a given module embedded within a network of interconnects presents challenges, even when identification is attempted locally. This complexity stems from the multitude of signals that interact with and alter measurements, obscuring the true dynamics of individual modules (BAZANELLA *et al.*, 2017; GEVERS; BAZANELLA; SILVA, 2018). Furthermore, determining the essential variables to measure becomes a daunting task, as inferring signal correlations within such intricate systems is far from trivial.

System identification in dynamic networks falls into four main categories: full network identification, local module identification, network topology identification and identifiability, where in both full & local network identification the network interconnections are assumed known. In full network identification, the objective is to unveil the dynamic behavior of the entire system. Several scalable methods have been proposed for this purpose, like those in Torres, Wingerden e Verhaegen (2015), Sarwar, Voulgaris e Salapaka (2010), which efficiently handle the addition of new modules. Due to the inherent complexity of large networks, full network identification typically emphasizes efficient numerical implementations and addresses concerns like identifiability (recovering network parameters) and optimal experimental conditions for precise parameter estimation, e.g., Hendrickx, Gevers e Bazanella (2019), Weerts, Hof e Dankers (2018b). While common practice assumes measurement of all nodes, studies like Bazanella *et al.* (2017) demonstrate successful network identification from just a subset of measured signals, highlighting an exciting avenue for further research.

In contrast, local module identification centers upon consistently estimating a specific module within the network, given a particular configuration. Classical identification methods often falter when faced with modules embedded in dynamic networks, yielding inaccurate or inconsistent transfer function estimates. This challenge has spurred the adaptation of closed-loop identification techniques for this purpose (RAMASWAMY;

BOTTEGAL; HOF, 2018; HOF *et al.*, 2013). Notably, the versatile Predictor Error Method (PEM) has seen numerous modifications for dynamic network applications (DANKERS; HOF; BOMBOIS, 2014; WEERTS; HOF; DANKERS, 2018b; DANKERS *et al.*, 2012). Examples include adapted direct methods, which employ one-step ahead predictors to identify a module based on input and output signals (HOF, 2006), and two-step methods, which strive to decorrelate signals prior to predictor application, a technique transferable from closed-loop identification (Van Den Hof; SCHRAMA, 1993; DANKERS; HOF; BOMBOIS, 2014).

1.2 Motivation

Dynamic networks, encompassing diverse systems from power grids to control systems, present a critical challenge in modern engineering. Accurately capturing their complex behavior through dynamic network identification is vital for their control, analysis, and ultimately, their safe and efficient operation.

The field of dynamic network identification is a rapidly evolving area, with various methods emerging to address the challenge. Existing methods share some similarities with established closed-loop system identification techniques, however, there is a need for a comprehensive approach that fully utilizes this analogy has not been comprehensively explored.

While advances in identification techniques have yielded significant progress, an aspect remains largely unaddressed: passivity. This fundamental property assures stable and predictable behavior in numerous physical systems. Without it, even the most accurate model can lead to undesirable consequences. For example, an improperly modeled passive power transformer in a grid, where instability could cascade, causing extensive disruptions.

Motivated by this critical gap, our research focuses on integrating passivity enforcement into dynamic network identification. We seek to answer the following question: **can we accurately identify passive modules within a given dynamic network while ensuring their passivity throughout the identification process?**

The potential impact of addressing this question is substantial. Our framework not only promises stable and reliable models but also holds a deeper understanding and improved control of interconnected systems. Imagine, for example, enhancing the resilience of power grids, optimizing decentralized control systems, or gaining new insights into biological networks.

Our approach tackles challenges in several key areas:

- **Bridging theory and practice**: We strive to develop robust and efficient numerical implementation strategies, translating theoretical advancements into real-world solutions.
- **Expanding beyond existing methods**: Exploring alternative frequency domain system identification frameworks will broaden the applicability and deepen our understanding of network dynamics.
- **Guaranteeing model passivity**: By incorporating passivity enforcement within the identification algorithm, we ensure the stability of estimated models, particularly for physical systems.

By addressing these challenges, we aspire to transform the field of dynamic network modeling. Our research carries the potential to contribute to the control and operation of interconnected systems, enhancing their stability, predictability, and resilience in the face of ever-increasing complexity.

The next section delves into a comprehensive review of existing network identification techniques, critically evaluating their strengths and limitations in the context of our goal. This review will pave the way for introducing our novel passivity-enforced dynamic network identification approach.

1.3 A Review of Network Identification Techniques

Network identification, or discerning the dynamics of a complex system from its observable outputs, is a fundamental issue in a variety of fields. This vast research area

can be categorized into four key areas of focus:

1. **Network Topology Detection**: In scenarios where the internal architecture is unknown, this category tackles the crucial challenge of topology detection, reconstructing the network's interconnection structure; it could be based solely on its outputs.

2. **Full Network Identification**: For systems where the overall behavior is paramount, this category focuses on estimating the complete set of interactions between all modules, reconstructing the full network dynamics.

3. **Local Identification in Dynamic Networks**: This category delves into the identification of individual internal components (modules) within the network, aiming to estimate their specific transfer functions and behavior.

4. **Network Identifiability**: In this research field, the aim is to comprehend the circumstances under which a dynamic network can be identified, as well as to determine the essential information required for detecting the topology of the network.

Note that the category 2 and 3 require knowledge of the underlying network topology. This means knowing how the individual components are connected and interact. This thesis and literature review will place particular emphasis on local identification. Understanding the behavior of individual modules forms the foundational step for characterizing the larger network, and it often carries direct practical value in fields like control and diagnosis.

While many applications in control and communication systems boast pre-defined network topologies, fields like biology and economics often face the additional complexity of unknown internal connections. This necessitates specialized techniques for not only understanding the individual components but also piecing together the network's topology.

The following subsections present a comprehensive review of the current state-of-the-art in each of these four crucial areas, offering a roadmap for navigating the diverse methodologies and insights within network identification research.

1.3.1 Network Topology Detection

Not all networks reveal their hidden blueprint readily. In many cases, the very structure that governs their internal interactions remains veiled, posing a crucial challenge to unraveling their functionalities. Here, the power of topology detection comes into play, providing a tool for deciphering the network architecture.

This ability to map the intricate web of connections, revealing how local modules interconnect and how the information flows within the network, lies at the heart of understanding complex systems. As aptly recognized by Goncalves, Howes e Warnick (2007), neither the order of elements nor the quest for minimal complexity can definitively paint the picture of a network's intricate architecture. This underscores the role of dedicated topology detection algorithms in unveiling the hidden wiring diagram.

Many topology detection approaches capitalize on a key assumption: that within a network, each internal variable exhibits a limited dependence on a few selected internal variables (WAARDE; TESI; CAMLIBEL, 2021; COUTINO *et al.*, 2020; SHAHRAMPOUR; PRECIADO, 2015; COUTINO *et al.*, 2021). This is a sparsity principle that translates into the network landscape and to identifying connections that are truly necessary, revealing the most impactful pathways of information flow.

While research focusing on networks built from simple single-input, single-output (SISO) systems has laid the groundwork for topology detection (SHAHRAMPOUR; PRECIADO, 2015; SUZUKI *et al.*, 2013), it often falls short in capturing the complexity of real-world systems. Here, the emergence of multi-input, multi-output (MIMO) heterogeneous networks paves the way for a more nuanced understanding. Entering MIMO networks introduces complexity with increased dimensionality from multiple inputs and outputs.

In numerous practical scenarios, achieving complete observability of a network remains a challenging endeavor. To address this issue, the authors in (COUTINO *et al.*, 2020) extend subspace techniques from system identification to graph topology identification. This work concentrates on inferring the network structure when only a partial

subset of node measurements is accessible. The authors employ a dynamic system model to represent the network, describing the evolution of node signals through a first-order differential representation. Applying their subspace approach to networks with up to 50 nodes, the study yields compelling results, effectively revealing the hidden topology despite the constraint of limited observations. Nevertheless, the authors appropriately recognize the challenges associated with extending their approach to larger graphs. They highlight the inherently ill-posed nature of topology detection, a foundational challenge demanding meticulous consideration of scalability and robustness as networks increase in size and complexity. Their study underscores the necessity for continued exploration of techniques adept at navigating the complexities of partial observations and ensuring resilience in the presence of uncertainty.

The exploration of topology detection extends beyond centralized approaches, incorporating the effectiveness of distributed strategies. As exemplified by Morbidi e Kibangou (2014), nodes within the network collaboratively contribute to the identification process, employing local least-squares algorithms to estimate individual time series. This collective effort weaves a tapestry of interconnected insights, unveiling the network's concealed architecture. In a different approach, Shahrampour e Preciado (2015) delves into spectral analysis, showcasing that subtle patterns in power distribution within a network can provide clues for topology identification.

While linear systems have often taken center stage in topology detection research, the tapestry of real-world systems often exhibits a nonlinear character. Venturing into this realm, (WANG *et al.*, 2011) and (SHEN; BAINGANA; GIANNAKIS, 2017) explore the potential for topology detection within nonlinear systems. The intricacies of nonlinear dynamics often necessitate careful consideration of model assumptions and identification methods, and the pursuit of rigorous guarantees regarding identification accuracy remains a vital area for further exploration.

In the work Shi, Bottegal e Hof (2019), the authors introduce a Bayesian model selection approach to identify the connectivity of networks composed of transfer functions. The algorithm integrates a Bayesian measure and a forward-backward search algorithm.

By representing the impulse responses of network modules as Gaussian processes, the authors estimate hyper-parameters through marginal likelihood maximization using the expectation-maximization algorithm, contributing to the acquisition of the Bayesian measure.

Recent contributions on the field highlight the limitations of relying on the linear independence condition (LIC), which has been widely used in the past decade. In Zhu *et al.* (2021), the authors introduce a regulation mechanism and constructing an auxiliary network with isolated nodes, the authors achieve successful topology identification through outer synchronization. This approach mitigates the risk of identification failure due to network synchronization and eliminates the need to verify the LIC.

1.3.2 Full Network Identification

Within the intricate framework of a network's interconnected modules, each component harbors distinctive insights into the entire system's behavior. Systematically discerning the dynamics of individual modules provides invaluable insights into the fundamental building blocks that contribute to the network's overall character. However, to fully comprehend the orchestration of interactions that govern the collective behavior of the network, it becomes imperative to embrace the inherent complexity of the entire system. While the identification of individual modules provides a focused examination of specific components, the pursuit of full network identification encourages a broader perspective. This marks the initiation of the pursuit for full network identification.

As networks extend in size, the intricate interconnection of modules poses a significant challenge for conventional identification methods. The exponential growth in complexity with increasing network size necessitates a delicate trade-off between precision and computational efficiency.

To address this computational challenge, researchers often resort to carefully crafted assumptions, providing a level of simplification while preserving essential network characteristics. These assumptions serve as foundational principles, facilitating the development of numerically efficient algorithms capable of extracting insights from large-scale systems.

One prevalent strategy involves assuming a network composed of identical modules (ALI *et al.*, 2011; MASSIONI; VERHAEGEN, 2009) significantly reducing computational overhead by leveraging inherent simplification in the system's structure.

Another approach focuses on networks where modules primarily interact with their immediate neighbors (HABER; VERHAEGEN, 2013; CHEN *et al.*, 2019). This assumption, frequently observed in physical and biological systems, allows the development of algorithms that exploit the locality of interactions, mitigating computational complexity while capturing essential network dynamics.

Although these assumptions offer valuable tools for large-scale network identification, it is imperative to acknowledge their limitations. Future research endeavors should aim to bridge the gap between accuracy and scalability, developing techniques capable of embracing the full complexity of real-world networks without succumbing to computational constraints.

While the Prediction Error Method (PEM) holds the potential for full network identification, its application often encounters the obstacle of non-convex optimization problems. To overcome these challenges, researchers have explored various extensions and modifications to the traditional PEM framework (DANKERS *et al.*, 2016; HOF *et al.*, 2013; DANKERS *et al.*, 2012).

One promising approach, proposed by Weerts, Hof e Dankers (2018b), involves incorporating rank-reduced process noise into PEM. This technique leverages the assumption that not all nodes within a network require individual measurement, as the number of independent white noise signals may be less than the total number of nodes. By acknowledging this inherent sparsity, the method reduces computational complexity and facilitates identification of networks with limited observability.

In addition to PEM-based techniques, alternative approaches have emerged to tackle full network identification. Zorzi e Chiuso (2017) demonstrate the efficacy of constructing sparse plus low-rank dynamic models, offering a powerful tool for capturing the interconnected dynamics of complex systems while maintaining computational tractability.

The quest for efficient and accurate full network identification techniques remains an active research area. Further exploration of optimization algorithms, model assumptions, and alternative identification frameworks holds the key to unlocking a deeper understanding of large-scale interconnected systems, paving the way for unprecedented insights and transformative applications.

1.3.3 Local Identification in Dynamic Networks

Shifting our focus, we turn to the intricate realm of single module identification within dynamic networks. This area delves into the challenge of isolating and understanding the behavior of individual components, a crucial step towards deciphering the complex symphony of interconnected dynamics. While many studies hinge on complete knowledge of the network's topology, work by Gevers, Bazanella e Silva (2018) has revealed a fascinating twist: only local topological information is necessary to identify a single module. This discovery opens up exciting possibilities for analyzing complex systems even when their full blueprint remains concealed.

To isolate the dynamics of a single module within the intricate web of network interactions, one often turns to the art of adaptation. By carefully tailoring closed-loop identification techniques, originally designed for traditional control systems, a path is forged towards understanding individual components within interconnected environments. The PEM proves its versatility once again in the context of dynamic networks. Researchers have successfully harnessed it to estimate individual transfer functions within these complex systems (DANKERS *et al.*, 2016; HOF *et al.*, 2013). However, this journey isn't without its challenges. The interconnected nature of dynamic networks often presents obstacles, even when focusing on a single module. The intricate presence of feedback loops, woven throughout the system's structure, can introduce complexities that challenge traditional identification methods. Reports frequently highlight the potential for issues arising due to this intricate interplay of interactions (HOF *et al.*, 2013; DANKERS *et al.*, 2014).

To enhance PEM's resilience amidst the complexities of dynamic networks, researchers have embarked on a journey of methodological refinement. One notable example

comes from Dankers *et al.* (2014), who extended the errors-in-variables (EIV) framework—a technique designed to handle uncertainties in both model inputs and outputs—to the realm of discrete-time network identification.

While PEM has enjoyed widespread exploration in the field of single module identification, a recent wave of research is venturing beyond its confines. Alternative methods with unique strengths are emerging, offering researchers a broader toolkit for deciphering the dynamics of individual components within dynamic networks.

- **Weighted Null-Space Fitting (WNSF)**: Fonken, Ferizbegovic e Hjalmarsson (2020) present WNSF, a technique that leverages the null space of the network transfer function matrix to identify individual modules. This approach offers promising results, showcasing performance comparable to PEM in both simulations and real-world data applications.

- **Regularized Kernel-Based Methods**: Ramaswamy, Bottegal e Hof (2021) introduce regularized kernel-based methods, harnessing the flexibility of non-parametric kernels to capture complex system dynamics. Their work demonstrates the potential of these methods to achieve performance on par with PEM, highlighting their ability to adapt to diverse network structures.

- **Subspace Methods**: Traditional subspace techniques, revisited and refined for the challenging setting of dynamic networks, are also showing promise. As demonstrated in works like (HABER; VERHAEGEN, 2014), these methods can effectively identify individual modules, offering a valuable addition to the available toolset.

- **Bayesian Refinement**: Everitt, Bottegal e Hjalmarsson (2018) take a distinct approach, employing a Bayesian framework to estimate individual modules. This probabilistic perspective helps to tackle challenges like parameter reduction and sensitivity variations. Notably, the use of a marginal likelihood estimator allows for efficient and robust parameter estimation, showcasing the potential of Bayesian methods in this domain. Also in Rajagopal, Ramaswamy e Hof (2020), the authors address the challenge of identifying a module within a dynamic network disrupted

by colored process noise sources. They extend the Empirical Bayes Direct Method to handle MIMO setups, avoiding the need for model order selection for each module and mitigating the estimation of a large number of parameters. Parameters are obtained by maximizing the marginal likelihood using the Empirical Bayes approach, facilitated by the Expectation Maximization algorithm for computational efficiency.

While most research in network identification has unfolded within the realm of discrete-time (DT) models, a growing appreciation for the subtleties of continuous-time dynamics is emerging. This shift in perspective acknowledges that many real-world systems inherently evolve in continuous-time (CT), and their accurate representation calls for methods that directly embrace this continuous nature.

(DANKERS; HOF; BOMBOIS, 2014) and (HOF *et al.*, 2013) explore both direct and indirect approaches to continuous-time module identification. Each path offers distinct advantages and considerations:

- **Indirect CT Methods**: These techniques first construct a discrete-time model and then meticulously translate it into an equivalent continuous-time representation. This approach often leverages the extensive toolkit of discrete-time identification methods, providing a bridge between well-established techniques and the continuous domain.

- **Direct CT Methods**: In contrast, direct methods seek to estimate continuous-time models directly from observed data. This approach eliminates the potential for distortions or information loss that might occur during discrete-time approximations, striving for a more faithful representation of the underlying continuous-time dynamics.

Dankers, Hof e Bombois (2014) further delve into the practical realities of data acquisition and its potential impact on continuous-time identification. They acknowledge the presence of Analog-to-Digital Converters (ADCs) and Digital-to-Analog Converters (DACs) in many experimental setups, carefully examining the effects of aliasing and

intersample behavior. These distortions, if unaddressed, can introduce artifacts into the identified models, potentially obscuring the true underlying dynamics.

Building upon the discussion of continuous-time identification, let's delve into a nuanced category of dynamic networks: systems characterized by diffusive couplings. These undirected interconnections, where signals flow bidirectionally between nodes, closely mirror the behavior of many physical systems.

Physical systems often evolve continuously, with forces and interactions playing out in a seamless temporal flow. Diffusive couplings, with their inherent two-way communication, offer a natural language for representing these dynamics. Think of a mass-spring-damper system, where vibrations ripple through interconnected components, continuously influencing and responding to each other's movements. Such intricate interplay demands a continuous-time perspective to faithfully capture the nuances of real-world behavior.

Typically, physical systems described by diffusive couplings are represented by vector difference equations of maximum second order (KIVITS; Van den Hof, 2023). The identification process for these models poses a unique challenge. Traditional identification approaches often involve converting differential equations into state-space models, followed by applying matrix manipulations or eigenvalue decompositions (KIVITS; HOF, 2019; KIVITS; HOF, 2022). While these techniques effectively extract model parameters, they often come at a cost: erasing the inherent network structure embedded within the original equations. This disconnect between model parameters and their spatial arrangement within the system poses a significant barrier to gaining a holistic understanding of the physical processes at play.

The quest for identification methods that not only capture the continuous-time dynamics of physical systems but also preserve the vital information encoded within their diffusive couplings remains an active research frontier. Exploring novel techniques that bridge the gap between mathematical rigor and physical plausibility has been little discussed by researchers in the area. Many questions posed for traditional dynamic network identification are open questions when it comes to diffusive couplings.

The preceding investigations have provided a comprehensive examination of time-domain identification; however, an equally significant dimension awaits exploration in the frequency domain. This relatively unexplored realm presents promising opportunities for dynamic network identification, forming the focus of the ensuing discussion in this section.

The pioneering work of (RAMASWAMY *et al.*, 2022) stands as a testament to its promise. Their semi-parametric approach breaks with tradition, offering a crucial advantage: minimal dependence on prior knowledge. The approach is two-folded: the first step estimates a non-parametric Frequency Response Functions (FRFs); this initial mapping reveals the system's fundamental behavior without imposing any preconceived model structures. The second step focuses on the module of interest, applying a parametric frequency domain estimator to refine its representation. This targeted refinement grants a clearer, more interpretable model for the module while preserving the insights gained from the non-parametric analysis. Given the developed semi-parametric approach, there is no need to pre-specify the number of poles and zeros for each module, what poses a significant boon when juggling multiple modules. However, this freedom comes at a cost – non-parametric estimates can often carry the burden of higher variance.

This semi-parametric approach offers two compelling advantages:

- **Scalability to Large Networks**: Unlike many time-domain techniques, its complexity remains unburdened by the network's size. The first step scales only with the number of local modules to be estimated, while the second step isolates the target module, elegantly sidestepping the intricacies of full network identification.
- **Model Flexibility**: By combining non-parametric and parametric steps, the method allows for adaptive model structures, accommodating a wide range of network dynamics without requiring extensive prior knowledge.

Notably, this approach deviates from the traditional Prediction Error Method (PEM) used in time-domain techniques, instead embracing a distinct cost function based on the 2-norm. This shift in optimization strategy reflects the unique nature of frequency-domain data and the nuances of semi-parametric model fitting.

A recent frequency-domain algorithm is discussed in Rodrigues *et al.* (2024), where the authors address the challenge of ensuring passivity, a key property in energy-based systems—during system identification. Their approach first employs the Indirect Local Polynomial Method (iLPM) to obtain a non-parametric frequency response estimate. This estimate is then refined using a modified version of Vector Fitting, termed Passive Vector Fitting (PVF), which integrates passivity constraints directly into the model estimation process via Linear Matrix Inequalities (LMIs). The proposed method ensures that the final identified model adheres to energy conservation principles, avoiding the need for post-processing passivity enforcement. Through numerical simulations on multi-node network systems, the authors demonstrate the effectiveness of their technique in providing accurate and consistent passive models, making it particularly relevant for applications in control systems and electrical networks.

Another research has also employed a semi-parametric approach to estimate local modules in dynamic networks (RODRIGUES *et al.*, 2023). In this paper an indirect Local Polynomial Method (LPM) is used to estimate the frequency response function of the target module. The curve is then smoothed through the Instrumental Variables Vector Fitting (IVVF) parametric estimator. The conference paper shows that the method is effective and can be used to identify local modules in complex dynamic networks.

1.3.4 Network Identifiability

Network identifiability plays a crucial role across various network identification studies, ensuring the validity and uniqueness of reconstructed network structures or individual module parameters. This section explores recent advancements in understanding and overcoming identifiability challenges in different network contexts.

- **Guaranteeing Identifiability in Network Topology Detection**

  Traditionally, accurate network topology detection relied heavily on the assumption of network identifiability. However, real-world networks often violate this assumption, leading to misleading results. To address this challenge, the work of Waarde, Tesi

e Camlibel (2021) provides rigorous identifiability conditions and a sophisticated algorithm based on the generalized Sylvester equation. This approach significantly enhances the reliability of network topology detection by ensuring identifiability before proceeding with reconstruction.

- **Overcoming Partial Measurement in Local Module Identification**

  Local module identification aims to isolate and understand the behavior of individual components within a network. However, limitations in measurements and excitations are often encountered. Shi, Cheng e Hof (2021) tackle this challenge by developing less stringent identifiability conditions that leverage unmeasured noise signals. Additionally, they propose graph-based verifications to assess identifiability based on network topology. These advancements enable strategizing excitation and measurement selection to guarantee module uniqueness, even with partial information.

- **Identifiability in Diffusively Coupled Networks**

  Kivits e Van den Hof (2023) address the identifiability challenge in diffusively coupled networks, which model symmetric interactions in systems like electrical circuits. Existing methods often struggle with higher-order networks due to complex state-space models. The work in (KIVITS; Van den Hof, 2023) presents generalized identifiability conditions applicable even with three-polynomial matrix fractions. This significantly improves our understanding of identifiability in diffusively coupled networks with limited observations.

1.4 Statement of the Problem

Despite a burgeoning body of research, the area of dynamic network identification remains a dynamic jigsaw puzzle itself, characterized by exciting advancements scattered within a framework that yearns for greater cohesion. While individual publications tackle specific challenges - from achieving consistent module estimates to boosting their accuracy - a unified theoretical foundation still awaits construction.

Moving forward, the field demands a shift from isolated pieces to a comprehensive picture. Beyond general model properties, specific considerations arise for physical systems. The passivity property, a crucial characteristic for many physical networks, deserves in-depth investigation within the context of module identification. Devising strategies to preserve and evaluate this property in identified models would significantly enhance their relevance and interpretability in interconnected systems context.

This thesis focuses on identifying passive modules of passive systems embedded in a dynamic network. Passivity enforcement has received little attention in the field of dynamic networks which is somewhat unjustified given its appealing algebraic closure property. On the other hand, the topic has been broadly explored in other realms such as power systems, microelectronics and RF contexts, see (GRIVET-TALOCIA; GUSTAVSEN, 2016). However, in these other research areas passivity is dealt with separately so that each device is enforced passive and then interconnected which is not quite the dynamic network context. The proposed approach tackles passive macromodeling within a dynamic network context from the very first step: measurement. Despite the differences, the advantages of considering passivity enforcement remain the same: numerical simulations are stable, energy balances are preserved and the model is consistent based on the energy balance conditions. As a consequence, addressing this question to the problem is a major concern to dynamic network analysis. Incorporating these estimators into the passivity framework in a integrated manner represents an innovative approach *per se*.

While existing literature offers diverse methods for dynamic network identification, as the ones herein presented, remarkably none delve into the crucial aspect of passivity enforcement. This property is surprisingly neglected despite its inherent benefits. While explored in contexts like power systems and microelectronics, passivity is typically analyzed on individual devices before interconnection, deviating from the dynamic network setting.

This thesis boldly steps into this uncharted territory, aiming to address passivity enforcement directly within the context of dynamic networks, right from the initial measurement stage. Initially focusing on the case where the interconnection structure is known. This simplification facilitates initial analysis and allows passivity results to be

readily extended to the unknown topology case later. While both scenarios exhibit some similarities from a passivity analysis standpoint, practical implementation in unknown topology scenarios may introduce additional challenges, particularly in topology detection.

Closed-loop identification methods are chosen as the initial framework due to their natural fit with the inherent feedback loops prevalent in dynamic networks. Furthermore, any dynamic network can be theoretically modelled as a single multi-variable feedback loop. However, applying closed-loop techniques requires careful consideration of certain assumptions like noiseless predictor inputs and zero-order-hold signals, which may not hold true in all dynamic network settings. This motivates further investigation and potentially exploring alternative identification approaches not limited by these assumptions, as discussed in (DANKERS, 2014).

The main motivating question for the research presented in this thesis is: **how to consistently identify a particular passive module for a passive system that is embedded in a dynamic network?**

Unlike traditional MIMO identification that aims to reconstruct the entire network, our focus is on identifying a smaller subset of transfer functions within a dynamic network, specifically targeting passive systems. This targeted approach allows for considerably relaxed identification conditions compared to full MIMO network identification. By focusing on local identification of passive systems, we can relax several strict assumptions often required in MIMO approaches. There is no need to:

- **Measure all internal variables**: References (GHALEBI *et al.*, 2018; HENDRICKX; GEVERS; BAZANELLA, 2019) highlights the reduced need for internal measurements in our approach.
- **Ensure external variables at every node**: References (SHI; CHENG; HOF, 2021;

MAPURUNGA; BAZANELLA, 2021b) demonstrate that local methods allows some nodes without external variables.

This targeted approach aligns with a distributed/local identification strategy compared to a centralized/global view inherent to traditional MIMO system identification. Only local measurements are required to identify a specific passive module within the dynamic network.

1.4.1 Objectives

This thesis aims at adding light on the hidden dynamics of individual modules within complex networks. The primary goal of this thesis is to reliably identify passive models for passive modules embedded within a dynamic network, with a focus on passive estimation. The specific objectives are:

Objective 1: Develop specialized formulation for passivity enforcement in the context of discrete-time network systems.

Objective 2: Design and implement a FD-VF algorithm for efficient and accurate module identification in dynamic networks.

Objective 3: Integrate passivity enforcement as a built-in procedure within the FD-VF algorithm, leveraging the KYP lemma to guarantee the passivity of estimated models at each step of the algorithm.

These objectives contribute to the field of dynamic network identification by providing researchers with a powerful toolkit for approximating model properties to their real-systems in the context of interconnected systems and paving the way for a plethora of exciting applications.

1.5 Thesis Layout

- **Chapter 2. Dynamic Network Modeling and Identifiability**

Provides a thorough grounding in dynamic network modeling and identifiability, focusing on physical systems within this framework. It outlines key definitions, identifiability conditions, and a practical toolbox for real-world implementation.

- **Chapter 3. Network Identification**

  Explores network identification, delving into direct and indirect methods for local module identification. It highlights the Predictor Error Method and introduces the projection indirect approach, showcasing their application through practical examples.

- **Chapter 4. System Dissipativity and Passivity**

  Elucidates concepts related to dissipativity and passivity in dynamic network systems. It examines various strategies for enforcing passivity, laying the groundwork for subsequent analysis.

- **Chapter 5. Frequency Domain Identification**

  Presents a Frequency Domain identification method employing a nonparametric step followed by a parametric step. This chapter offers a complex case study illustrating the practical application and efficacy of the proposed approach in a real-world scenario.

- **Chapter 6. Conclusions**

  Synthesizes the key findings and insights gleaned from the research, consolidating knowledge acquired on dynamic network modeling, identifiability, dissipativity, passivity, and both time- and frequency-domain identification. This concluding chapter not only summarizes contributions but also provides a comprehensive perspective on the current state of the research within this domain.

2 Dynamic Network Models and Modeling

Imagine navigating a bustling city, its streets forming a intricate network of connections. Imagine untangling the hidden patterns within a flock of birds in flight, their movements governed by an unseen choreography. This, in essence, is the power of dynamic network models. The primary question addressed in the present chapter is: how do we capture the dynamic essence of dynamic networks? This is where models come in. Think of them as simplified maps, highlighting the crucial pathways and interactions within a system while filtering out unnecessary details. Just like traditional models, dynamic network models feature internal and external variables, representing the system's own workings and its interactions with the outside world. Importantly, they also account for the ever-present noise – the unpredictable fluctuations that inject an extra layer of complexity into real-world systems. This chapter delves into the world of dynamic network models, providing you with the essential tools to decipher the intricate dance of interactions within complex systems.

2.1 Introduction

Linear system theory offers a variety of model representations, including state-space, transfer function, and impulse response. These fundamental models serve as building blocks for constructing complex, structured models that analyze interconnected systems, or networks.

Building on these fundamental models, dynamic networks offer a powerful framework for analyzing interconnected systems. While traditional closed-loop models provide compact transfer functions for individual or multiple subsystems, they lack information on how these subsystems interact within the network. This "structural information" is crucial for comprehensive network analysis. Understanding, analyzing, and controlling these intricate structures become challenging without proper models. In fact, operating, designing, or maintaining such systems would be impossible without an appropriate representation.

This underscores the inherent significance of delving deeper into the concept of a model for dynamic networks.

This chapter establishes the fundamental framework of dynamic network models. We formally define a dynamic network model, highlighting its similarities to closed-loop models through shared internal, external, and noise variables. Furthermore, we show that the dynamic network model can be viewed as a natural extension of its closed-loop counterpart. To illuminate this interconnections, we initially provide a graph representation that visually captures the structure of a dynamic network.

2.2 Graph Theory concepts

This section provides a concise review of the essential definitions in graph theory, with examples to illustrate each concept.

A graph $\mathcal{G}$ is an ordered pair $(V(\mathcal{G}), E(\mathcal{G}))$ consisting of a nonempty set $V(\mathcal{G})$ of vertices and a set $E(\mathcal{G})$ of edges that associates pairs of vertices, thus the elements of E are 2-element subsets of V (BONDY; MURTY, 1982).

Consider the following example of a graph $\mathcal{H}$, as ilustrated in Figure 1.

Example 2-3.

$$\begin{aligned} &\mathcal{H} = (V(\mathcal{H}), E(\mathcal{H})) \\ &\textit{where} \\ &V(\mathcal{H}) = \{1,2,3,4,5,6,7,8\} \\ &E(\mathcal{H}) = \{\{1,2\},\{1,5\},\{2,3\},\{2,4\},\{4,6\},\{6,7\},\{7,8\}\} \end{aligned} \tag{2.1}$$

The number of vertices of a graph is its *order*. A graph is *finite* if both its vertex set and edge set are finite. An *infinite* graph would have an infinite order (BONDY; MURTY, 1982). Unless otherwise stated, the graphs we consider in this thesis are all finite. Furthermore, we call a graph with just one vertex *trivial*, i.e., a graph of order 1 (DIESTEL, 2017).

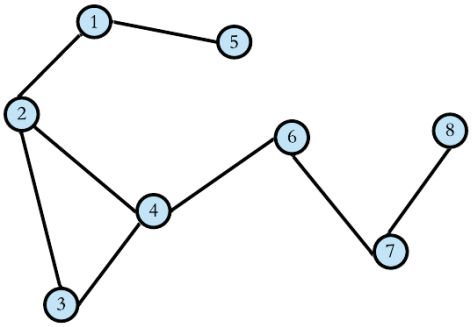

Figure 1 – Diagram of graph $\mathcal{H}$.

A graph with multiple edges, or simply *multigraph*, is a special case when two vertices are linked by more than one edge, as shown in Figure 2. Graphs withtout multiple edges are called *simple graphs*.

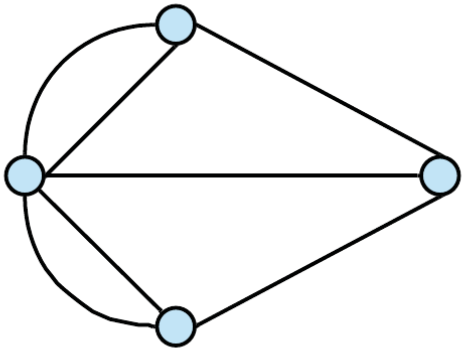

Figure 2 – Multigraph (with multiple edges).

In all the aforementioned examples, the edges were not directed. In Figure 3, however, the directions of the one-way edges are being indicated by arrows. Graphs with such characteristic are called *directed graphs*, or simply *digraphs*.

We often refer to a *walk* as a way of getting from one vertex to another. It consists of a sequence of edges that leads from vertex i, for $i = 1, 2, \ldots, V$, to vertex j, $j = 1, 2, \ldots, V$, where V is the number of vertexes in the graph. For example, consider the graph in Figure 3, $1 \to 2 \to 4$ is a walk of length 2. Likewise, $1 \to 3 \to 1 \to 4$ is a walk of length 3.

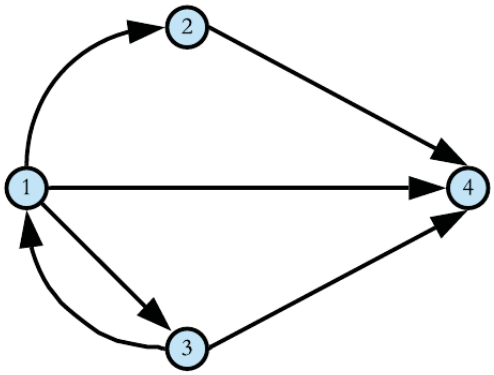

Figure 3 – Digraph.

2.2.1 Adjacency and Incidence Matrices

While a graph can be intuitively represented by a diagram of points connected by lines, this approach becomes impractical for large graphs. Instead, matrices offer an efficient and structured way to represent graph information.

We define the network's topology using a directed graph, which specifies both the locations and the causal directions of module transfers within the network. This directed graph can be represented by an adjacency matrix, as outlined below.

Consider a directed graph $\mathcal{G}$ with vertex set $V = \{v_1, v_2, \ldots, v_n\}$. The *adjacency matrix* $\mathbf{A} = (a_{ij})_{n\times n}$ is defined as in (2.2), where each entry a_{ij} indicates whether there is a directed edge from vertex v_i to vertex v_j:

$$a_{ij} := \begin{cases} 1 & \text{if } (v_i, v_j) \in E, \\ 0 & \text{otherwise.} \end{cases} \tag{2.2}$$

Here, E represents the set of directed edges in $\mathcal{G}$.

If the edges of $\mathcal{G}$ are also labeled as $E = \{e_1, e_2, \ldots, e_m\}$, we can construct the *incidence matrix* $\mathbf{M} = (m_{ij})_{n\times m}$, which is defined as in (2.3). For each vertex v_i and edge e_j, the incidence matrix $\mathbf{M}$ records the relationship between vertices and edges as follows:

$$m_{ij} := \begin{cases} 1 & \text{if } v_i \text{ is the start or end of edge } e_j, \\ 0 & \text{otherwise.} \end{cases} \tag{2.3}$$

Consider a directed graph with an adjacency matrix $\mathbf{A}$. For $k \geq 1$, the entry $[\mathbf{A}^k]_{ji}$ represents the number of distinct paths of length k from node i to node j.

Example 2-4.

Consider, for example, the graph in Figure 4, which is the same as Figure 3, but with the edges enumerated. Its adjacency matrix is

$$\mathbf{A} = \begin{bmatrix} 0 & 0 & 1 & 0 \\ 1 & 0 & 0 & 0 \\ 1 & 0 & 0 & 0 \\ 1 & 1 & 1 & 0 \end{bmatrix}. \tag{2.4}$$

Its incidence matrix is

$$\mathbf{M} = \begin{bmatrix} 1 & 0 & 0 & 1 & 1 & 1 \\ 1 & 1 & 0 & 0 & 0 & 0 \\ 0 & 0 & 1 & 1 & 0 & 1 \\ 0 & 1 & 1 & 0 & 1 & 0 \end{bmatrix}. \tag{2.5}$$

Note that the information provided by both adjacency and incidence matrices are sufficient to characterize the topology of the graph.

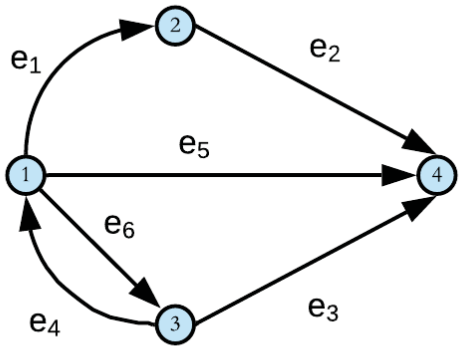

Figure 4 – Graph of Example 2-4.

The rich toolbox of theorems and concepts within graph theory provides valuable insights into network dynamics. For instance, topological properties of the graph, such as

connectivity and the presence of loops, can reveal inherent network characteristics like identifiability (the ability to uniquely determine internal states based on observations). Furthermore, graph coloring techniques, when applied with specific constraints, can aid in identifying network behavior and controllability.

However, it's important to recognize that while network interconnections are often visualized as direct "paths", the underlying physical reality may be more intricate. Physical laws govern the relationships between variables, not merely the fact that they share information. This raises a question: How can we rigorously model interconnected systems while faithfully representing their underlying physical principles?

This section illustrates how to derive models for interconnected systems, considering:

- Individual subsystem models.
- Interconnection structure (captured by the graph).
- The nature of interconnections (physical relationships between variables).

2.2.2 Electrical Circuits - An RLC example

Electrical circuits, consisting of interconnected components like resistors, capacitors, and inductors, provide an illustrative example of the link between graphs and dynamic networks. Each component within the circuit can be modeled as a "node" in the corresponding graph, with its internal voltages and currents represented as the node's variables.

The terms "network" and "circuit" are often used interchangeably, reflecting their shared concept of interconnected elements (as noted in (DESOER; KUH, 1969)). However, the term "network" often carries an implicit connotation of complexity, typically referring to circuits with a large number of components.

Similar to many other systems, an electrical circuit can be analyzed effectively as a dynamic network due to the interconnected nature of its individual components. These components, such as resistors, inductors, and capacitors, become the nodes in the graph representation, as shown in Figure 5.

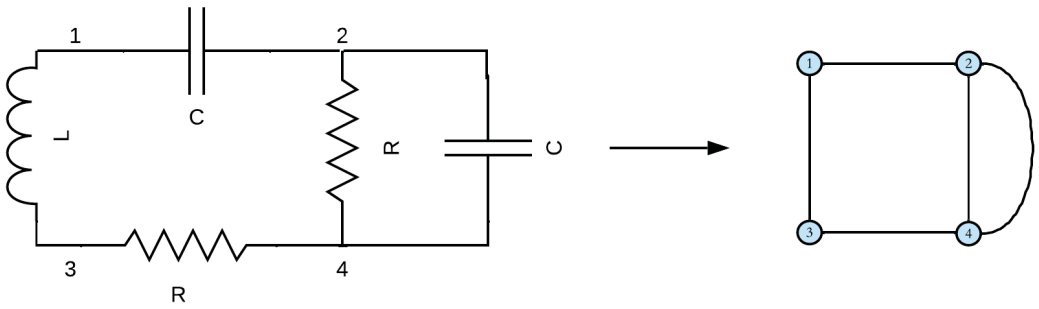

Figure 5 – An electrical circuit represented by a graphical network.

The connections between these components translate to "edges" in the graph. This graphical network representation allows us to model the entire circuit's behavior by leveraging individual component models and their interactions captured by the edge connections. By applying the principles of graph theory and network analysis, we can then extract valuable insights into the circuit's dynamics, such as current flow, voltage distribution, and overall circuit response.

2.2.3 Control Systems

Control systems, ubiquitous in various engineering applications, offer a prime example of leveraging graphs to represent their interconnected dynamics. These systems maintain a desired state (output) of a process by manipulating its inputs through feedback mechanisms.

Consider the example depicted in Figure 6 where G_{21} is the controller, G_{32} and G_{23} are systems and G_{14} is a sensor. The graph representation translate all dynamic systems as directed edges and all summation points as the network's nodes.

This graphical approach complements traditional control system analysis techniques, providing a tool for engineers to design, analyze, and optimize control systems across diverse applications.

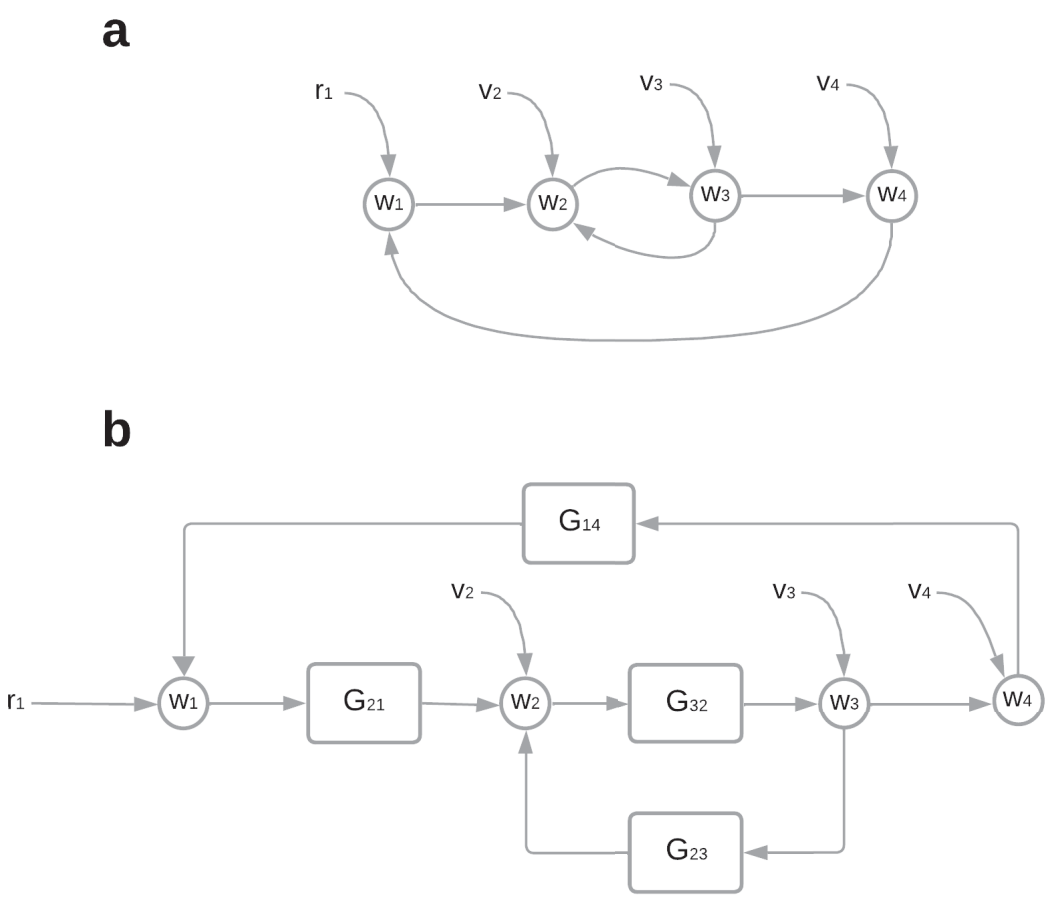

Figure 6 – A control system (dynamic network) represented as a digraph: **a**. Graph visualization; and **b**. Transfer function representation.

2.2.4 Electrical Circuits- An RC example

Figure 7 illustrates an RC electrical circuit that can be modeled as a dynamic network. In this setup, the system's internal signals correspond to the voltages across capacitors, labeled V_1, V_2, and V_3, while the external input signal is the applied voltage u.

In the circuit representation shown in Figure 7, each node represents a capacitor voltage, and the connections between nodes are the physical components of the circuit: the voltage source, resistors, and capacitors. In the dynamic network form, as shown in Figure 8, the nodes continue to represent the capacitor voltages; however, the connections between nodes are now described by transfer functions.

$$
\begin{aligned}
G_1(s) &= \frac{R_2}{sR_1R_2C_1 + R_1 + R_2}, \\
G_{12}(s) &= \frac{R_1}{sR_1R_2C_1 + R_1 + R_2}, \\
G_{21}(s) &= \frac{R_3}{sR_3R_3C_2 + R_2 + R_3}, \\
G_{23}(s) &= \frac{R_2}{sR_2R_3C_2 + R_2 + R_3}, \\
G_{32}(s) &= \frac{1}{sR_3C_3 + 1}.
\end{aligned}
\tag{2.6}
$$

This example ilustrated how an RC electrical circuit (in Figure 7), where each node represents the voltage across a capacitor, and the interconnections correspond to the resistors, capacitors, and the voltage source can be transformed into a dynamic network model (Figure 8), where the nodes continue to represent the capacitor voltages, but the interconnections are now described by continuous-time transfer functions.

In what follows, we intend to show that the dynamic network in Figure 7 can be represented either using a directed graph or undirected graph.

To further illustrate the abstraction, Figure 9 presents the directed graph representation of the circuit. In this graph, each node still represents a capacitor voltage,

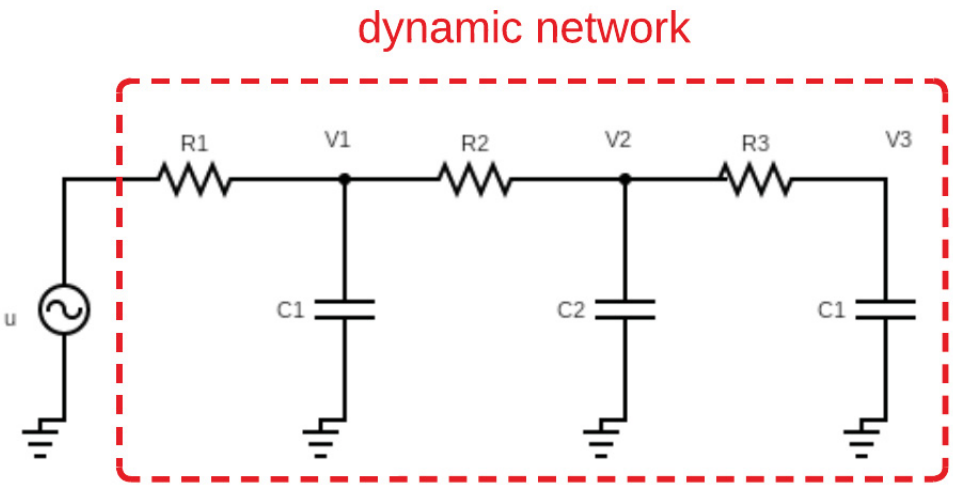

Figure 7 – Schematic of an RC electrical circuit with nodes representing capacitor voltages. Adapted from (MELO, 2022).

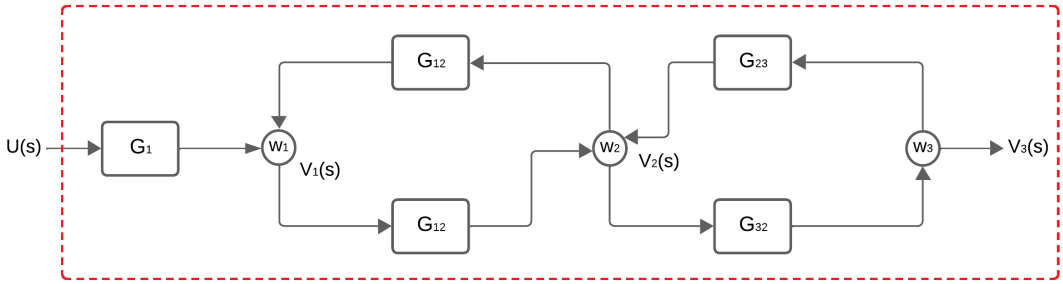

Figure 8 – Dynamic network representation of the RC circuit, where nodes denote capacitor voltages.
Adapted from (MELO, 2022).

and the edges indicate dependencies between nodes, reflecting the influence of transfer functions between each pair of connected nodes. This transformation allows for a simplified visualization of the network's structure, focusing on the relational dependencies between internal signals.

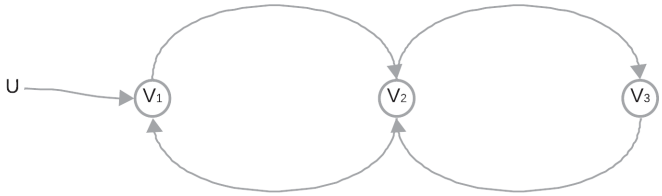

Figure 9 – Directed graph representation of the RC circuit.

The undirected graph of the dynamic network without the input signal is shown in Figure 10. Please note that the signals flow both ways in the nodes of the dynamic network, as it happens in the electrical circuit of Figure 7. We use the notation in (DORFLER; BULLO, 2013) to represent the reference/ground point in the electrical circuit into its graphical representation.

Figure 10 – Undirected graph representation of the RC circuit.

2.3 Module Representation for Dynamic Networks

The concept of module representation offers a distinct perspective on analyzing dynamic networks. It focuses on the causal dependencies existing between internal signals within the network. This section explores three prevalent models built upon this representation, each distinguished by its assumptions regarding available signals and the presence of noise.

We consider a dynamic network comprised of interconnected nodes. Each node represents a scalar, measurable internal signal denoted as $w_l(t)$, where $l \in \{1, 2, ...L\}$ and L is the total number of nodes. The dynamics of each node's signal are defined based on existing signals within the network.

A Linear Dynamical Graph (LDG) operates under the assumption that no external input signals are directly measurable (YEUNG *et al.*, 2011). It envisions the network as a stochastic linear system driven by unknown process noise. Mathematically, LDGs are represented by Equation (2.7), where:

- $w_j(t)$ denotes the signal of node j at time t.
- $v_j(t)$ represents the process noise affecting node j.
- $G_{ji}(q)$ is the transfer function characterizing the dynamic relationship from node i to node j [1]. A non-zero value for $G_{ji}(q)$ indicates the presence of a module (or edge) connecting nodes j and i.

$$w_j(t) = \sum_{i \in \mathcal{N}_j} G_{ji}(q) w_i(t) + v_j(t) \tag{2.7}$$

with q^{-1} the forward/backward operator, i.e., $q^{-1}u_j(t) = u_j(t-1)$, $G_{ji}(q)$ the proper rational transfer function between nodes j and i, and $\mathcal{N}_j$ denotes the set of indices of node signals w_k, $k \neq j$ for which G_{jk} are nonzero.

[1] Moving forward we will keep the notation herein adopted for G_{ji} being the transfer function from node i to note j.

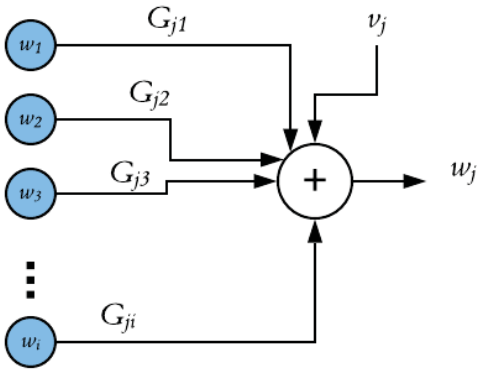

Figure 11 – A basic linear dynamical graph structure.

The noise vector associated with the internal variable vector $\mathbf{w} = \begin{bmatrix} w_1 & \cdots & w_L \end{bmatrix}^T$ is denoted by $\mathbf{v} = \begin{bmatrix} v_1 & \cdots & v_L \end{bmatrix}^T$. This noise vector is modeled as a stationary stochastic process with a rational spectral density. Consequently, there exists a p-dimensional white noise process $\mathbf{e} = \begin{bmatrix} e_1 & \cdots & e_p \end{bmatrix}^T$, where $p \leq L$, with covariance matrix $\Sigma > 0$, such that

$$\mathbf{v}(t) = \mathbf{H}(q)\mathbf{e}(t). \tag{2.8}$$

where $\mathbf{H}(q)$ is a diagonal matrix. In addition, we can define the external signals vector $\mathbf{r} = \begin{bmatrix} r_1 & \cdots & r_L \end{bmatrix}^T$.

The Dynamical Structure Function (DSF) builds upon Linear Dynamic Graphs (LDGs) by factoring in the impact of known external signals, denoted $r_j(t)$, on node dynamics (GONCALVES; HOWES; WARNICK, 2007). These external signals are scaled by elements from the system matrices, $G_{ji}(q)$ and $R_{ji}(q)$, which themselves may represent dynamic transfer functions (BAZANELLA *et al.*, 2017). The DSF is mathematically defined by Equation (2.9):

$$w_j(t) = \sum_{i \in \mathcal{N}_j} G_{ji}(q) w_i(t) + \sum_{i \in \mathcal{N}_r} R_{ji}(q) r_i(t), \tag{2.9}$$

where $\mathcal{N}_r$ is the set indices of existing external signals in the network nodes.

DSFs can also be expressed in a compact matrix form, as shown in Equations (2.10) and (2.11). This form explicitly highlights the interactions between nodes and the impact

of external inputs.

$$\mathbf{w} = \mathbf{G}\mathbf{w} + \mathbf{R}\mathbf{r}, \tag{2.10}$$

where we omit the time dependency for convenience. Alternatively, **??** can be written as,

$$\begin{bmatrix} w_1(t) \\ w_2(t) \\ \vdots \\ w_L(t) \end{bmatrix} = \begin{bmatrix} 0 & G_{12}(q) & \cdots & G_{1L}(q) \\ G_{21}(q) & 0 & \cdots & G_{2L}(q) \\ \vdots & \ddots & \ddots & \vdots \\ G_{L1}(q) & G_{L2}(q) & \cdots & 0 \end{bmatrix} \begin{bmatrix} w_1(t) \\ w_2(t) \\ \vdots \\ w_L(t) \end{bmatrix} + \begin{bmatrix} R_{11}(q) & R_{12}(q) & \cdots & R_{1L}(q) \\ R_{21}(q) & R_{22}(q) & \cdots & R_{2L}(q) \\ \vdots & \ddots & \ddots & \vdots \\ R_{L1}(q) & R_{L2}(q) & \cdots & R_{LL}(q) \end{bmatrix} \begin{bmatrix} r_1(t) \\ r_2(t) \\ \vdots \\ r_L(t) \end{bmatrix}. \tag{2.11}$$

2.3.1 General Module Representation

This subsection introduces a specialized variant of the DSF model (GONCALVES; HOWES; WARNICK, 2007), frequently employed to describe input-output relationships within dynamic networks (KIVITS; HOF, 2018; DANKERS *et al.*, 2016). This variant is characterized by the presence of a process noise $v_j(t)$, incorporated into each node's equation. This term captures the influence of internal disturbances within the network. In addition, $\mathbf{R}$ is an identity matrix.

Equation (2.12) formalizes this specialized model:

$$w_j(t) = \sum_{i \in \mathcal{N}_j} G_{ji}(q) w_i(t) + r_j(t) + v_j(t), \tag{2.12}$$

In matrix notation, the dynamic network can be represented as

$$\mathbf{w}(t) = \mathbf{G}(q)\mathbf{w}(t) + \mathbf{r}(t) + \mathbf{H}(q)\mathbf{e}(t),$$

where $\mathbf{w}(t)$ is the vector of internal variables, $\mathbf{G}(q)$ represents the network dynamics, and $\mathbf{H}(q)$ a diagonal matrix that models the effect of noise $\mathbf{e}(t)$ on the system.

This generalized model exhibits adaptability by accommodating vector-valued signal handling through appropriately sized transfer functions, as detailed in (HOF *et al.*, 2013). It's important to note that the following equation presents a single matrix formulation applicable to all measured nodes, simplifying the external signal $\mathbf{r}(t)$ and $\mathbf{v}(t)$.

This formulation is mathematically equivalent to Equation (2.12).

$$\begin{bmatrix} w_1(t) \\ w_2(t) \\ \vdots \\ w_L(t) \end{bmatrix} = \begin{bmatrix} 0 & G_{12}(q) & \cdots & G_{1L}(q) \\ G_{21}(q) & 0 & \cdots & G_{2L}(q) \\ \vdots & \ddots & \ddots & \vdots \\ G_{L1}(q) & G_{L2}(q) & \cdots & 0 \end{bmatrix} \begin{bmatrix} w_1(t) \\ w_2(t) \\ \vdots \\ w_L(t) \end{bmatrix} + \begin{bmatrix} r_1(t) \\ r_2(t) \\ \vdots \\ r_L(t) \end{bmatrix} + \begin{bmatrix} v_1(t) \\ v_2(t) \\ \vdots \\ v_L(t) \end{bmatrix}, \tag{2.13}$$

or, equivalently

$$\mathbf{w} = \mathbf{G}\mathbf{w} + \mathbf{r} + \mathbf{v}, \tag{2.14}$$

$$\mathbf{w} = (\mathbf{I} - \mathbf{G})^{-1}(\mathbf{r} + \mathbf{v}). \tag{2.15}$$

The topology of the network is embedded in the matrix $\mathbf{G}$.

The dynamic network description presented in this section considers the following properties.

- **Direct Connections**: The set of $\mathcal{N}_j$ defines the nodes directly influencing node j (w_k). Non-zero transfer functions, G_{jk}, signify these connections.
- **Proper Transfer Functions**: G_{ji} functions are all proper. Zero values for specific G_{ji} indicate no direct connection from node j to node i.
- **Absence of Self-Loops**: No node directly influences itself, as denoted by $G_{jj} = 0$ for all nodes.
- **Well-Posed Network**: All transfer functions are proper, and the determinant of the identity matrix minus the overall transfer matrix det(**I-G**) is non-zero. This ensures the network's mathematical solvability.
- **Known Network Topology**: We possess complete knowledge of the network's connection structure. This means it is known which G_{ij} are zero and which are non-zero.

The following example illustrates the graphical representation of a network equation. This will showcase how the graphical structure aligns with the mathematical description.

2.3.2 A continuous-time representation

The continuous-time counterpart of the module representation has been presented in Dankers, Hof e Bombois (2014). It can be mathematically written similiarly to (2.12), with the following differences

- t is now a continuous-time variable;
- G_{ij} is now a proper continuous-time transfer function;
- the forward/backward operator becomes a differential operator, i.e. $pu_j(t) = \frac{\mathrm{d}}{\mathrm{d}t}u_j(t)$.

$$w_j(t) = \sum_{i \in \mathcal{N}_j} G_{ji}(p) w_i(t) + r_j(t) + v_j(t). \tag{2.16}$$

The set of nodes and edges $\mathcal{N}_j$ and the signals r_j and v_j have the usual definition. Likewise, it is also assumed that the following matrix equations are well-posed.

$$\begin{bmatrix} w_1(t) \\ w_2(t) \\ \vdots \\ w_L(t) \end{bmatrix} = \begin{bmatrix} 0 & G_{12}(p) & \cdots & G_{1L}(p) \\ G_{21}(p) & 0 & \cdots & G_{2L}(p) \\ \vdots & \ddots & \ddots & \vdots \\ G_{L1}(p) & G_{L2}(p) & \cdots & 0 \end{bmatrix} \begin{bmatrix} w_1(t) \\ w_2(t) \\ \vdots \\ w_L(t) \end{bmatrix} + \begin{bmatrix} r_1(t) \\ r_2(t) \\ \vdots \\ r_L(t) \end{bmatrix} + \begin{bmatrix} v_1(t) \\ v_2(t) \\ \vdots \\ v_L(t) \end{bmatrix}, \tag{2.17}$$

Equivalently, in the matrix form

$$\mathbf{w} = \mathbf{G}\mathbf{w} + \mathbf{r} + \mathbf{v}. \tag{2.18}$$

Equations (2.17) and (2.18) define a continuous-time dynamic network.

We'll make it explicit whenever t refers to a continuous-time (CT) variable in this document. We shall omit the discrete-time (DT) specification whenever it is not essential because the majority of the content refers to DT variables.

2.4 Network Identifiability

In this section, we formally define the concept of network identifiability within the context of dynamic networks. Identifiability establishes the conditions under which the

network structure, including individual modules and their connections, can be uniquely recovered from measured data. These conditions guide the design of experiments, specifying which nodes require excitation (external influence) and measurement. Two fundamental aspects of identifiability are explored: local module identifiability and path-based identifiability.

Local identifiability focuses on the ability to uniquely determine the dynamics of a single module based solely on the measured data. This typically requires exciting all incoming nodes to the module and measuring the outgoing node. By doing so, the influence of other modules on the target module is fully accounted for, enabling the unique characterization of its internal dynamics (WEERTS; DANKERS; Van den Hof, 2015; WEERTS; HOF; DANKERS, 2018a).

Path-based identifiability focuses on reconstructing the connections between modules within a network. It transcends local identifiability by strategically selecting nodes for excitation and measurement along specific paths. This selection ensures the isolation and distinction of each traversed module's influence. By adhering to these conditions, researchers can design experiments that guarantee the unique identification of inter-modular connections, leading to a comprehensive understanding of the network's architecture. Notably, path-based identifiability leverages the concept of generic rank, considering all feasible parameter configurations within the model class (excluding only a set of measure zero). This stricter definition ensures the identified connections hold true for almost all possible parameter values within the network (WEERTS; DANKERS; Van den Hof, 2015; BAZANELLA *et al.*, 2017).

2.4.1 Some background on power spectra

Defining the network's open-loop response, the data's spectral density allows us to characterize the information embedded within the data.

The network transfer function that maps the external signals $\mathbf{r}(t)$ and $\mathbf{e}(t)$ into the

node signals (input) $\mathbf{w}$ is given by:

$$\mathbf{T}(q) = [\mathbf{T_{wr}}(q) \quad \mathbf{T_{we}}(q)], \tag{2.19}$$

$$\mathbf{T_{wr}}(q) = (\mathbf{I} - \mathbf{G}(q))^{-1}\mathbf{R}(q), \tag{2.20}$$

and

$$\mathbf{T_{we}}(q) = (\mathbf{I} - \mathbf{G}(q))^{-1}\mathbf{H}(q). \tag{2.21}$$

Where the notation $\mathbf{T}(q) = (\mathbf{I} - \mathbf{G}(q))^{-1}\mathbf{U}(q)$ with

$$\mathbf{U}(q) = [\mathbf{H}(q) \quad \mathbf{R}(q)] \tag{2.22}$$

is also used. This is also know as the open-loop response of the network corresponding with

$$\mathbf{w}(t) = \mathbf{T_{wr}}(q)\mathbf{r}(t) + \mathbf{T_{we}}(q)\mathbf{e}(t). \tag{2.23}$$

Nodes $w(t)$ can be represented as a spectral density in the following way:

$$\phi_w(\omega) = \mathbf{T}_{wr}(\omega)\phi_r(\omega)\mathbf{T}_{wr}^T(\omega) + \phi_v(\omega). \tag{2.24}$$

2.4.2 Conditions for a local module identification

Methods for identifying network structure from data often rely on additional assumptions to infer connections and dynamics. However, the validity of these assumptions in ensuring a unique network solution is often uncertain, as they may lack rigorous characterization. For instance, the commonly used sparsity assumption suggests that the simplest network, which best explains the observed behavior, is likely to represent the real system (HAYDEN *et al.*, 2016). While this assumption is intuitively appealing, it has limitations: we can demonstrate that any input-output behavior could also be produced by a completely disconnected network structure, thus challenging the reliability of sparsity as a sole assumption.

Building on this, Weerts, Dankers e Van den Hof (2015) propose relaxing some of the stringent conditions imposed by previous network identification methods. Earlier approaches to network identification, such as those based on prediction error methods and

topology reconstruction, typically required extensive prior knowledge of the entire network structure or strong assumptions like uncorrelated noise at each node. These methods also often relied on specific excitation conditions across all modules to uniquely determine the full network structure. The approach in (WEERTS; DANKERS; Van den Hof, 2015), however, introduces a more flexible framework that allows for the identification of a single module within a network, even if the dynamics of other modules remain unknown. This innovation enables targeted identification of specific components without needing to reconstruct the entire network, thus expanding the applicability of identification methods to more complex and partially known networks.

In Weerts, Dankers e Van den Hof (2015), identifiability concepts are presented for the dynamic network case. In this thesis, we are interested in guaranteeing that a local module, or set of modules, can be identified based on data from the network measurements. This section delves into a definition and provides relaxed conditions to explore how a single module can be uniquely estimated in a dynamic network.

While identifiability traditionally focuses on distinguishing a single model G_{ji} from others, a stronger concept exists: local network identifiability of the entire model matrix $\mathbf{G}$. This property ensures all models in $\mathbf{G}$ can be obtained based on data features obtainable from its underlying properties. This is advantageous because, in practice, the true model G_{ji} is often unknown. This concept builds upon previous work on identifiability at a specific model level (GONCALVES; WARNICK, 2008).

The notion of *network identifiability* in dynamic networks ensures that the dynamics and structure of a network can be uniquely determined based on measured data. This property is crucial when identifying network topology and individual modules, as it guarantees that the identified model represents the true network configuration. In this context, network identifiability extends classical system identifiability concepts by considering the complexity of interconnected modules, correlated disturbances, and structured excitation sources.

To formalize network identifiability, let us consider a network model matrix $\mathbf{G}$, which is defined over a set of parameters θ, where θ conveys the parameters of a given

transfer fucntion. For the network model to be identifiable, it must be possible to uniquely determine each transfer function G_{ji} based on the data, including both excitation signals and noise properties.

This identifiability condition states that if two models G^0 and G_{ji} generate the same open-loop behavior ϕ_w, for a given ϕ_r, as represented by the transfer function $\mathbf{T}_{wr}$ and the spectral density ϕ_v, then they must be identical, ensuring a unique mapping from the model matrix $\mathbf{G}$ to the underlying network structure.

This identifiability condition we evaluate in this thesis is influenced by the following factors:

- **Excitation Signal Requirements**: Adequate external signals must be applied at specific points in the network to ensure that each module's dynamics are distinguishable. This requirement, often referred to as data informativity, is crucial to separate the influence of individual modules.
- **Disturbance Modeling**: The network disturbance $\mathbf{v}(t)$, driven by a reduced-rank white noise process $\mathbf{e}(t)$, requires proper modeling.
- **Structural Prior Knowledge**: Certain network identification approaches may require structural assumptions, such as knowing which nodes are connected, to simplify the identification task. For example, Hof *et al.* (2013) developed methods based on predictor input selection, which utilize known module interconnections.

These identifiability concepts allow us to assess whether a specific module or the entire network can be consistently identified from measured data, considering both excitation and disturbance characteristics. For example, in (WEERTS; DANKERS; HOF, 2015) the authors showed that network identifiability depends not only on excitation and noise placement but also on the uniqueness properties of the network's parametrization and topology.

Thus, $\mathbf{G}$ is globally identifiable if the items above holds for all G_{ji}, guaranteeing that the network dynamics can be reconstructed without ambiguity from the available

data.

In this thesis, we apply the identifiability concepts presented in Weerts, Dankers e Hof (2015), which satisfy the aforementioned described factors. The identifiability analysis is made in the basis of a toolbox for dynamic network identification (Van den Hof, www.sysdynet.net, 2023), where local identifiability conditions are verified.

To apply the identifiability framework described in Weerts, Dankers e Hof (2015), the following outlined steps should hold [2].

Formulate the Network Model

- Define the transfer function matrices $G(q)$, $H(q)$, and $R(q)$ to describe the system's internal dynamics, noise, and external excitation inputs.
- Verify which nodes are influenced by external excitations and disturbances.

Check Identifiability Conditions

- Ensure that the transfer function matrix $G(q)$ is fully parameterized or satisfies structural constraints that guarantee unique identification.
- Verify that each node has independent excitation using the theoretical conditions.

Construct the Predictor Model

- Define the one-step-ahead predictor equation (WEERTS; DANKERS; HOF, 2015):

$$\hat{w}(t|t-1) = [I - H^{-1}(q)(I - G(q))]w(t) + H^{-1}(q)R(q)r(t). \tag{2.25}$$

- Compute the matrix $T(q, \theta)$ from measured data.

Analyze Identifiability

- Check whether the estimated $T(q, \theta)$ uniquely maps to a single model structure.
- If multiple models fit the observed data, the network might not be identifiable.

[2] These steps are outlined in depth in (WEERTS; DANKERS; HOF, 2015).

Use Excitation Design for Robust Identification

- If identifiability is not guaranteed, adjust the experimental setup by:
  - Placing additional excitation sources in strategic nodes.
  - Introducing structural constraints based on prior system knowledge.

By following these steps, the network identifiability framework can be effectively applied to ensure that the estimated model is unique and accurately represents the underlying dynamic system.

2.4.3 Summarizing Network Identifiability

For network identification to be successful, the network itself needs to be identifiable. In simpler terms, we need to ensure that the network's dynamic properties can be uniquely determined from the collected data.

Network identifiability is a multifaceted concept, as highlighted by (SHI; CHENG; HOF, 2021). It refers to the ability to distinguish between different network models within a set of candidate models based solely on the measurement data. Additionally, as emphasized by Mapurunga e Bazanella (2021a), identifiability depends on several factors beyond just the experimental setup. These factors include:

- **Excitation Signal Richness:** The quality and design of the input signals used to excite the network can significantly impact identifiability.
- **Model Set Parametrization:** The chosen model structure (e.g., transfer functions, state-space models) can influence identifiability.
- **Data Generating System:** The inherent properties of the system that generated the data play a role in identifiability.

The first perspective focuses on the practicalities of data collection and designing effective experiments. Here, the goal is to determine which nodes within the network

should be excited with input signals and which ones need to be measured to obtain the most accurate parameter estimates during identification (MAPURUNGA; BAZANELLA, 2021b). This concept is crucial for designing efficient experiments and is independent of the specific identification method chosen.

The second perspective takes a more theoretical approach, looking at identifiability from the standpoint of the network model set itself. This set is defined by the parameterized transfer matrices of the network, as discussed in (WEERTS; DANKERS; HOF, 2015; WEERTS; HOF; DANKERS, 2018a). Here, the focus is on whether the chosen model structure allows for a unique set of parameters to be recovered from the data. In other words, this definition emphasizes the ability to distinguish between different network models based solely on their mathematical representations (transfer functions).

This distinction between the two perspectives is important. The first perspective focuses on designing experiments that will yield the most accurate data, while the second perspective focuses on the mathematical properties of the network models themselves. Both perspectives are crucial for successful network identification.

Since this thesis centers on identifying individual modules within a network, a more in-depth discussion on network identifiability in this context can be found in (MAPURUNGA; BAZANELLA, 2021a).

2.5 Closing Remarks

This chapter has established a foundation for the analysis of dynamic network models. We commenced by formally defining dynamic networks and emphasizing the significance of mathematical models in elucidating their intricate temporal characteristics. Subsequently, we explored the fundamental building block of network representation: graphs. Graph theory provides a powerful visual and mathematical tool for analyzing the interconnected nature of complex systems.

Following this, we delved deeper into the nexus between graphs and dynamic networks. We established how graph theory equips us with essential tools to analyze network

dynamics, such as identifiability. We further explored the construction of dynamic network models by considering the constituent subsystem models, the network's interconnection structure, and the underlying physical relationships between system variables.

Electrical circuits and power systems served as illuminating examples of how graphs can effectively model real-world dynamic networks. The chapter then proceeded to explore three prominent model representations built upon the concept of module interaction: Linear Dynamical Graphs (LDGs), Dynamical Structure Functions (DSFs), and a generalized variant of the DSF model. These models provide a framework for analyzing and predicting network behavior under varying assumptions regarding the availability of signals and the presence of noise.

By attaining an understanding of these core concepts and models, we can effectively analyze and control complex dynamic networks. This knowledge has far-reaching implications for advancements in various disciplines, including engineering, biology, and the social sciences. The insights gleaned from this chapter serve as a springboard for further exploration into the fascinating realm of dynamic network analysis and its diverse applications.

Moving forward, the subsequent chapters will primarily adopt the discrete-time version of the standard network structure presented in equation (2.13). This framework assumes a network comprising L nodes. Notably, the network identification procedure to be introduced in Chapter **5** caters specifically to discrete-time models embedded within this type of network representation.

While the focus rests on discrete-time models, acknowledging the importance of continuous-time systems is crucial. Many physical systems often find natural descriptions as continuous-time networks. Additionally, the underlying physical characteristics of the system under study frequently have a close connection to continuous-time transfer functions. Notably, estimating physical system parameters sometimes involves identifying a continuous-time transfer function within a continuous-time network model.

3 Dynamic Network Identification

Extracting a mathematical model that captures the essence of dynamic networks poses a significant challenge. This chapter delves into the realm of network identification, exploring techniques to unveil the hidden dynamics that govern these interconnected systems. We'll navigate the complexities arising from feedback loops, noise, and the sheer number of interacting elements. By exploring established methods, this chapter equips you with the tools to undestand passive identification in dynamic networks, paving the way for their effective analysis and control.

3.1 Introduction

Extracting a mathematical model from real-world data is a challenging task, prone to errors at various stages. Most system identification methods focus on systems operating in either open-loop (no feedback) or closed-loop (with feedback) configurations. While closed-loop systems introduce complexities due to feedback, network identification presents an even greater challenge. Networks, by their very nature, can contain multiple loops, leading to strong correlations between signals, the presence of algebraic loops (circular dependencies), and noise corrupting both inputs and outputs.

Figure 12, adapted from (LJUNG, 1999), illustrates a typical system identification process. It involves three main steps: data acquisition, model selection and parameter estimation & validation. Data acquisition focuses on gathering measurements from the system. This may involve designing an experiment to excite the system with specific inputs and measure relevant outputs.

The second step involves choosing a model structure (e.g., state-space, transfer function) and an estimation algorithm. This step requires the user to select a model that can effectively map past inputs and outputs to the current system behavior. Additionally, an estimation method is needed to determine the model's parameters. A common approach

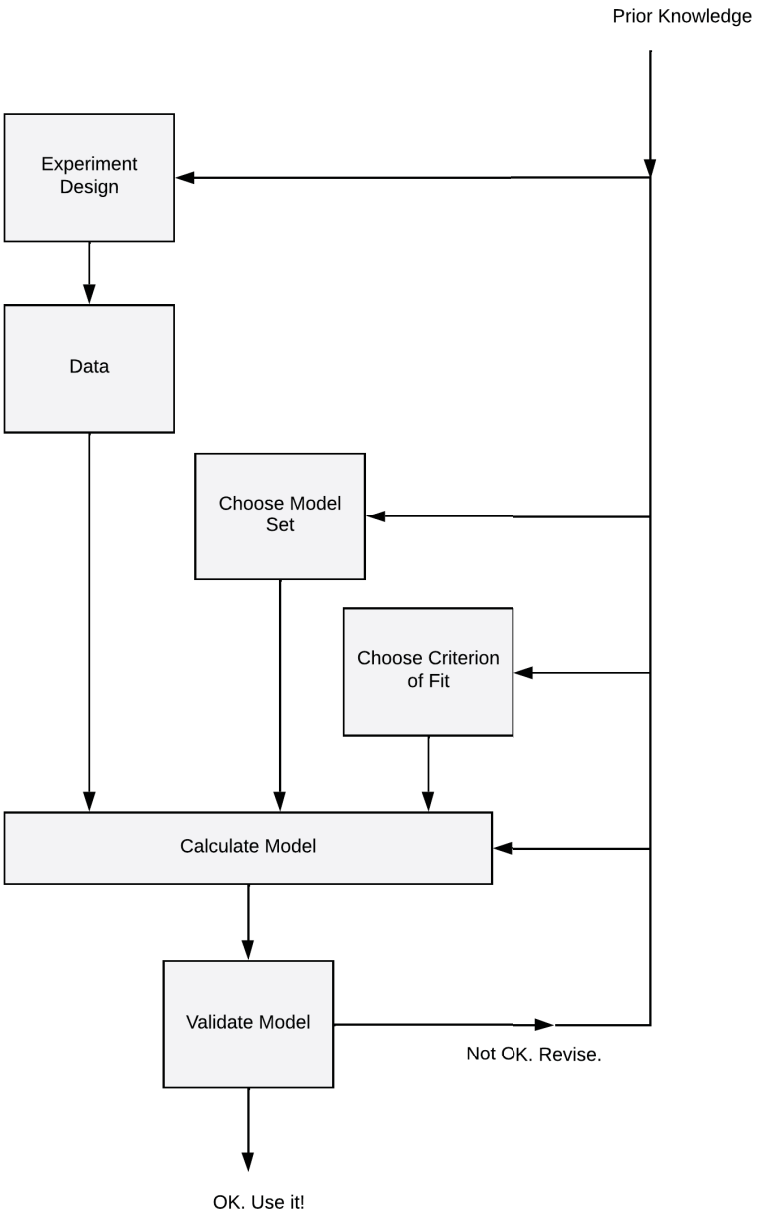

Figure 12 – A generic system identification flowchart.

is to minimize the sum of squared prediction errors between the model's output and the actual system output (LJUNG, 1999). Finally, the validation step assesses the obtained model's performance. Key aspects include evaluating the model's accuracy, potential biases, and output variance.

Traditional system identification methods primarily target open-loop or closed-loop systems. This chapter ventures beyond these established techniques to explore the identification of individual modules embedded within dynamic networks. A critical challenge in network identification lies in determining suitable experimental conditions. This involves

identifying which network nodes require excitation (input signals) and which ones need measurement to ensure the network's parameters are identifiable. Section 2.4.2 addressed this crucial aspect.

Building upon the foundation of closed-loop system identification, this chapter introduces two key approaches for network identification:

- The Direct Method (presented in Section 3.3)
- The Two-Stage Method (introduced in Section 3.4)

3.1.1 Data Generating System

To analyze the properties of identification methods, we will assume the data originates from a dynamic network, as introduced in Chapter 2. This framework allows us to explore how well different identification techniques perform under controlled conditions.

Consider a network with internal variables denoted by $w_1(t), w_2(t), \cdots, w_L(t)$. We use the superscript 0 to denote the transfer function of the true underlying system (data generating system) as G^0. These internal variables are related through the following equation (Equation 3.1):

$$\begin{bmatrix} w_1(t) \\ w_2(t) \\ \vdots \\ w_L(t) \end{bmatrix} = \begin{bmatrix} 0 & G_{12}^0(q) & \cdots & G_{1L}^0(q) \\ G_{21}^0(q) & 0 & \cdots & G_{2L}^0(q) \\ \vdots & \ddots & \ddots & \vdots \\ G_{L1}^0(q) & G_{L2}^0(q) & \cdots & 0 \end{bmatrix} \begin{bmatrix} w_1(t) \\ w_2(t) \\ \vdots \\ w_L(t) \end{bmatrix} + \begin{bmatrix} r_1(t) \\ r_2(t) \\ \vdots \\ r_L(t) \end{bmatrix} + \begin{bmatrix} v_1(t) \\ v_2(t) \\ \vdots \\ v_L(t) \end{bmatrix}, \tag{3.1}$$

or, given a single internal variable defined as

$$w_j(t) = \sum_{i \in \mathcal{N}_j} G_{ji}^0(q) w_i(t) + r_j(t) + v_j(t). \tag{3.2}$$

The data generating system also satisfy the following assumptions.

- $\mathcal{N}_j$ denotes the set of indices of node signals w_i, $i \neq j$ for which G_{ji}^0 are nonzero, i.e., the set of measured variables with direct causal connections.

- G_{ij}^0 are proper transfer functions. Absence of G_{ij}^0 corresponds to $G_{ij}^0 = 0$, indicating that there is no direct link from w_j to w_i.
- The dynamic network has no self loops, or, $G_{jj}^0 = 0$.
- The network is well posed, meaning all transfer functions are proper and $det(\mathbf{I}-\mathbf{G}^0) \neq 0$.
- The topology of the network is known, i.e., one knows which G_{ij}^0 are zero.

Embedded models within the network are parameterized as linear, discrete-time transfer functions of the form shown in Equation 3.3:

$$G_{ji}^0(q) = \frac{B(q)}{A(q)} = \frac{b_1 q^{-1} + b_2 q^{-2} + \cdots + b_{n_b} q^{-n_b}}{1 + a_1 q^{-1} + a_2 q^{-2} + \cdots + a_{n_a} q^{-n_a}}, \tag{3.3}$$

where n_a and n_b represent the orders of the denominator and numerator, respectively. Therefore, the following parameter vector can be defined:

$$\theta^0 = [b_1\ b_2\ \cdots\ b_{n_b}\ a_1\ a_2\ \cdots\ a_{n_a}]\,. \tag{3.4}$$

Equivalently, we consider the error model as

$$H_j(q, \theta_j) = \frac{c_0 + c_1 q^{-1} + c_2 q^{-2} + \cdots + c_{n_c} q^{-n_c}}{1 + d_1 q^{-1} + d_2 q^{-2} + \cdots + d_{n_d} q^{-n_d}}, \tag{3.5}$$

where n_d and n_c represent the orders of the denominator and numerator, respectively.

3.2 System Identification Framework

In this section, we shift the attention from data generating system and related themes to a parametric identification structure that is based on solving a minimization problem. The objective is to estimate the parameters of a given model by minimizing its prediction error.

In system identification, a crucial aspect lies in the model's ability to predict the system's behavior (LJUNG, 1981; GEVERS *et al.*, 2003; WEERTS; HOF; DANKERS, 2018b). Therefore, a logical criterion for evaluating model quality is its prediction ability

(BOSCH; KLAUW, 1994). Prediction Error Methods (PEMs) offer a way to assess this ability by calculating the difference between measured and predicted outputs. Essentially, PEMs evaluate candidate models based on how well they can predict future behavior.

We will now formally define the concept of PEMs and introduce some notation. For a more in-depth treatment of this material, refer to (LJUNG, 1999; AGUIRRE, 2015).

3.2.1 Prediction Error Methods

This section focuses on one-step-ahead predictor models. Let $w_j(t)$ denote the internal variable to be predicted, and $w_i(t)$ denotes the internal variable that will be used to predict $w_j(t)$. Recalling the relationship between these variables:

$$w_j(t) = \sum_{i \in \mathcal{N}_j} G_{ji}(q, \theta) w_i(t) + r_j(t) + v_j(t).$$

Consider $v_j(t) = H_j(q)e_j(t)$, where $e_j(t)$ is a white noise process and $H_j^0(q)$ is a stable and inversible transfer function. From the estimation perspective, both $H_j^0(q)$ and $G_{ji}^0(q)$ are unknown transfer functions, and they are modeled using parametrized rational transfer functions as

$$\begin{aligned} G_{ji}(q, \theta_{ji}) &= \frac{b_1 q^{-1} + b_2 q^{-2} + \cdots + b_{n_b} q^{-n_b}}{1 + a_1 q^{-1} + a_2 q^{-2} + \cdots + a_{n_y} q^{-n_a}}, \\ H_j(q, \theta_j) &= \frac{c_0 + c_1 q^{-1} + c_2 q^{-2} + \cdots + c_{n_c} q^{-n_c}}{1 + d_1 q^{-1} + d_2 q^{-2} + \cdots + d_{n_d} q^{-n_d}}. \end{aligned} \tag{3.6}$$

The corresponding parameter vectors are defined in Equation 3.7:

$$\begin{aligned} \theta_{ji} &= [b_1\, b_2\, \cdots\, b_{n_b}\, a_1\, a_2\, \cdots\, a_{n_a}], \\ \theta_j &= [c_0\, c_1\, c_2\, \cdots\, c_{n_c}\, d_1\, d_2\, \cdots\, d_{n_d}], \\ \theta &= [\theta_{jk_1}\, \cdots\, \theta_{jk_n}\, \theta_j], \{k_1, \cdots, k_n\} \in \mathcal{D}_j. \end{aligned} \tag{3.7}$$

where $k_j \in \mathcal{D}_j$ denotes the parameters of the transfer functions that will be used to predict the value of $w_j(t)$.

In (3.2), $w_j(t)$ is the measured process output at instant t, suppose that we have complete knowledge of past samples $(w_j(t-1), w_j(t-2), \ldots)$ in addition to current and past values of $w_i(t)$, i.e., $(w_i(t), w_i(t-1), w_i(t-2), \ldots)$.

The one-step-ahead predictor defined in (LJUNG, 1999) is defined as follows.

$$\hat{y}(t \mid t-1, \theta) = H^{-1}(q,\theta)G(q,\theta)u(t) + \left(1 - H^{-1}(q,\theta)\right) y(t). \tag{3.8}$$

Then it is defined the one-step-ahead predictor adapted to the dynamic network case where $u = w_i$ and $y = w_j$. The network equation expresses $w_j(t)$ as a sum of influences from multiple nodes $w_i(t)$, meaning that instead of a single $G(q,\theta)u(t)$, we must sum over all influencing nodes in $\mathcal{N}_j$:

$$\hat{w}_j(t \mid t-1, \theta) = H_j^{-1}(q,\theta) \sum_{i \in \mathcal{N}_j} G_{ji}(q,\theta)w_i(t) + \left(1 - H_j^{-1}(q,\theta)\right) w_j(t). \tag{3.9}$$

The network equation also contains the external variable $r_j(t)$, which is known and does not need prediction. It is added as a direct term:

$$\hat{w}_j(t \mid t-1, \theta) = \sum_{i \in \mathcal{N}_j} H_j^{-1}(q,\theta)G_{ji}(q,\theta)w_i(t) + r_j(t) + \left(1 - H_j^{-1}(q,\theta)\right) w_j(t). \tag{3.10}$$

The prediction error is:

$$\epsilon_j(t,\theta) = w_j(t) - \hat{w}_j(t|t-1,\theta). \tag{3.11}$$

The identification criterion must select the model with the best predictive ability. It is common to choose the model with the smallest sum of squared prediction errors (LJUNG, 1999). The dynamic system parameters can be obtained by minimizing the following cost function

$$V_N(\theta) = \frac{1}{N}\sum_{t=1}^{N} \epsilon_j(t,\theta)^2, \tag{3.12}$$

therefore, the parameter estimates are given by

$$\hat{\theta} = arg\min_{\theta} V_N(\theta). \tag{3.13}$$

Methods that determine the parameter vector based on the minimization of $V_N(\theta)$ are called Predictor Error Methods.

3.2.2 Statistical Properties of Estimators

The previous subsection introduced an estimator that minimizes a cost function based on the squared errors between measured data and one-step-ahead predictions.

This approach using Prediction Error Methods is attractive due to its straightforward calculations and the resulting estimator's ability to handle errors in the regression equation. This is particularly beneficial when dealing with noisy data, a common scenario in real-world applications.

In addition, throughout this work, it is assumed that the order of the model G_{ji} is equal to the order of the true data-generating system G_{ji}^0. This assumption ensures that the model is capable of accurately capturing the dynamics of the underlying system.

The term *convergence* refers to the behavior of an estimator as the sample size grows. Convergence in probability ensures that, for any arbitrarily small positive number $\epsilon > 0$, the infimum that the estimate $\hat{\theta}$ deviates from the true parameter θ by no more than ϵ approaches zero as N increases:

$$inf\left(\|\hat{\theta} - \theta^0\| < \epsilon\right) \to 0 \quad \text{as} \quad N \to \infty.$$

This form of convergence is distinct from other types, such as almost sure convergence or mean square convergence, which are stronger but may not always be required for consistency.

An essential property of estimators is their *consistency*. An estimator is consistent if it provides parameter estimates that converge in probability to the true parameter value as the number of data samples N approaches infinity. Specifically, for the estimated transfer function $G_{ji}(q, \hat{\theta})$, the parameter vector estimate $\hat{\theta}$ is consistent if:

$$\hat{\theta} \xrightarrow{\mathbb{P}} \theta^0 \quad \text{as} \quad N \to \infty, \tag{3.14}$$

where $\xrightarrow{\mathbb{P}}$ denotes convergence in probability. This ensures that:

$$G_{ji}(q, \hat{\theta}) \to G_{ji}(q, \theta^0) \quad \text{as} \quad N \to \infty. \tag{3.15}$$

In simpler terms, a consistent estimator guarantees that the estimated parameter vector $\hat{\theta}$ becomes arbitrarily close to the true value θ^0 as more data is collected. However, achieving consistency often depends on specific experimental conditions, such as sufficient excitation of the system or accurate noise modeling (DANKERS, 2014).

In practical situations, the number of data samples N is finite. This limitation can introduce bias into otherwise consistent estimators. Bias is defined as the difference between the expected value (average) of the estimator $\hat{\theta}$ and the true value θ^0 of the parameter vector:

$$\mathrm{b} = \mathrm{E}[\hat{\theta}] - \theta^0, \tag{3.16}$$

where $\mathrm{E}[\hat{\theta}]$ is the mathematical expectation. Note that despite θ being deterministic, $\hat{\theta}$ is a vector with stochastic variables, therefore the expected value is used because b is also stochastic.

3.3 Direct Method

The direct method is a straightforward approach for system identification that originated in the context of closed-loop systems. It leverages the predictor introduced in Equation (3.10) to estimate the transfer function G_{ji} by minimizing the cost function in Equation (3.12). This method requires an input signal w_i and an output signal w_j.

The method can be readily applied to dynamic networks as well. The key aspect lies in selecting the appropriate set of input signals for the predictor. While a simple choice might be to use w_i as the sole input, this can often lead to biased estimates. This is because other variables with direct connections to the output w_j can also influence its value, as noted in (FORSSELL; LJUNG, 1999; HOF *et al.*, 2012).

Under specific conditions, the direct method can provide a way to estimate the module transfer function $G_{ji}(q)$ (DANKERS *et al.*, 2012). These conditions are:

(i) **Uncorrelated Noise:**

there exists a noise model $H(q)$ such that the filtered version of the process noise, or $v_j(t) = H(q)e_j(t)$, is uncorrelated to the input signal[1];

(ii) **True Parameter Vector:**

there exists a parameter vector θ such that $G_{ji}(q, \theta) = G^0_{ji}(q)$;

[1] The main point of preposition (i) is that if the (filtered) noise $v_j(t)$ is uncorrelated to the input signal w_i then consistent estimates of $G_{ji}(q)$ are possible.

(iii) **Loop Delays:**

for the data generating system, every loop through w_j has a delay, meaning that every loop has at least one dynamic system in between nodes;

(iv) **Positive Definite Excitation:**

the spectral density of w_j, denoted as ϕ_j, is positive definite for $\omega \in [-\pi, \pi]$ [2].

It is important to highlight that the direct method in the original closed-loop framework ignores the existence of feedback, treating the data as though no feedback loops are present (SöDERSTRöM; STOICA, 1989). In the context of dynamic networks, Condition (iii) adapts this principle by restricting the loop delay requirement specifically to the output signal being identified.

Example 3.1-

Consider the dynamic network depicted in Figure 13. Suppose we want to estimate the transfer function G_{32} using the direct method. In this scenario, a possible choice would be to use w_2 as the input signal and w_3 as the output signal for identification.

Under the condition that a delay is present in the loop ($G_{32}G_{23}$) and by the use of an appropriate model set that includes accurate noise modeling, the transfer function G_{32} can be estimated.

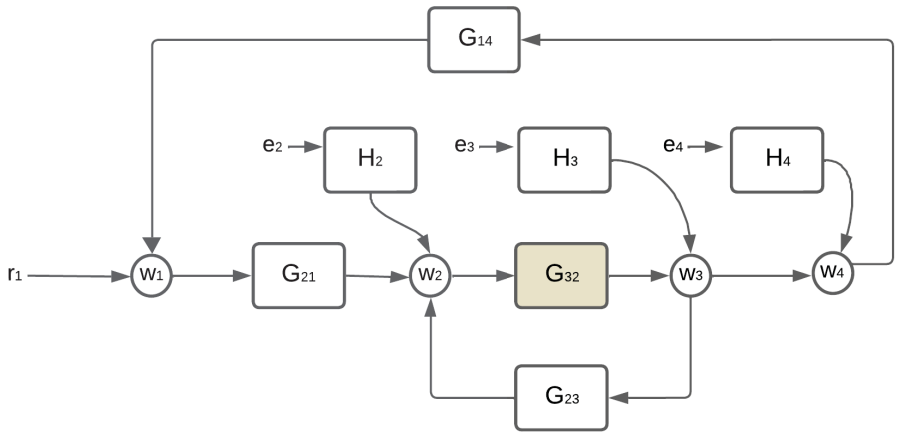

Figure 13 – Dynamic network of Example 3.1.

[2] The excitation condition (*iv*) is a rather generic condition for informative data (LJUNG, 1999).

3.4 Two-Stage Method

This section introduces an indirect/projection method capable of estimating a module transfer function within a dynamic network. The two-stage identification method, originally proposed in (Van Den Hof; SCHRAMA, 1993) and revisited in (FORSSELL; LJUNG, 1999), offers an advantage over the Direct Method by utilizing external variables to achieve consistent identification.

The method leverages classical Prediction Error Methods (PEM) and standard identification tools. The core idea lies in decorrelating the input signal and process noise through an orthogonal projection in the first stage. Then, in the second stage, the decorrelated input signal is used to estimate the module transfer function. This approach allows for estimation without explicitly modeling the noise dynamics.

The method we present in this subsection was adapted to the dynamic network identification case in Hof *et al.* (2013).

Consider estimating the module G_{ji} based on the following variables: w_i (input signal), w_j (output signal) and r_i (external signal). Note that r_i and w_i are quasi-stationary signals (LJUNG, 1999), such that the cross-correlation function

$$R_{w_i r_i}(\tau) = \overline{\mathbb{E}}\left[w_i(t) r_i(t-\tau)\right] \tag{3.17}$$

is zero for $\tau < 0$ and non-zero for $\tau \geq 0$. Given that

$$\overline{\mathbb{E}}\left[x(t)\right] = \lim_{N\to\infty} \frac{1}{N} \sum_{t=1}^{N} \mathbb{E}\left[x(t)\right], \tag{3.18}$$

where $\mathbb{E}$ is the expectation operator.

Stage 1:

An initial set of external variables $\{r_m\}$ is selected with $m \in \mathcal{T}_j$. Each of the external variables in $\{r_m\}$ is correlated with w_i.

We assume a proper MISO transfer function $F^0_{w_i r_m}$ exists such that

$$w_i(t) = \sum_{m \in \mathcal{T}j} F^0_{w_i r_m}(q) r_m(t) + z(t), \tag{3.19}$$

where $z(t)$ uncorrelated with all $\{r_m\}$ with $m \in \mathcal{T}_j$. This equation allows us to decompose the input signal $w_i(t)$ into two parts:

$$w_i(t) = w_i^{(r_m)}(t) + w_i^{(\perp r_m)}(t). \tag{3.20}$$

Here, $w_i^{(r_m)}$ represents the projection of w_i onto the space spanned by all external signals $\{r_m\}$, and $w_i^{\perp(r_m)} = z(t)$ captures the part uncorrelated with the selected external variables.

If the set $\{r_m\}$ is sufficiently informative[3], then $F^0_{w_i r_m}(q)$ can be consistently estimated based on the measured signals $\{r_m\}$ and w_i. This leads to an estimated transfer function $F^0_{w_i r_m}(q)$, which can then be used to calculate the projection:

$$\hat{w}_i^{(r_m)}(t) = \sum_{m \in \mathcal{T}_j} \hat{F}_{w_i r_m}(q) r_m(t) \tag{3.21}$$

where $\hat{F}_{w_i r_i}(q)$ is the estimated transfer function, providing an estimation of $w_i^{(r_m)}(t)$.

Stage 2:

In the second stage, the decorrelated input estimate $\hat{w}_i^{(r_i)}(t)$ is used as the input to the predictor model. However, the predictor's output needs a correction term (HOF *et al.*, 2013):

$$\tilde{w}_j(t) = w_j(t) - \sum_{i \in \mathcal{N}_j} G^0_{ji}(q) w_i(t) - r_j(t) \tag{3.22}$$

This corrected output, denoted by $\tilde{w}_j(t)$, removes the contributions from other internal signals and the external reference signal $r_j(t)$.

The predictor model is adjusted to incorporate the decorrelated input signal and the corrected output signal:

$$\hat{w}_j(t \mid t-1, \theta) = \sum_{i \in \mathcal{N}_j} H_j^{-1}(q,\theta) G_{ji}(q,\theta) \hat{w}_i^{(r_i)}(t) + \left(1 - H_j^{-1}(q,\theta)\right) \tilde{w}_j(t). \tag{3.23}$$

As a result, estimates of $G_{ji}(q)$ are obtained by minimizing the sum of prediction errors (3.11).

This section presents two algorithmic approaches for the two-stage identification method, originally described in (HOF *et al.*, 2013). The key concept to remember is that

[3] Sufficiently informative signals are inputs that excite all dynamics of the system, ensuring the identifiability of the model parameters.

limiting the predictor model to a Single-Input, Single-Output (SISO) format treats the influence of all other inputs affecting the output signal w_j as noise. This, in turn, can lead to increased variance in the estimated parameters.

Two-stage SISO algorithm

1. **Select External Variables:** Choose a set of external signals, denoted by $\{r_m\}$, that have a path to the input signal w_i within the network.
2. **Estimate Projected Input:** Determine the projected component, $w_i^{(r_i)}(t)$, of the input signal w_i using the estimated transfer function $\hat{w}_i^{(r_i)}(t)$ obtained from Eq. (3.21). his essentially isolates the contribution of the external variables to w_i.
3. **Construct Corrected Output:** Construct the corrected output signal $\tilde{w}_j$ as in (3.22). This step removes the influence of other internal inputs and the reference signal from the measured output.
4. **Estimate Transfer Function:** Finally, estimate the transfer function $G_{ji}(q)$ on the basis of a predictor model (3.23) with the prediction error (3.11).

The MISO (Multiple-Input, Single-Output) algorithm addresses the limitations of the SISO approach by incorporating the effects of other relevant internal variables. However, this comes at the cost of increased complexity due to the need for more models and parameter estimates. Here's a summary of the steps:

Two-stage MISO algorithm

1. **Select External Variables:** Similar to the SISO approach, select a set of external signals $\{r_m\}$, with paths to the input w_i.
2. **Identify Correlated Internal Variables:** Determine the set of internal variables, denoted by w_i, that exhibit correlation with any of the external variables r_i.
3. **Estimate Projected Input:** As in the SISO case, estimate the projected component $w_i^{(r_m)}(t)$ of the input signals using the estimated transfer functions $F_{w_i r_m}(q)$ as shown in (3.21).

4. **Construct Corrected Output:** Construct the corrected output signal $\tilde{w}_j$ using Eq. (3.22).

5. **Estimate Transfer Function:** Estimate the transfer function $G_{ji}(q)$ using a MISO predictor model (Eq. 3.23) that minimizes the prediction error (Eq. 3.11).

The choice between the SISO and MISO algorithms depends on the specific application and the desired balance between accuracy and complexity. The SISO approach offers a simpler implementation but may suffer from higher variance in parameter estimates, while the MISO approach can provide more accurate results at the expense of increased computational cost.

3.5 Case Studies

This section showcases the two identification methods (Direct and Two-Stage) through a practical example. We'll demonstrate how these methods can be used to estimate transfer functions within a closed-loop system.

The Coefficient of Variation

To compare the variances of parameter estimates from both methods, we'll use the Coefficient of Variation (CV). Let's consider an estimated parameter x, with a mean of $\tilde{x}$ and variance of δ_x. The CV is defined as:

$$CV(x) = \frac{\delta_x}{\tilde{x}} 100. \tag{3.24}$$

The CV encompasses the relative variability of a parameter compared to its average value. The same variance might have a different impact on the analysis of models depending on the mean value.

3.5.1 A simple feedback

We begin by validating the techniques discussed in previous chapters using a synthetic system designed to generate data. Since our focus is on closed-loop identification,

Table 1 – Results for estimation of simple feedback modules using the direct method.

Model Parameter	True Value	Estimate Mean	Estimate Variance
a_1	-0.7	-0.7001	4×10^{-4}
a_2	-0.5	-0.5002	3.6×10^{-3}
b_1	1.0	1.0006	1×10^{-4}
b_2	0.3	0.3010	7×10^{-4}

we'll use a simple feedback case to illustrate the methodology. This closed-loop system represents the simplest possible network example. This case study has been presented in Rodrigues *et al.* (2022).

The closed-loop system generating data is shown in Figure 14. The external signal r_1 is zero-mean, normally distributed white noise with a unit variance. Notice that an additional disturbance signal has been introduced at node 2. This disturbance is also zero-mean Gaussian distributed random noise, but with a variance of 0,1.

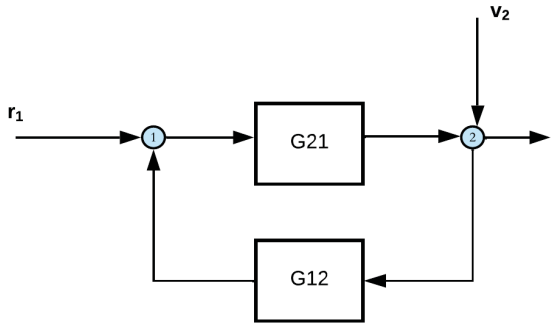

Figure 14 – A simple feedback.

The module transfer functions G_{21} and G_{12} are defined as follows

$$\begin{aligned} G_{21}^0(q) &= \frac{b_1}{q + a_1} = \frac{1}{q - 0.7}, \\ G_{12}^0(q) &= \frac{b_2}{q + a_2} = \frac{0.3}{q - 0.5}. \end{aligned} \tag{3.25}$$

To verify that the two modules in the feedback system can be consistently estimated using the direct method, we generated 500 samples for each experiment. We also performed 1000 identification experiments and computed the mean and variance of the estimated parameters. The results are summarized in Table 1.

Table 2 – Results for estimation of simple feedback modules using the two-stage method.

Model Parameter	True Value	Estimate Mean	Estimate Variance
a_1	-0.7	-0.6999	4×10^{-5}
a_2	-0.5	-0.5000	7×10^{-5}
b_1	1.0	1.0002	9×10^{-5}
b_2	0.3	0.2999	9×10^{-5}

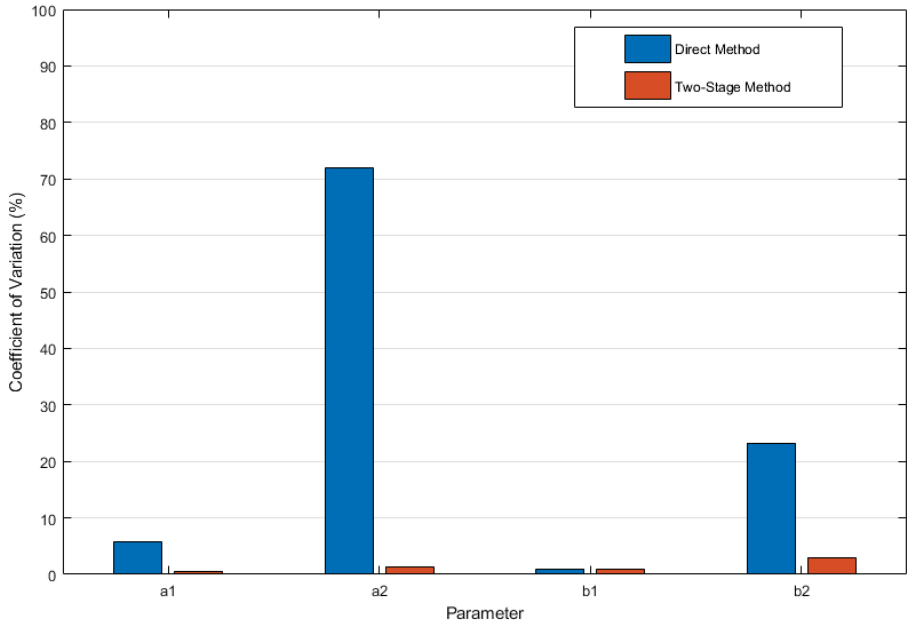

Figure 15 – Coefficient of Variation- a simple feedback.

For comparison, we used the two-stage method to estimate SISO models for the modules in the feedback system. We employed the same dataset used for the direct method. Table 2 shows the mean and variance of the estimates from the two-stage method. As you can see, there's a significant reduction in the variance of the estimates compared to the direct method.

Figure 15 illustrates the CV comparison for both methods. The decrease in variability of the parameters is confirmed by the CV analysis. It is worth noting that the parameters a_2 and b_2 presented a larger discrepancy between methods based on CV.

3.5.2 A dynamic network: example 1

This example explores a dynamic network scenario to illustrate the application of network identification methods herein presented. This case study has been presented in

Rodrigues *et al.* (2022).

Network Description: Consider the dynamic network represented in Figure 16. The excitation signal r_1 is white noise with mean 1 and variance 0.1 and the signals v_2, v_4 and v_5 are white noise with mean 0 and variance 0.1. The measured signals are illustrated in red in the image, they are: the nodal signals w_1, w_2, w_3, w_4 and w_5 and the excitation signal r_1.

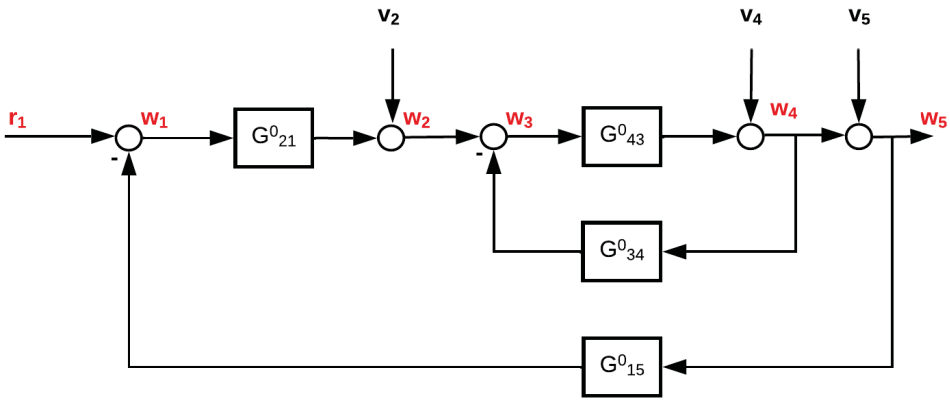

Figure 16 – A dynamic network with 5 nodes and 4 modules.

The module transfer functions are defined as follows

$$\begin{aligned} G_{21}^0(q) &= \frac{b_1}{q+a_1} = \frac{1}{q-0.7}, \\ G_{43}^0(q) &= \frac{b_2}{q+a_2} = \frac{0.5}{q-0.4}, \\ G_{34}^0(q) &= \frac{b_3}{q+a_3} = \frac{0.2}{q-0.9}, \\ G_{15}^0(q) &= \frac{b_4}{q+a_4} = \frac{0.3}{q-0.5}. \end{aligned} \tag{3.26}$$

Experiment Design: 500 samples are used per experiment, and 1000 identification experiments were generated. Table 3 shows the mean and variance results of the parameter estimation for the direct method and Table 4 shows the results for the two-stage method.

The comparison in relation to the CV of the estimates is shown in Figure 17. For all model parameters, variances were reduced, as illustrated in Tables 3 and 4.

In this case study, it is worth noting that the direct method presented a biased estimate for G_{34}^0. This was reduced with the two-stage method, but there is still a bias in

Table 3 – Results of the estimation of dynamic network modules using the direct method.

Parameter	True value	Mean	Variância
a_1	-0.7	-0.7046	1.2981×10^{-4}
a_2	-0.4	-0.3980	2.1834×10^{-4}
a_3	-0.9	-0.9014	6.3329×10^{-4}
a_4	-0.5	-0.4929	4.5200×10^{-4}
b_1	1.0	0.9997	3.1984×10^{-5}
b_2	0.5	0.4993	1.1392×10^{-4}
b_3	0.2	0.3022	3.0032×10^{-4}
b_4	0.3	0.2985	3.6816×10^{-3}

Table 4 – Results of the estimation of dynamic network modules using the two-stage method.

Parameter	True value	Mean	Variância
a_1	-0.7	-0.7001	7.5513×10^{-5}
a_2	-0.4	-0.3999	3.8815×10^{-5}
a_3	-0.9	-0.9007	1.6921×10^{-4}
a_4	-0.5	-0.4993	5.3856×10^{-5}
b_1	1.0	1.0005	1.9081×10^{-5}
b_2	0.5	0.5002	8.3981×10^{-5}
b_3	0.2	0.2101	3.1684×10^{-4}
b_4	0.3	0.3003	3.0344×10^{-4}

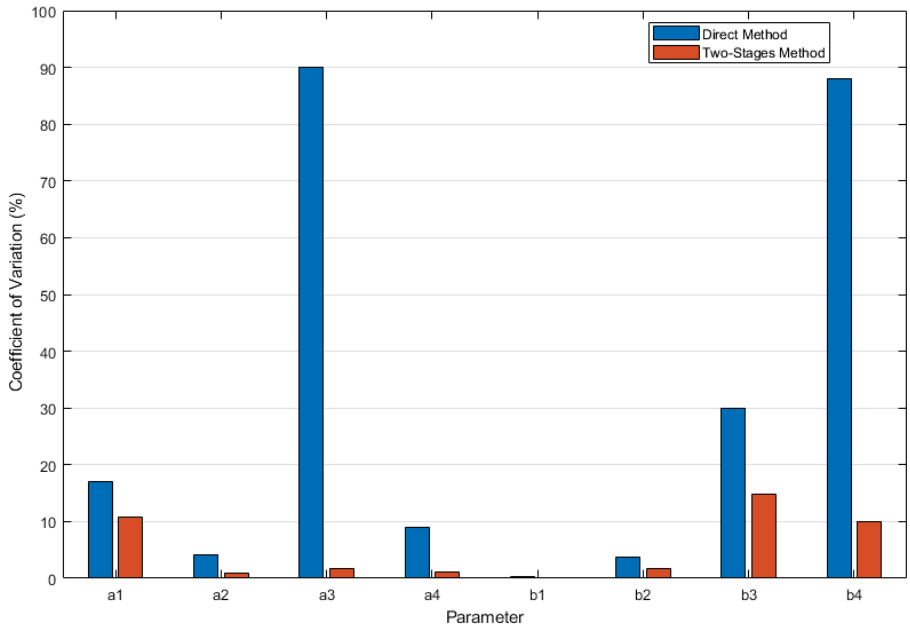

Figure 17 – Coefficient of Variation- a dynamic network example.

the b_3 parameter. The literature indicates that a possible solution to mitigate such effects is to add more excitation signals, for example, adding r_2 in the Figure 16 network can improve the estimates for the two-stage method.

3.5.3 A dynamic network: example 2

In this part, a complex network with 5 nodes and 6 modules is simulated in order to generate data to validate the methodology. The network topology is presented in Hof *et al.* (2013).

Consider the dynamic network depicted in Figure 18. The objective of this case study is to apply the direct method and the two-stage method to estimate SISO modules (green boxes) of the network. The MISO modules (yellow boxes) estimate will be discussed in the following sections of this chapter.

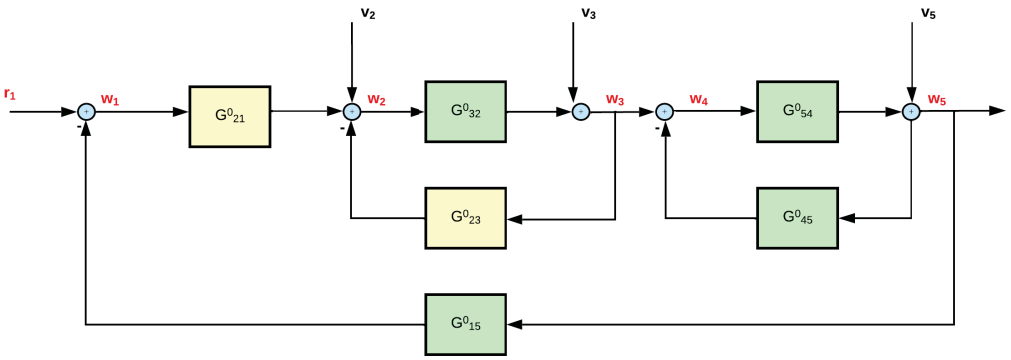

Figure 18 – A complex network example (HOF *et al.*, 2013).

Let us define the SISO module transfer functions parameters:

$$\begin{aligned} G_{32}^{0}(q) &= \frac{b_1}{q+a_1} = \frac{1}{q-0.7}, \\ G_{54}^{0}(q) &= \frac{b_2}{q+a_2} = \frac{0.1}{q-0.2}, \\ G_{45}^{0}(q) &= \frac{b_3}{q+a_3} = \frac{0.15}{q-0.2}, \\ G_{15}^{0}(q) &= \frac{b_4}{q+a_4} = \frac{0.4}{q-0.6}. \end{aligned} \tag{3.27}$$

Network Description: The external signal r_1 is a zero mean normally distributed white noise with variance equal to 1. Also the noise signals v_2, v_3 and v_4 are zero mean normally distributed white noise with variances 0.1. For the estimation procedure, the data generating system considers the node signals w_1, w_2, w_3, w_4 and w_5, and the external signal r_1.

Experiment Design: 500 samples are extracted and used in the identification experiment. 1000 experiments are simulated and the information we display are the mean of the estimates and the estimate variance as results of the procedure.

Initially, the direct method is used to estimate all SISO modules (G_{32}, G_{15}, G_{54}, G_{45}). Table 5 shows the results of the identification concerning each parameter.

Table 5 – Results for estimation of modules in a dynamic network using the direct method.

Model Parameter	True Value	Estimate Mean	Estimate Variance
a_1	-0.7	-0.6994	1.1636×10^{-4}
a_2	-0.2	-0.1986	2.2200×10^{-3}
a_3	-0.2	-0.1998	5.9580×10^{-5}
a_4	-0.6	-0.5956	1.5400×10^{-2}
b_1	1.0	0.9999	7.2607×10^{-5}
b_2	0.1	0.1002	7.1000×10^{-3}
b_3	0.15	0.1479	5.3000×10^{-3}
b_4	0.4	0.4000	5.4100×10^{-3}

Note that the estimation via the direct method is performed locally, as a consequence it neglects the rest of the network signals. The method uses only the input/output signals regarding the local module and discards the external signal r_1. This may incur into biased estimates of the modules parameters. However, Table 5 shows that consistent estimates are possible, provided that the input node signal is sufficiently exciting.

In what follows, results of the two-stage method applied to estimate the same SISO modules are given in Table 6.

Table 6 – Results for estimation of modules in a dynamic network using the two-stage method.

Model Parameter	True Value	Estimate Mean	Estimate Variance
a_1	-0.7	-0.6998	8.0382×10^{-5}
a_2	-0.2	-0.1900	8.6217×10^{-5}
a_3	-0.2	-0.2000	1.8431×10^{-31}
a_4	-0.6	-0.5934	5.5400×10^{-3}
b_1	1.0	0.9994	2.2568×10^{-5}
b_2	0.1	0.1007	3.2941×10^{-5}
b_3	0.15	0.1500	3.6280×10^{-34}
b_4	0.4	0.3968	5.0846×10^{-4}

On the other hand, the two-stage method relies on measured external signal r_1 and

a similar least squares criterion is applied. Consistent estimates are possible provided that the input signal is sufficiently exciting.

Figure 19 illustrates the CV comparison for both methods. The decrease in variability of the parameters are also stated by the CV analysis. When comparing the results using the direct and the two-stage methods, it is clear that there has been a decrease in the variance of the estimates.

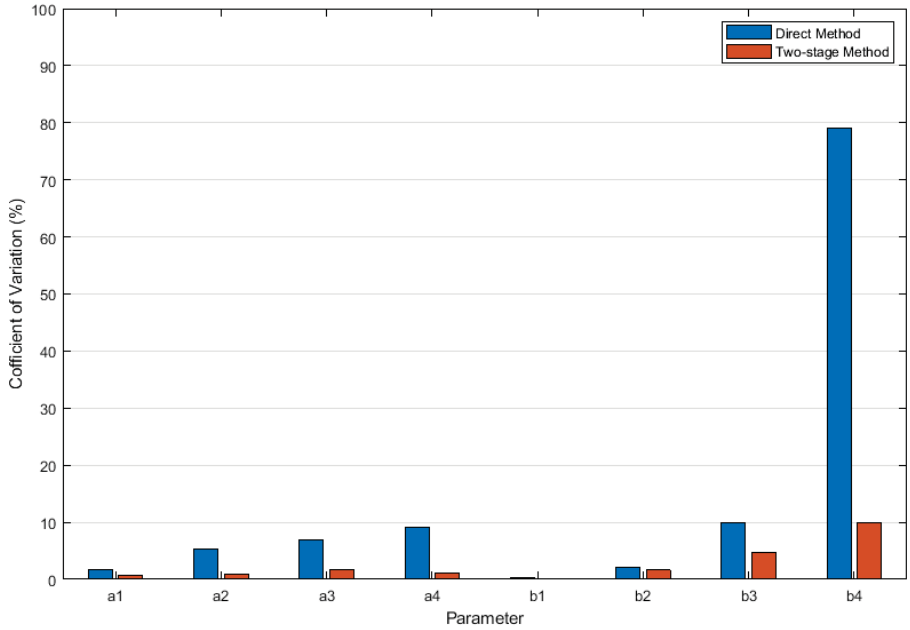

Figure 19 – Coefficient of Variation- a well-known dynamic network.

3.6 Closing Remarks

This chapter delved into the intricacies of network identification, exploring techniques to unveil the hidden dynamics governing interconnected systems. We navigated the complexities arising from feedback loops, noise, and the sheer number of interacting elements. By equipping the reader with established methods for network identification, this chapter paves the way for their effective analysis and control.

Summary of this chapter:

- Traditional system identification methods primarily target open-loop or closed-loop

systems. Network identification presents a distinct challenge due to the presence of multiple loops and the potential for algebraic loops.

- The Direct Method and Two-Stage Methods offer two key approaches for tackling network identification.
- The success of network identification hinges on the concept of identifiability. This refers to the ability to uniquely determine the network's dynamic properties from collected data.
- Prediction Error Methods offer a framework for evaluating model quality based on their ability to predict future system behavior.
- The Direct Method leverages a predictor model to estimate the transfer function, but may suffer from bias under certain conditions.
- The Two-Stage Method employs an external signal for decorrelating the input and process noise, enabling consistent identification without explicit noise modeling.

4 Dissipative and Passive Systems

In the realm of system identification, ensuring physical meaning and stability of identified models is paramount. This chapter is intended to be a first step in order to bring light to questions that were not well discussed in the dynamic network systems literature: how can we identify a passive module from a passive system embedded in a dynamic network? how the relationship between dissipativity and passivity impact on the system identification of dynamic networks? We delve into the fundamental concepts of dissipativity and passivity, which provide a framework for understanding a system's energy exchange and storage behavior.

4.1 Introduction

This chapter delves into the theoretical foundations of system dissipativity and passivity. These concepts are fundamental for understanding the energy exchange and storage behavior of dynamical systems. By incorporating passivity constraints into system identification, we can ensure that the resulting models are energetically consistent and stable.

Dissipativity is a fundamental property that characterizes a system's interaction with its environment in terms of energy. A dissipative system does not generate energy but rather exchanges it with its surroundings. Passivity is a specific form of dissipativity, requiring that the system's stored energy does not increase indefinitely.

For linear time-invariant (LTI) systems, dissipativity can be related to mathematical concepts such as positive-realness and the bounded-real lemma (WILLEMS, 1972; KOTTENSTETTE *et al.*, 2014; GAWTHROP; BEVAN, 2007). These concepts provide tools for analyzing and verifying the passivity of a given system model.

Incorporating dissipativity constraints into system identification ensures that the resulting models are energetically consistent and stable. This is particularly important for

systems where energy considerations are crucial, such as electrical networks, mechanical systems, and control systems. By enforcing passivity, we can avoid obtaining models that violate the laws of physics and may lead to unstable or non-realistic behavior. Additionally, incorporating passivity constraints can improve the accuracy of system identification algorithms.

Implications for System Identification

Enforcing passivity constraints in system identification can lead to several benefits:

- **Stable Time-Domain Simulations:** under any kind of interconnection and excitation, which is a closure property.
- **Improved Model Accuracy:** Passivity constraints can help to ensure that the identified model accurately reflects the physical behavior of the system.
- **Stability:** Passive models are inherently stable, which is crucial for many applications.

While incorporating passivity constraints into system identification offers significant advantages, it also presents challenges. One of the main challenges is ensuring that the identified model remains passive while maintaining accuracy. Developing efficient algorithms for passivity enforcement remains an active area of research.

4.2 Dissipativity in Dynamic Networks

The characterization of dissipative systems involves formulating energy balance inequalities, which require the definition of functions mapping energy exchange for a system (WILLEMS, 1972). Two key functions are usually considered: a supply function $\Phi(\cdot)$ and a storage or Lyapunov function $V(\cdot)$. The supply function represents energy inputs and outputs, while the storage function represents the energy stored within the system. The power balance equation in (4.1) reflects the fundamental principle of physical systems which cannot store more energy than it receives from external sources (GRIVET-TALOCIA;

GUSTAVSEN, 2016):

$$V(x(t+1)) - V(x(t)) \leq \Phi(u(t), y(t))^{1}. \tag{4.1}$$

The class of disipative LTI systems encompasses both passive and non-expansive (contractive) LTI systems and dissipativity generalizes the concepts of stability and causality (GRIVET-TALOCIA; GUSTAVSEN, 2016; TRIVERIO *et al.*, 2007). Intuitively, dissipative, passive and non-expansive systems entail these are formed out of energy absorbing elements.

Evaluating a given system for compliance with dissipative behavior is a process known as passivity assessment. Assuming an LTI system described by a SISO transfer function $G(z)$ with an input signal u and an output signal y, this property can be assessed by the existence of a symmetric and positive-definite ($\mathbf{P} = \mathbf{P}^T > 0$) such that:

$$\begin{bmatrix} \mathbf{A}^T\mathbf{P}\mathbf{A} - \mathbf{P} & \mathbf{A}^T\mathbf{P}\mathbf{b} - \mathbf{c}^T \\ (\mathbf{A}^T\mathbf{P}\mathbf{b} - \mathbf{c}^T)^T & \mathbf{b}^T\mathbf{P}\mathbf{b} - (d^T + d) \end{bmatrix} \preceq 0 \tag{4.2}$$

where the quadruple (**A**,**b**,**c**,d) is a state-space realization of $G(z)$.

$$x(t+1) = \mathbf{A}x(t) + \mathbf{b}u(t), \tag{4.3a}$$

$$y(t) = \mathbf{c}x(t) + du(t), \tag{4.3b}$$

where $x(t) \in \mathbb{R}^n$ is the state vector, $u(t) \in \mathbb{R}$ is the input vector, $y(t) \in \mathbb{R}$ is the output vector, and the system matrix $\mathbf{A} \in \mathbb{R}^{n \times n}$ and vectors $\mathbf{b} \in \mathbb{R}^n$, $\mathbf{c} \in \mathbb{R}^n$, and $d \in \mathbb{R}$.

As a sufficient and necessary condition, feasibility of the aforementioned LMI corresponds to a dissipativity certificate for the quadruple (**A**,**b**,**c**,d). Unfeasibility of this LMI indicates a non-dissipative system.

4.3 Passivity Assessment

Given the necessity to study the behavior of the energy in time-varying networks, the term "passive element" comes as a clear formulation of elements that absorb energy.

[1] Considering the sampling time as 1 for convenience.

Passivity is a primal property of several physical systems, it qualifies the energy balance of a system in an input-output sense. A system is said to be passive when it is not capable of generating energy by itself. In other words, it can consume energy only from the sources that excite it (GRIVET-TALOCIA; GUSTAVSEN, 2016; MAHANTA; YAMIN; ZADEHGOL, 2017).

Generally, passive equipment only absorbs active power given any voltage excitation, in any frequency range. In order to be physically consistent, electrically interconnected models must satisfy causality, stability and passivity properties. Typically, the model is subjected to a passivity enforcement stage with the intention to avoid further instability in simulations (KUO, 1968; TRIVERIO *et al.*, 2007).

The passivity property either can be assessed in data or in a model, and literature shows a few formulations with different levels of details (BRUNE, 1931; WILLEMS, 1972; RAISBECK, 1954). If one is interested in the passivity assessment in raw data, then the techniques based on a model structure can not be employed. In Subsection 4.3.1, the sweep method checks passivity over measured frequencies, and it is appropriate to verify the property in raw data. Should a state-space realization be available, the evaluation of the passivity can be made using Linear Matrix Inequalities (LMI), as discussed in Subsection 4.3.2. In fact, many other techniques are accessible and a broad discussion on passivity assessment methods based on technical literature is delivered in (IHLENFELD, 2015).

Given the importance of the passivity property in some complex systems, especially the ones composed by interconnected models, many authors direct their research to develop techniques to ensure passivity in models as further discussed in (GRIVET-TALOCIA; UBOLLI, 2008; GAO *et al.*, 2005; IHLENFELD, 2015). There are available a few passivity enforcement schemes for LTI lumped systems. Some are based on direct enforcement of Positive Real Lemma (PRL) constraints via optimization, some others via discrete frequency samples and there is also a class based on Hamiltonian eigenvalue perturbation. All of them are intended to ensure the model's dynamic to be strictly passive. This thesis is focused on passivity enforcement via PRL using a Linear Matrix Inequality (LMI).

4.3.1 Frequency sweeping assessment

In Triverio *et al.* (2007), a frequency sweep assessment is described for passive LTI systems with $\mathbf{G}(z)$, a transfer function matrix, it is possible to define

$$\mathbf{G}(z) + \mathbf{G}^H(z) \succeq \mathbf{0} \Leftrightarrow \lambda_{\min}(\mathbf{G}(z)) \geq 0, \quad \forall z,\ s.t.\ z = e^{j\theta} \ \text{ and } \theta = [0, \pi] \tag{4.4}$$

where $(\cdot)^H$ denotes an Hermitian matrix. $\mathbf{G}$(z) is positive real if the following conditions are satisfied.

1. $\mathbf{G}$(z) is defined and analytic;
2. $\mathbf{G}(z^*) = \mathbf{G}^*(z)$, where $(\cdot)^*$ represents the complex conjugate.
3. $\mathbf{\Phi}(z) = \mathbf{G}(z) + \mathbf{G^H}(z) \succeq \mathbf{0}$.

These three conditions are equivalent to a "positive resistivity". As noted in (TRIVERIO *et al.*, 2007), condition (1) implies BIBO (Bounded-Input Bounded-Output) stability, while condition (2) ensures that the system impulse response to be real. Condition (3) is a generalization for the fact that any passive device has a positive real part.

As a result, a simple assessment for passivity, widely used in literature is:

$$\mathbf{\Phi}(z) \succeq 0 \quad for\ \ all\ \ z, \tag{4.5}$$

Should the inequality in (4.4) hold, passivity requires the matrix $\mathfrak{G}(z) = Re[\mathbf{G}(z)]$ to be positive real. If all eigenvalues of $\mathfrak{G}$ are strictly positive, so is the smallest one. Consequently, the passivity criteria can take the even simpler form in (4.6).

$$eig_{min}(\mathfrak{G}(z)) > 0. \tag{4.6}$$

Passivity is assessed only at sampled frequencies, which means violations may occur between these sampled points. Therefore, even if passivity is violated at a specific sampled frequency z_k it does not necessarily imply that the assessment will indicate a violation at a neighboring frequency ω_{k+k_1}.

4.3.2 LMI based assessment

The concept of passivity, fundamentally tied to the energy exchange properties of a system, can be rigorously analyzed using Linear Matrix Inequalities (LMIs). By formulating the passivity conditions as LMIs, we can leverage the power of convex optimization to efficiently assess and enforce passivity.

The idea of the passivity assessment based on LMI arose from control systems theory (KALMAN, 1964; KUO, 1966; KUO, 1968) where the authors state the relation between positive realness of a transfer matrix and feasibility of a state-space realization.

The foundation of LMI-based passivity assessment lies in the energy balance of a system. Recalling the balance expressed in the following equation:

$$V(x(t+1)) - V(x(t)) \leq \Phi(u(t), y(t))$$

where:

- $V(\mathbf{x}(t))$ is a storage function (often quadratic), representing the stored energy in the system at time t.
- $\Phi(\mathbf{u}(t), \mathbf{y}(t))$ is a supply function, representing the supplied power to the system.

For linear time-invariant (LTI) systems, these functions can be expressed in quadratic forms, leading to conditions that can be cast as LMIs.

$$\Phi(\mathbf{u}, \mathbf{y}) = \mathbf{y}^T\mathbf{L}\mathbf{y} + \mathbf{u}^T\mathbf{R}\mathbf{u} + \mathbf{y}^T\mathbf{W}\mathbf{u} = \begin{bmatrix} \mathbf{y}(t) \\ \mathbf{u}(t) \end{bmatrix}^T \begin{bmatrix} \mathbf{L} & \mathbf{W} \\ \mathbf{W}^T & \mathbf{R} \end{bmatrix} \begin{bmatrix} \mathbf{y}(t) \\ \mathbf{u}(t) \end{bmatrix} \tag{4.7}$$

The PRL establishes a direct link between the positive-realness of the transfer function and the feasibility of certain LMIs. The following matrices are defined ($\mathbf{L} = \mathbf{0}, \mathbf{R} = \mathbf{0}, \mathbf{W} = \mathbf{I}$)

$$\Phi(\mathbf{u}, \mathbf{y}) = \mathbf{y}^T\mathbf{0}\mathbf{y} + \mathbf{u}^T\mathbf{0}\mathbf{u} + \mathbf{y}^T\mathbf{I}\mathbf{u} = \mathbf{y}^T\mathbf{u} = \begin{bmatrix} \mathbf{y}(t) \\ \mathbf{u}(t) \end{bmatrix}^T \begin{bmatrix} \mathbf{0} & \mathbf{I} \\ \mathbf{I} & \mathbf{0} \end{bmatrix} \begin{bmatrix} \mathbf{y}(t) \\ \mathbf{u}(t) \end{bmatrix} \tag{4.8}$$

Considering a quadratic form for the storage/Lyapunov function, that is:

$$V(x) = x^T P x$$

all functions involved in modeling the system's energy balance or exchange are quadratic forms. Note that the supply function depends on the input-output pair, while the storage function depends on the system's state. It's crucial to ensure that the definitions of input, output, and state variables are consistent with the units of the quantities they represent.

Given these specific choices, we can derive convenient matrix expressions to verify the energy balance. Invoking the condition of a dissipative system, we can state:

$$x(t+1)V(x(t)) \leq \Phi(y(t), u(t)) \tag{4.9}$$

Both the left and right sides of the inequality are scalar expressions with vector arguments and matrix parameters (under the aforementioned assumptions). Furthermore, these scalar expressions aim to capture the concept of energy/power balance. In this sense, it's clear that both expressions represent power: $x(t+1)V(x(t))$ as the rate of change of stored energy in the states, and $\Phi(y(t), u(t))$ as the net power injection into the system.

$$\begin{aligned}
V(\mathbf{x}(t+1), \mathbf{u}(t+1)) - V(\mathbf{x}(t), \mathbf{u}(t)) &\leq \Phi(\mathbf{y}(t), \mathbf{u}(t)) \\
\frac{dV}{d\mathbf{x}}\left(\mathbf{x}^T\mathbf{P}\mathbf{x}\right) &\leq \Phi(\mathbf{y}(t), \mathbf{u}(t)) \\
(\mathbf{A}\mathbf{x} + \mathbf{B}\mathbf{u})^T\mathbf{P}\mathbf{x} + \mathbf{x}^T\mathbf{P}(\mathbf{A}\mathbf{x} + \mathbf{B}\mathbf{u}) &\leq \Phi(\mathbf{y}(t), \mathbf{u}(t)) \\
\begin{bmatrix} \mathbf{x}(t) \\ \mathbf{u}(t) \end{bmatrix}^T \begin{bmatrix} \mathbf{A}^T\mathbf{P} + \mathbf{P}\mathbf{A} & \mathbf{P}\mathbf{B} \\ \mathbf{B}^T\mathbf{P} & 0 \end{bmatrix} \begin{bmatrix} \mathbf{x}(t) \\ \mathbf{u}(t) \end{bmatrix} &\leq \Phi(\mathbf{y}(t), \mathbf{u}(t))
\end{aligned} \tag{4.10}$$

In the previous step, we developed the balance equation based on the premise that the system dynamics are governed by a state-space representation (LTI). Since in the state-space representation, the output equation is a function of both the states and inputs, we can eliminate the output vector.

$$
\begin{aligned}
&V(\mathbf{x}(t+1),\mathbf{u}(t+1)) - V(\mathbf{x}(t),\mathbf{u}(t)) \leq \Phi(\mathbf{y}(t),\mathbf{u}(t)) \\
&V(\mathbf{x}(t+1),\mathbf{u}(t+1)) - V(\mathbf{x}(t),\mathbf{u}(t)) \leq \begin{bmatrix}\mathbf{y}(t)\\ \mathbf{u}(t)\end{bmatrix}^T \begin{bmatrix}\mathbf{L} & \mathbf{W}\\ \mathbf{W}^T & \mathbf{R}\end{bmatrix} \begin{bmatrix}\mathbf{y}(t)\\ \mathbf{u}(t)\end{bmatrix} \\
&V(\mathbf{x}(t+1),\mathbf{u}(t+1)) - V(\mathbf{x}(t),\mathbf{u}(t)) \leq \begin{bmatrix}\mathbf{C}\mathbf{x}(t)+\mathbf{D}\mathbf{u}(t)\\ \mathbf{u}(t)\end{bmatrix}^T \begin{bmatrix}\mathbf{L} & \mathbf{W}\\ \mathbf{W}^T & \mathbf{R}\end{bmatrix} \begin{bmatrix}\mathbf{C}\mathbf{x}(t)+\mathbf{D}\mathbf{u}(t)\\ \mathbf{u}(t)\end{bmatrix} \\
&V(\mathbf{x}(t+1),\mathbf{u}(t+1)) - V(\mathbf{x}(t),\mathbf{u}(t)) \leq \begin{bmatrix}\mathbf{x}(t)\\ \mathbf{u}(t)\end{bmatrix}^T \begin{bmatrix}\mathbf{C}^T\mathbf{L}\mathbf{C} & \mathbf{C}^T\mathbf{L}\mathbf{D}+\mathbf{C}^T\mathbf{W}\\ \mathbf{D}^T\mathbf{L}\mathbf{C}+\mathbf{W}^T\mathbf{C} & \mathbf{D}^T\mathbf{L}\mathbf{D}+\mathbf{D}^T\mathbf{W}+\mathbf{W}^T\mathbf{D}+\mathbf{R}\end{bmatrix} \\
&\qquad\qquad \begin{bmatrix}\mathbf{x}(t)\\ \mathbf{u}(t)\end{bmatrix} \\
&V(\mathbf{x}(t+1),\mathbf{u}(t+1)) - V(\mathbf{x}(t),\mathbf{u}(t)) \leq \begin{bmatrix}\mathbf{x}(t)\\ \mathbf{u}(t)\end{bmatrix}^T \begin{bmatrix}\tilde{\mathbf{L}} & \tilde{\mathbf{W}}\\ \tilde{\mathbf{W}}^T & \tilde{\mathbf{R}}\end{bmatrix} \begin{bmatrix}\mathbf{x}(t)\\ \mathbf{u}(t)\end{bmatrix} \\
&V(\mathbf{x}(t+1),\mathbf{u}(t+1)) - V(\mathbf{x}(t),\mathbf{u}(t)) \leq \tilde{\Phi}(\mathbf{x}(t),\mathbf{u}(t))
\end{aligned}
\tag{4.11}
$$

Depending on the choice of supply function (Positive Real or Bounded Real) and the type of dynamics involved (Continuous Time or Discrete Time), the energy balance can be expressed in different ways. In this thesis, we are particularly interested in analyzing and enforcing the passivity of Discrete-Time Positive Real systems, therefore we achieve the following equation.

$$
\begin{bmatrix}\mathbf{A}^T\mathbf{P}\mathbf{A}-\mathbf{P} & \mathbf{A}^T\mathbf{P}\mathbf{b}-\mathbf{c}^T\\ (\mathbf{A}^T\mathbf{P}\mathbf{b}-\mathbf{c}^T)^T & \mathbf{b}^T\mathbf{P}\mathbf{b}-(d^T+d)\end{bmatrix} \preceq 0 \tag{4.12}
$$

4.4 Passivity Enforcement

Passivity, a fundamental property reflecting a system's energy exchange behavior, is crucial for ensuring the stability and physical realizability of identified models. Various techniques have been proposed to enforce passivity, often involving post-processing steps to modify non-passive models.

In this thesis, we present a different approach to enforce passivity to local modules in dynamic network. We do not treat passivity as a post-processing but, rather, we incorporate the LMI in a convex optimization problem by treating certain system matrices as free parameters for the parametric estimator in a way to iteratively refine the model to ensure it adheres to the desired properties. This method leverages the power of convex optimization to efficiently solve the optimization problem.

Key Considerations:

- **Model Structure:** The choice of model structure (e.g., state-space, transfer function) can influence the effectiveness of passivity enforcement techniques.
- **Optimization Algorithm:** The selection of a suitable convex optimization algorithm is crucial for efficient and accurate passivity enforcement.
- **Trade-offs:** There may be trade-offs between the accuracy of the identified model and the degree of passivity enforcement.

Frequency-domain methods, such as Vector Fitting (VF), have also been widely used for passivity enforcement out of the dynamic network context. These techniques involve fitting a rational function to the measured frequency response data while ensuring that the resulting model satisfies passivity constraints, usually as a post-processing strategy. Subspace-based methods offer an alternative approach to passivity enforcement (RODRIGUES; IHLENFELD; OLIVEIRA, 2021). By incorporating passivity constraints directly into the subspace identification algorithm, we can obtain a passive model without the need for post-processing steps. This can lead to more efficient and accurate results.

4.5 Closing Remarks

This chapter has delved into the theoretical foundations of system dissipativity and passivity. We have explored the concepts of energy exchange, storage, and their implications for system identification. By understanding the relationships between dissipativity,

positive-realness, and bounded-realness, we can ensure that identified models are physically meaningful and stable.

Dissipativity characterizes a system's energy exchange behavior, while passivity is a specific form of dissipativity that ensures the system's stored energy does not increase indefinitely.

Positive-realness and bounded-realness are properties closely related to dissipativity, assessed using mathematical tools like the positive-real lemma and bounded-real lemma.

Incorporating passivity constraints into system identification ensures physically meaningful and stable models. Various techniques, including convex optimization, frequency-domain methods, and subspace-based approaches, can enforce passivity.

5 Frequency Domain Passive System Identification

This chapter explores the identification of passive systems in the frequency domain. One consequence of system passivity is that it guarantees system stability. By leveraging a two-stage approach, the methodology first estimates the Frequency Response Function (FRF) using a non-parametric estimator and then refines the model using a parametric identification technique with built-in passivity enforcement. The contribution introduced in this chapter is the Passive Vector Fitting (PVF) method, which guarantees passivity throughout the estimation process, unlike traditional approaches that impose it as a post-processing step. These techniques provide a framework for modeling passive modules within dynamic networks.

5.1 Introduction

This chapter presents a frequency-domain approach to identify passive local models in dynamic networks by incorporating the Positive-Real Lemma (PRL) constraints into the parametric identification stage. The methodology and some of the case studies presented in this chapter were published in (RODRIGUES *et al.*, 2024).

Existing literature applies a semi-parametric approach to estimate local modules in the frequency domain (RAMASWAMY *et al.*, 2022). In this thesis, this method was the starting point to find a way to estimate passive models for passive modules in dynamic network using a frequency-domain approach.

The methodology comprises two main stages: (i) a time-domain non-parametric estimation of the Frequency Response Function (FRF) for the local module(s) of interest using the indirect Local Polynomial Method (iLPM); and (ii) a parametric identification that estimates a transfer function for the previously estimated FRF through an extension of the frequency-domain Vector Fitting (VF) method, which directly estimates a passive

model.

The second stage introduces a novel approach, referred to as *Passive Vector Fitting (PVF)*, which ensures passivity during the Sanathanan-Koerner iterations by constructing a sequence of passive models. Unlike conventional VF, which typically enforces passivity only through post-processing of a potentially non-passive model, PVF guarantees that the final estimated model is inherently passive. This advance brings a passivity assurance into the local module identification framework, addressing a challenge in dynamic network identification.

5.1.1 A Brief Background and Notation

The problem of identifying passive systems in the frequency domain has received significant attention due to its relevance in ensuring stability within interconnected systems. Passivity, a property ensuring that the system does not produce energy, is typically enforced by conditions derived from the Positive-Real Lemma (PRL). The PRL relates a system's transfer function to a positive-real criterion in the frequency domain, which is key to ensuring that the estimated models comply with energy conservation laws. The PVF method leverages this framework by enforcing passivity conditions directly in the estimation process, thereby guaranteeing the model's passivity.

The proposed two-stage approach achieves computational efficiency by decoupling local module identification from the complexity of the entire network. This allows the method's complexity to depend primarily on the local environment—specifically, the number of adjacent modules connected to the target—rather than on the network's overall size or intricacy.

5.1.2 Overview of the Approach

The first stage begins with an indirect estimation of the correlation between excitation signals and node responses (HOF *et al.*, 2013), reconstructing the node signals based on the available excitation data. The goal is to isolate the frequency response of the local module, minimizing external influence from adjacent modules. This stage utilizes

the Local Polynomial Method (LPM), a non-parametric estimator that effectively reduces spectral leakage errors that often occur when applying Fourier transform techniques to non-periodic data (DANKERS; HOF, 2015). The LPM is particularly advantageous for processing finite data sets, as it can accurately estimate the FRF even for signals that are not periodic.

The combination of signal reconstruction and LPM constitutes the *indirect Local Polynomial Method (iLPM)*, which has been shown to yield robust FRF estimates for specific modules in dynamic networks (RAMASWAMY *et al.*, 2022). By avoiding the need for a predefined model order in this initial stage, the iLPM approach allows for flexible model selection in subsequent parametric estimation.

The second stage utilizes the estimated FRF as input for parametric identification, wherein the PVF method is applied. Unlike standard VF, which requires post processing of a non-passive model to enforce passivity, PVF ensures that passivity is preserved throughout the Sanathanan-Koerner iterative process. This iterative approach constructs a passive model at each step, resulting in a final model that is inherently passive. The PVF algorithm, therefore, produces a parametric model for the local module represented by the quadruple $(\mathbf{A}, \mathbf{b}, \mathbf{c}, c_0)$, tailored for the target module G^0_{ji} based on the network data.

The benefit of this approach is particularly notable for its computational efficiency. By focusing on a local module within a dynamic network, the complexity of the PVF method remains bounded by the local module's neighborhood, rather than by the overall network size. Thus, this method addresses a key challenge in network identification: achieving accurate, passive model estimates without requiring global network information.

This chapter proceeds as follows: Section 5.2 details the non-parametric estimation process; Section 5.3 describes the parametric identification method, including the implementation of PVF; Section 5.4 presents case studies to validate the approach; and Section 5.5 provides concluding remarks and insights on future directions.

5.2 Non-parametric estimator

In this section, we introduce the Local Polynomial Method (LPM), a non-parametric approach for estimating the Frequency Response Function (FRF) of a linear system. Non-parametric estimation is particularly valuable for system identification when it is necessary to obtain a high-quality FRF without assuming a parametric model structure. The LPM, known for its effectiveness in reducing leakage errors associated with non-periodic input signals, has proven advantageous over traditional Fourier Transform-based methods (CSURCSIA, 2022; CSURCSIA; PEETERS; SCHOUKENS, 2020).

5.2.1 Overview of the Local Polynomial Method

The LPM estimates a FRF by utilizing a polynomial approximation within a narrow frequency band around each frequency of interest. This approach effectively mitigates spectral leakage- a common problem when analyzing finite-length data or non-periodic signals by treating the FRF and the transient response as smooth functions of frequency. The LPM, therefore, delivers more accurate frequency-domain estimates by fitting a polynomial locally to each frequency band, reducing both variance and bias in the estimation (CSURCSIA, 2022).

Consider a linear Single-Input Single-Output (SISO) discrete-time system $G_0(q)$ with input $u(t)$ and output $y(t)$, where the system is subject to additive noise $v(t)$ modeled as a quasistationary process. The system can be described by:

$$y(t) = G_0(q)u(t) + H_0(q)e(t), \tag{5.1}$$

where $G_0(q)$ is the transfer function of the system, $H_0(q)$ represents the noise model, and $e(t)$ is zero-mean white noise with variance σ_e^2 (CSURCSIA, 2022).

5.2.2 Frequency Domain Representation

In practice, we deal with a finite record of data, leading to transient terms in the frequency domain representation of the output. Taking the Discrete Fourier Transform

(DFT) of the input and output signals yields the following exact frequency-domain relation:

$$Y(k) = G_0(\Omega_k)U(k) + T_G(\Omega_k) + H_0(\Omega_k)E(k) + T_H(\Omega_k), \tag{5.2}$$

where $Y(k)$, $U(k)$, and $E(k)$ denote the DFTs of $y(t)$, $u(t)$, and $e(t)$, respectively, at frequency $\Omega_k = e^{j2\pi k/N}$, with $T_G(\Omega_k)$ and $T_H(\Omega_k)$ representing the transient terms associated with the system and noise models, respectively (CSURCSIA, 2022). These transients are rational functions of the frequency variable and decay as the data record length increases, but in finite records, they can introduce bias and error in FRF estimates.

5.2.3 Local Polynomial Approximation

The core idea of the LPM is to leverage the smoothness of both G_0 and the transient terms as functions of frequency. Within a narrow frequency window centered on Ω_k, the FRF and transient terms are approximated by a Taylor series expansion. For frequencies Ω_{k+r} in a neighborhood of Ω_k, the FRF $G_0(\Omega_k)$ can be locally represented as:

$$G_{k+r} = G_k + \sum_{s=1}^{R} g_s(k) r^s + O\left(\left(\frac{r}{N}\right)^{R+1}\right), \tag{5.3}$$

where $g_s(k)$ are the coefficients of the polynomial expansion, r represents the frequency offset, and R is the polynomial order. Similarly, the transient terms can be expanded as:

$$T_{k+r} = T_k + \sum_{s=1}^{R} t_s(k) r^s + O\left(\left(\frac{r}{N}\right)^{R+1}\right). \tag{5.4}$$

The estimation task thus reduces to solving for the coefficients

$$\theta_k = [G_k, g_1(k), \ldots, g_R(k); T_k, t_1(k), \ldots, t_R(k)]^T,$$

which represent both the FRF and transient terms in a local polynomial form (CSURCSIA, 2022).

5.2.4 Least Squares Estimation

To estimate θ_k for each frequency Ω_k, we set up a least squares problem using data in a window centered on Ω_k. Define the observed frequency-domain data vector $\overline{Y}_{k,n}$ and

input vector $\overline{U}_{k,n}$ as:

$$\overline{Y}_{k,n} = [Y_{k-n}, Y_{k-n+1}, \ldots, Y_k, \ldots, Y_{k+n}]^T, \tag{5.5}$$

$$\overline{U}_{k,n} = [U_{k-n}, U_{k-n+1}, \ldots, U_k, \ldots, U_{k+n}]^T. \tag{5.6}$$

The local polynomial estimate $\hat{\theta}_k$ is obtained by solving:

$$\hat{\theta}_k = \arg\min_{\theta_k} \left\| \overline{Y}_{k,n} - K_{k,n}(R, \overline{U}_{k,n})\theta_k \right\|^2, \tag{5.7}$$

where $K_{k,n}(R, \overline{U}_{k,n})$ is a matrix constructed based on the polynomial structure and input data, incorporating the information on r for all frequencies in the window. This least squares formulation allows the estimation of G_k with reduced leakage errors by fitting the polynomial coefficients across the frequency window (CSURCSIA; PEETERS; SCHOUKENS, 2020).

5.2.5 Practical Considerations and Performance

Choosing an appropriate polynomial order R and window width n is crucial for achieving a good balance between bias and variance. A higher-order polynomial reduces leakage errors by fitting the local FRF and transient more accurately but may increase interpolation error if the window width n is too small. Typically, second-order polynomials (i.e., $R = 2$) provide a reasonable balance between leakage reduction and computational efficiency (CSURCSIA; PEETERS; SCHOUKENS, 2020).

Furthermore, the LPM performs well under noisy conditions as it averages noise over multiple spectral lines within the frequency window. By incorporating additional constraints between neighboring frequency intervals, enhanced versions of the LPM, such as the Constrained LPM (LPMC), further reduce estimation variance by enforcing smoothness across neighboring estimates (CSURCSIA; PEETERS; SCHOUKENS, 2020).

In summary, the LPM provides an effective non-parametric approach to FRF estimation by locally approximating the system's frequency response with polynomial models, thereby reducing leakage errors and offering robustness against noise. This approach is particularly well-suited for dynamic network applications where accurate non-parametric estimates are needed to guide subsequent parametric modeling.

5.2.6 Indirect LPM (iLPM)

We employ an indirect implementation of LPM. Traditionally, identifying a FRF for a given system via LPM involves selecting a set of signals as predictor inputs and then estimate a MISO model (CSURCSIA, 2022). Conversely, the indirect approach hereby advocated entails the following steps (HOF *et al.*, 2013):

1. Defining a MISO setup with w_j as output and w_k as inputs, $w_k \in \mathcal{N}_j$;
2. Defining for each w_k a set of external excitation signals $\{r_m\}_k$, $m \in \mathcal{R}$ with a path from r_m to w_k;
3. Estimating for each w_k the transfer functions between $\{r_m\}_k$ and the node w_k.

   It consists of a decomposition of node signals w_k as $w_k = w_k^{\{r_m\}_k} + w_k^{\perp\{r_m\}_k}$ with $w_k^{\perp\{r_m\}_k}$ and r_m uncorrelated so that the component of w_k correlated with r_m be denoted $w_k^{\{r_m\}_k}$.
4. Reconstructing the MISO setup of step 1. only with all correlated components $w_k^{\{r_m\}_k}$ to be used for the target module's FRF estimation.

In order to estimate a FRF using the iLPM, all components $w_k^{\{r_m\}_k}$ are first pre-processed by dividing it into overlapping segments of equal length. During this procedure, a narrow sliding processing window is employed. Within each segment, a polynomial of degree M is fitted to each $w_k^{\{r_m\}_k}$ using a least square approach. The polynomial coefficients are then used to compute the FRF of the MISO model from step 4. which includes the target module G_{ji}, using a Fast Fourier Transform (FFT).

The FRF of the target module obtained via the iLPM algorithm is denoted as $\widetilde{G}_{ji}(\omega_\kappa)$, where $\kappa = 0, \cdots, N_f$, N_f is the number of frequency samples.

5.3 Passive Vector Fitting

The objective is to compute a passive parametric model $\breve{G}_{ji}(\omega)$ so that $\breve{G}_{ji}(\omega) \approx \widetilde{G}_{ji}(\omega)$ for all frequencies $\omega = \omega_\kappa$ in a least square sense. To achieve this objective,

we implement modifications to the Vector Fitting (VF) algorithm to include passivity conditions within the estimation process.

VF implementations are numerically robust implementations of the Sanathanan-Koerner/Steiglitz-McBride iterations (SANATHANAN; KOERNER, 1963; STEIGLITZ; MCBRIDE, 1965) in which the minimization of the non-linear objective function is achieved iteratively via a sequence of linear least square problems. The modification includes passivity conditions as constraints in each iteration and is discussed as follows.

The target passive model $\breve{G}_{ji}(\omega)$ has the following structure:

$$\breve{G}_{ji}(z) = \frac{N(z)}{D(z)} = \frac{c_0 + \sum_{\alpha=1}^{n} \frac{c_\alpha}{z-p_\alpha}}{1 + \sum_{\alpha=1}^{n} \frac{\tilde{c}_\alpha}{z-p_\alpha}} \tag{5.8}$$

where $\breve{G}_{ji}(z)$ is an n-th order transfer function parameterized by a set of poles $\{p_\alpha\}_{\alpha=1}^{n}$, $\{c_\alpha\}_{\alpha=0}^{n}$ and $\{\tilde{c}_\alpha\}_{\alpha=1}^{n}$. Also, we henceforth denote θ and $\tilde{\theta}$ the set of c_α and $\tilde{c}_\alpha$, respectively.

$\breve{G}_{ji}(\omega)$ admit a minimal state-space equivalence as in (4.3), namely $\{\mathbf{A}, \mathbf{b}, \mathbf{c}, d\}$ such that:

$$N(z) = \Big((z\mathbf{I}_\mathrm{n} - \mathbf{A})^{-1}\mathbf{b} \quad 1\Big)\theta$$
$$D(z) = 1 + \Big((z\mathbf{I}_\mathrm{n} - \mathbf{A})^{-1}\mathbf{b}\Big)\tilde{\theta}$$

The algorithm follows the subsequent steps.

5.3.0.1 Step 1

The algorithm initiates assigning an initial set of poles $\{p_\alpha\}_{\alpha=0}^{n}$. These poles are typically defined as lightly damped poles with imaginary parts logarithmically spaced along the frequency axis.

5.3.0.2 Step 2

Within each iteration, we seek to minimize the linearized version of the weighted least square error (SANATHANAN; KOERNER, 1963) defined as following:

$$\mathrm{J}(\theta, \tilde{\theta}) = \sum_{\kappa=1}^{N_f} W(z_\kappa)^2 \left| N(z_\kappa) - D(z_\kappa)\widetilde{G}_{ji}(z_\kappa) \right|^2, \tag{5.9}$$

where $W(z_\kappa)$ is a weighting function, defined as in (SCHUMACHER; OLIVEIRA, 2019), to consider measurements with resonance peaks and exhibit significant variations in magnitude. Then, the optimization problem which should be solved at each iteration is:

$$\begin{aligned} \min_{\theta,\tilde{\theta},\mathbf{P}} \quad & \mathrm{J}(\theta,\tilde{\theta}) \\ \text{s.t.} \quad & \begin{bmatrix} \mathbf{A}^T\mathbf{P}\mathbf{A}-\mathbf{P} & \mathbf{A}^T\mathbf{P}\mathbf{b}-\mathbf{c}^T \\ (\mathbf{A}^T\mathbf{P}\mathbf{b}-\mathbf{c})^T & \mathbf{b}^T\mathbf{P}\mathbf{b}-2c_0 \end{bmatrix} \preceq 0, \end{aligned} \tag{5.10}$$

This guarantees that a sequence of passive models is obtained during the VF iterations. Minimizing cost function (5.10) is equivalent to minimizing

$$\mathrm{J}(\theta,\tilde{\theta}) = \left\| \mathbf{M}\begin{bmatrix}\theta \\ \tilde{\theta}\end{bmatrix} - \mathbf{F} \right\|^2, \tag{5.11}$$

in which $\mathbf{F} = \begin{bmatrix} \mathrm{Re}(\mathbf{F}^c) \\ \mathrm{Im}(\mathbf{F}^c) \end{bmatrix}$ and $\mathbf{M} = \begin{bmatrix} \mathrm{Re}\,(\mathbf{M}^c) & \mathbf{1} & -\mathrm{Re}\,(\mathbf{M}^c) \\ \mathrm{Im}\,(\mathbf{M}^c) & \mathbf{1} & -\mathrm{Im}\,(\mathbf{M}^c) \end{bmatrix}$,

$$\mathbf{F}^c = \begin{pmatrix} \widetilde{G}_{ji}(z_1) \\ \widetilde{G}_{ji}(z_2) \\ \vdots \\ \widetilde{G}_{ji}(z_N) \end{pmatrix}, \mathbf{M}^c = \begin{pmatrix} W(z_1)(z_1\mathbf{I}_\mathrm{n}-\mathbf{A})^{-1}\mathbf{b} \\ W(z_2)(z_2\mathbf{I}_\mathrm{n}-\mathbf{A})^{-1}\mathbf{b} \\ \vdots \\ W(z_N)(z_\mathrm{N}\mathbf{I}_\mathrm{n}-\mathbf{A})^{-1}\mathbf{b} \end{pmatrix},$$

superscript $(\cdot)^c$ stands for a complex valued matrix and both $\mathrm{Re}(\cdot)$ and $\mathrm{Im}(\cdot)$ stand for its real and imaginary parts, respectively. Equation (5.11) is

$$\mathrm{J}(\theta,\tilde{\theta}) = \left[\mathbf{M}\begin{bmatrix}\theta \\ \tilde{\theta}\end{bmatrix} - \mathbf{F}\right]^T \left[\mathbf{M}\begin{bmatrix}\theta \\ \tilde{\theta}\end{bmatrix} - \mathbf{F}\right]. \tag{5.12}$$

Using the following QR decomposition $\mathbf{M} = \mathbf{Q}\mathbf{R}$ with $\mathbf{Q}^T\mathbf{Q} = \mathbf{I}$ and after some algebra we conclude that:

$$\mathrm{J}(\theta,\tilde{\theta}) = \left(\mathbf{R}\begin{bmatrix}\theta \\ \tilde{\theta}\end{bmatrix} - \mathbf{Q}^T\mathbf{F}\right)^T \left(\mathbf{R}\begin{bmatrix}\theta \\ \tilde{\theta}\end{bmatrix} - \mathbf{Q}^T\mathbf{F}\right) + \mathbf{F}^T\left(\mathbf{I}-\mathbf{Q}\mathbf{Q}^T\right)\mathbf{F}$$

or

$$J(\theta,\tilde{\theta}) = \mathbf{E}^T\mathbf{E} + \delta^2,$$

with $\mathbf{E} = \mathbf{R}\begin{bmatrix}\theta \\ \tilde{\theta}\end{bmatrix} - \mathbf{Q}^T\mathbf{F}$ and $\delta^2 = \mathbf{G}^T\Big(\mathbf{I} - \mathbf{Q}\mathbf{Q}^T\Big)\mathbf{G}$.

Minimizing $\mathrm{J}(\theta, \tilde{\theta})$ is equivalent to minimizing $\mathrm{J}(\theta, \tilde{\theta}) - \delta^2 = \mathrm{J}_\delta(\theta, \tilde{\theta}) = \mathbf{E}^T\mathbf{E}$. Using Schur complements leads to an epigraph convex formulation and a standard Semi-Definite Programming (SDP) problem results as in Equation (5.13). μ is an auxiliary optimization variable introduced to reformulate the problem into a convex Semi-Definite Programming problem using the epigraph form. In Equation (5.13), it serves as an upper bound on the objective function.

$$\begin{aligned}
\min_{\mathbf{c},\tilde{\mathbf{c}},\mathbf{P},\mu} \quad & \mu \\
\text{s.t.} \quad & \begin{bmatrix}\mu & \mathbf{E}^T \\ \mathbf{E} & \mathbf{I}\end{bmatrix} \succeq 0 \\
& \mathbf{P} \succ 0 \\
& \mu \succeq 0 \\
& \begin{bmatrix}\mathbf{A}^T\mathbf{P}\mathbf{A} - \mathbf{P} & \mathbf{A}^T\mathbf{P}\mathbf{b} - \mathbf{c}^T \\ (\mathbf{A}^T\mathbf{P}\mathbf{b} - \mathbf{c})^T & \mathbf{b}^T\mathbf{P}\mathbf{b} - 2c_0\end{bmatrix} \preceq 0
\end{aligned} \tag{5.13}$$

with $\mathbf{A}$ and $\mathbf{b}$ problem data previously derived via the *Step 1* at first iteration or *Step 3* otherwise. This problem can be solved to find the optimal pair $[\mathbf{c}, \tilde{\mathbf{c}}]^T$ with the CVX solver (COELHO; PHILLIPS; SILVEIRA, 2004).

5.3.0.3 Step 3

On terminating each iteration, poles are updated using:

$$\{p_1, \cdots, p_n\} = eig(\mathbf{A} - \mathbf{b}\tilde{\mathbf{c}}), \tag{5.14}$$

and them Step 2 is called.

The procedure is repeated recursively until convergence of (5.14)[1]. On completion of the PVF algorithm, a passive model $\breve{G}_{ji}(z)$ is obtained as either a transfer function or an equivalent minimal state-space realization.

[1] For detailed insights into the convergence challenges associated with Vector Fitting, we recommend consulting Chapter 7 of the reference book (GRIVET-TALOCIA; GUSTAVSEN, 2016).

In summary, by adopting the approach hereby described accurate guaranteed passive models for the target modules are obtained. The two stages leading to a passive estimate are: (i) use of the iLPM to obtain a FRF for the local module(s) of interest; (ii) use of the PVF to achieve a passive parametric description based on the FRF by incorporating the PRL constraints into the optimization problem.

5.4 Case studies

This section presents numerical simulations to demonstrate the practical application of our proposed methodology. We use a benchmark case study of a network system with complex interconnections, visualized in Figure 20 and previously analysed in (RAMASWAMY *et al.*, 2022). All noise, external sources, and module specifications remain unchanged, except for module G_{31}^0, which is defined in this section. This specific modification serves a crucial purpose: to illustrate the estimation of a passive model for a passive system. This necessitates the original transfer function to be positive real. For the purpose of statistical analysis in this section, the model order of the system to be estimated, G_{31}^0, is assumed to be known.

The dynamics embedded in the network are defined as follows, with a sampling time of 0.01s:

$$G_{32}^0 = \frac{0.09q^{-1}}{1+0.5q^{-1}};$$

$$G_{34}^0 = \frac{1.184q^{-1} - 0.647q^{-2} + 0.151q^{-3} - 0.082q^{-4}}{1 - 0.8q^{-1} + 0.279q^{-2} - 0.048q^{-3} + 0.01q^{-4}};$$

$$G_{14}^0 = G_{21}^0 = \frac{0.4q^{-1} - 0.5q^{-2}}{1+0.3q^{-1}};$$

$$H_1^0 = \frac{1}{1+0.2q^{-1}};$$

$$G_{12}^0 = G_{23}^0 = \frac{0.4q^{-1} + 0.5q^{-2}}{1+0.3q^{-1}};$$

$$H_2^0 = \frac{1}{1+0.3q^{-1}};$$

$$H_3^0 = \frac{1 - 0.505q^{-1} + 0.155q^{-2} - 0.01q^{-3}}{1 - 0.729q^{-1} + 0.236q^{-2} - 0.019q^{-3}};$$

$$H_4^0 = 1.$$

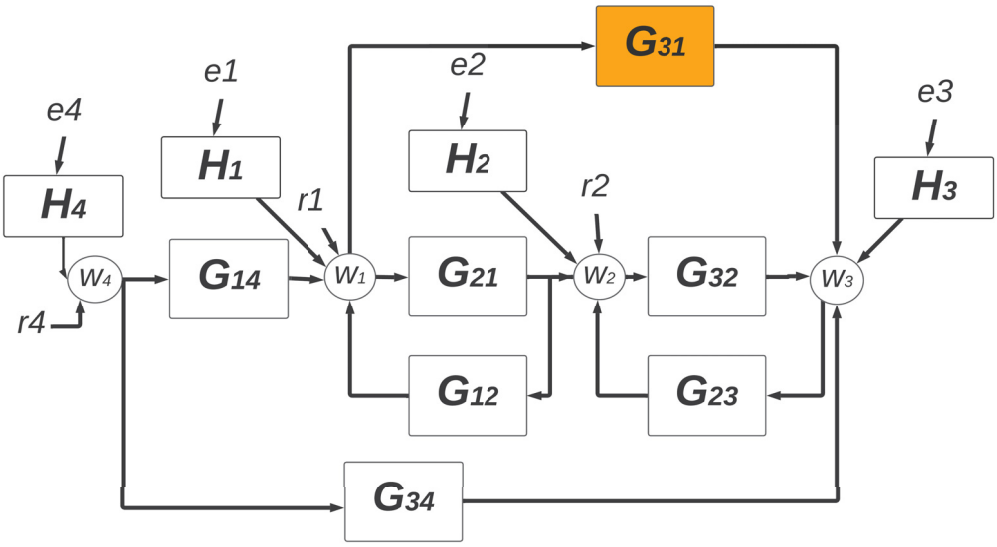

Figure 20 – Network example with 4 nodes, 3 reference signals and noise sources at each node (RAMASWAMY *et al.*, 2022).

5.4.1 A second-order passive model

We aim to estimate the following target module:

$$G_{31}^0(z) = \frac{0.1717z^2 + 0.0202z - 0.1515}{z^2 - 1.771z + 0.8857} = G_{31}(z, \theta_{31}). \tag{5.15}$$

The MATLAB Toolbox for Dynamic Network Identification (beta version 0.1.0) (Van den Hof, www.sysdynet.net, 2023) was employed to initially assess the identifiability of the target module G_{31}^0 based on the network's topology. The toolbox confirmed that G_{31}^0 is identifiable. As established in (HENDRICKX; GEVERS; BAZANELLA, 2019) and (BOMBOIS *et al.*, 2023), for targets satisfying graphical identifiability conditions, ensuring an informative excitation signal suffices. We conducted 100 independent Monte-Carlo experiments in Simulink, each comprising 1300 samples. For each experiment, the data is generated using known reference signals $r_1(t)$, $r_2(t)$ and $r_4(t)$ that are realizations of independent white noise with variance of 0.1, also the noise sources $e_1(t)$, $e_2(t)$, $e_3(t)$ and $e_4(t)$ have variance 0.05, 0.08, 1, 0.1 respectively. Each experiment yielded a parametric state-space model for G_{31}^0.

To facilitate parameter comparison independent of units or scale, we also employed the Coefficient of Variation (CV) defined as:

$$CV(x) = \frac{\delta_x}{\tilde{x}} \cdot 100$$

where x represents a normally distributed random variable, δ_x its standard deviation, and $\tilde{x}$ its mean.

We now discuss the parameterization choices for each stage of our approach.

iLPM: We proceed to estimate G_{31}^0 as a MISO identification problem with three inputs (w_1, w_2, w_4) and one output (w_3). For the iLPM, we opted for a second-degree polynomial. This choice improves the smoothness of the non-parametric estimate across the frequency range by providing broader bandwidth. However, it's important to be mindful of introducing bias through excessive bandwidth. Since the subsequent Vector Fitting step also introduces some smoothing, this initial parameterization becomes less critical.

As shown in (RAMASWAMY *et al.*, 2022), the minimum required number of frequencies for this configuration is 12. We opted for a wider bandwidth of 24 frequencies due to the presence of substantial noise. This reduces the impact of noise while minimizing bias error.

Passive Vector Fitting: During the PVF step, a linear weighting procedure is employed (see (SCHUMACHER; OLIVEIRA, 2019)) to estimate a passive second-order model. We have empirically concluded that a maximum of 50 iterations is enough to reach convergence.

The combined pole and residue estimates for G_{31}^0 across all experiments are summarized in Figures 21 and 22. In Figure 21, a boxplot of the parameters for the estimated coefficients while in Figure 22, their coefficient of variation.

The experiment reveals $\mathbf{c} = [c_1\ c_2] = [0.3243\ \ -0.3036]$ suggesting dominant real and imaginary components of the poles at $a = 0.8855$ and $b = 0.3187$.

Figure 23 showcases the frequency response curves for the data and the estimated model for the iLPM step and for the PVF step. A particular experiment is depicted in Figure 23 for which the RMSE between the $\breve{G}_{31}$ curve and the data is 0.07682. Across 100

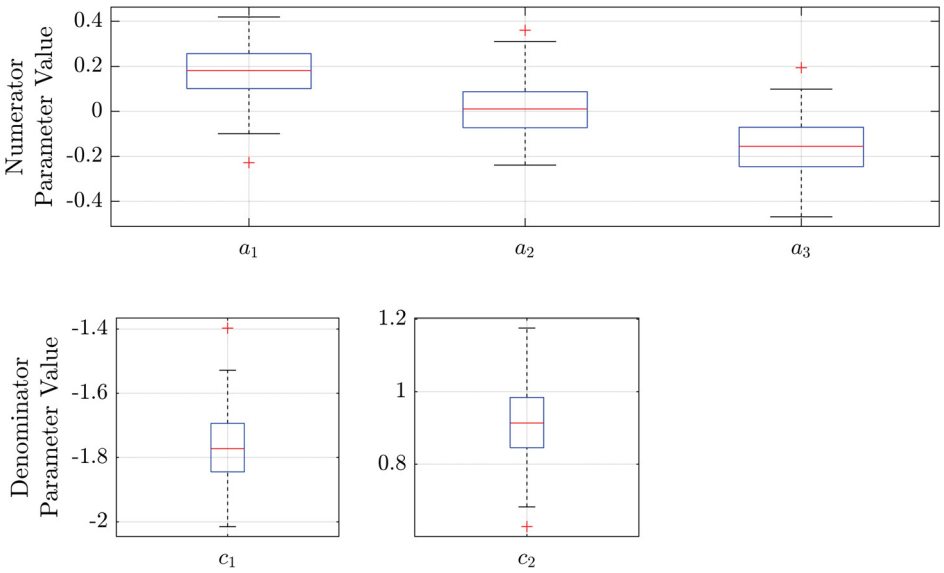

Figure 21 – Boxplot of the parameters of $\hat{G}_{31}$, estimated via 'iLPM+IVVF'.

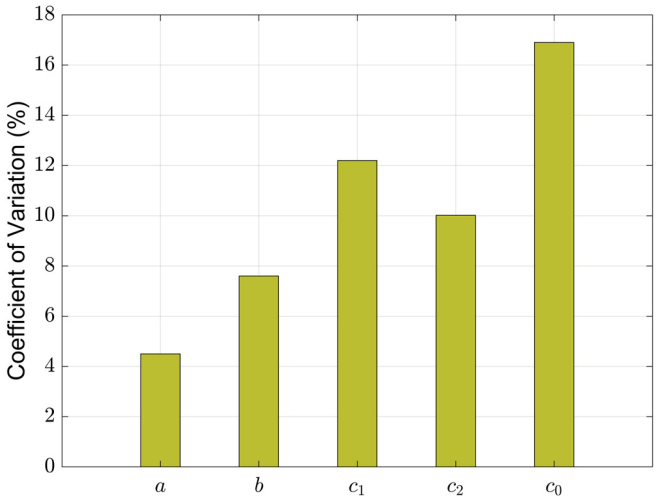

Figure 22 – Coefficient of Variation of the parameters of $\hat{G}_{31}$, estimated via 'iLPM+IVVF'.

experiments, the achieved RMSE error has mean and variance values 0.08634 and 0.0131, respectively. This figure effectively demonstrates the efficacy of the proposeed methodology in achieving passivity while preserving the desired system dynamics.

This case study successfully demonstrates the effectiveness of incorporating energy consistency criteria into the developed approach for passive model estimation. By focusing on the system matrices $\mathbf{c}$ and c_0, our passive identification method ensures compliance with energy balance principles while minimizing parameter deviations. Importantly, the

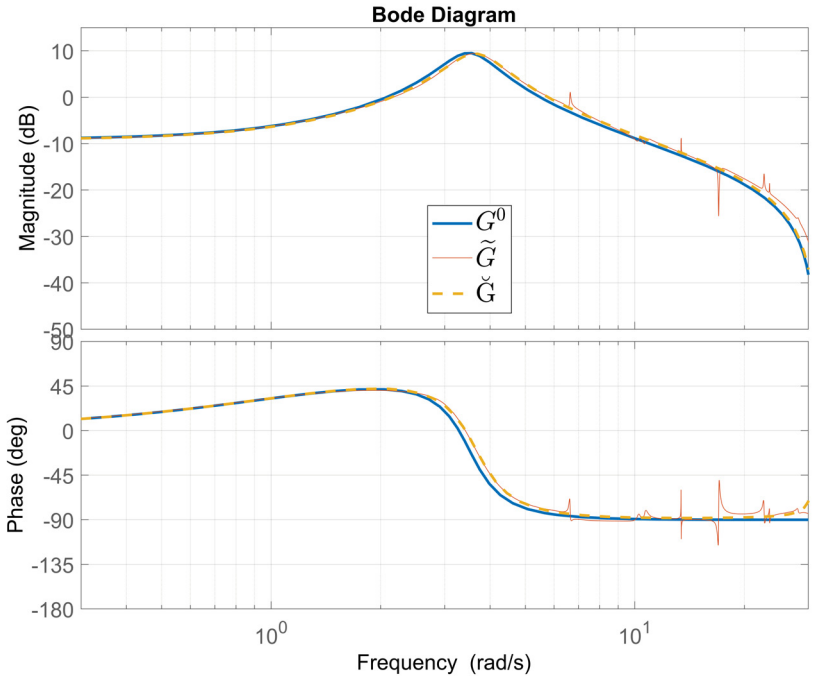

Figure 23 – Frequency response diagram of data and estimated models (2^{nd} order).

method proves successful in a complex 7-module network, highlighting its suitability for systems with intricate structures and correlated input and output signals.

5.4.2 A third-order passive model

Building upon the previous case study, we now consider a modified network scenario where the target module G_{31}^0 is defined as a 3rd order transfer function, with a sampling time of 0.01s:

$$G_{31}^0(z) = \frac{10^{-4}(7.214z^3 - 7.018z^2 - 7.196z + 7.036)}{z^3 - 2.707z^2 + 2.418z - 0.7107} = G_{31}(z, \theta_{31}).$$

All other network module specifications remain unchanged from the previous case study. The key objectives of this second case study are to demonstrate the ability of the Passive Vector Fitting (PVF) method to estimate a 3rd order passive model for the target module G_{31}^0, and to analyze the estimation accuracy and the required compensation to enforce passivity compared to the previous 2nd order case. Similar to the first case study, we conducted 100 independent Monte-Carlo experiments, each with 1300 samples of data generated using the same noise and reference signal specifications.

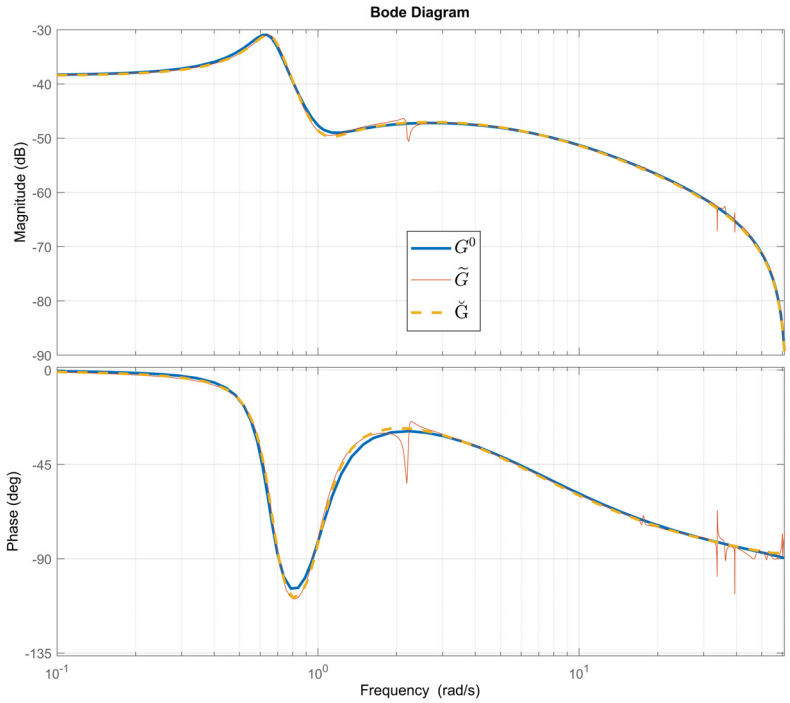

Figure 24 – Frequency response diagram of data and estimated models (3rd order).

In the iLPM step, we increased the polynomial order to 3 to better capture the higher order dynamics of the target module. The minimum required number of frequency points was also increased to 18 to ensure sufficient bandwidth coverage.

During the PVF step, the algorithm was configured to estimate a 3rd order passive state-space realization for G_{31}^0. The maximum number of iterations was maintained at 50.

Estimation Accuracy: The average RMSE between the estimated 3rd order passive model $\breve{G}_{31}$ and the true 3rd order G_{31}^0 across the 100 experiments was 0.001948, with a variance of 0.0009276. Figure 24 illustrate the frequency response curves for the data and the estimated models and, for that instance, the RMSE is 0.002439.

Passivity Enforcement: The analysis revealed that 92% of the 3rd order model estimates required passivity enforcement, compared to 94% in the 2nd order case. The overall compensation remained moderate, suggesting that the proposed PVF method can effectively estimate passive models even for higher order target modules.

Figures 25 and 26 provides a visual representation of the parameter variations in

the estimated model.

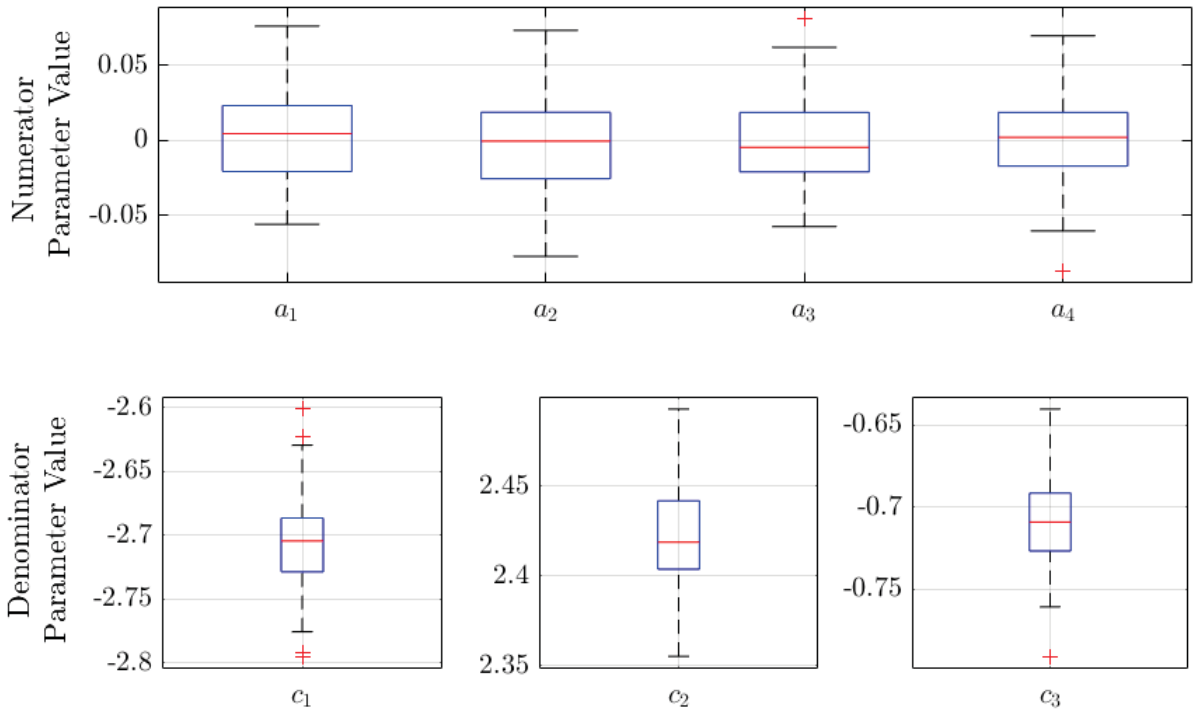

Figure 25 – Boxplot of the parameters of $\hat{G}_{31}$, estimated via 'iLPM+IVVF'.

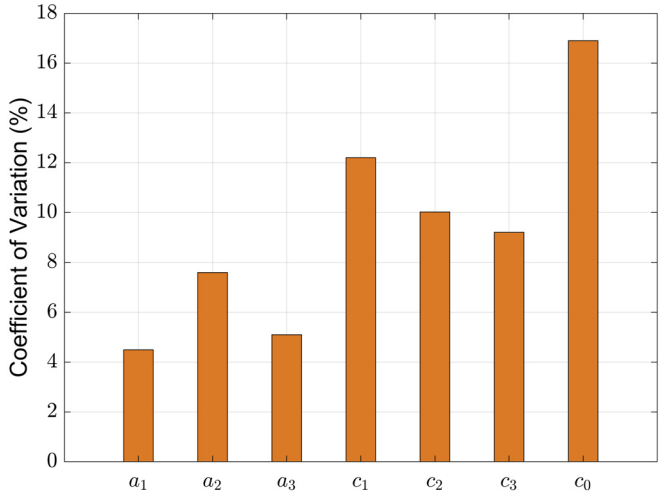

Figure 26 – Coefficient of Variation of the parameters of $\hat{G}_{31}$, estimated via 'iLPM+IVVF'.

5.4.3 A 6-node example

To demonstrate the applicability and effectiveness of the proposed methodology, this case study considers a dynamic network comprising six interconnected nodes. The network is designed to reflect realistic complexities, including feedback loops, delayed connections, and disturbances, providing a rigorous testbed for the methods developed in this thesis. Each node represents a subsystem with unique dynamic characteristics, while the edges correspond to transfer functions governing the interactions between nodes.

The network topology is represented by a directed graph, where the nodes are labeled $w_1, w_2, \ldots, w_6$. Each edge is associated with a transfer function $G_{ji}(q)$, describing the relationship between nodes w_j (output) and w_i (input). Feedback loops are present between certain nodes.

External excitation signals r_3, r_5, r_6 are applied at select nodes to ensure sufficient excitation for identification. Additive noise $v_i(t)$ is introduced at each node to simulate measurement disturbances, with noise modeled as a quasistationary process. The overall system can be described in state-space form or using the network transfer matrix, depending on the analysis focus.

We consider the 6-node network example as illustrated in Figure 27 with target module G_{12}. The dynamics embedded in the network are defined as follows, with a sampling time of 0.01s:

$$G_{32}^0 = \frac{0.09q^{-1}}{1 + 0.5q^{-1}};$$

$$G_{34}^0 = \frac{1.184q^{-1} - 0.647q^{-2} + 0.151q^{-3} - 0.082q^{-4}}{1 - 0.8q^{-1} + 0.279q^{-2} - 0.048q^{-3} + 0.01q^{-4}};$$

$$G_{14}^0 = G_{21}^0 = \frac{0.4q^{-1} - 0.5q^{-2}}{1 + 0.3q^{-1}};$$

$$H_1^0 = \frac{1}{1 + 0.2q^{-1}};$$

$$G_{21}^0 = G_{23}^0 = G_{52}^0 = G_{43}^0 = \frac{0.4q^{-1} + 0.5q^{-2}}{1 + 0.3q^{-1}};$$

$$H_2^0 = \frac{1}{1 + 0.3q^{-1}};$$

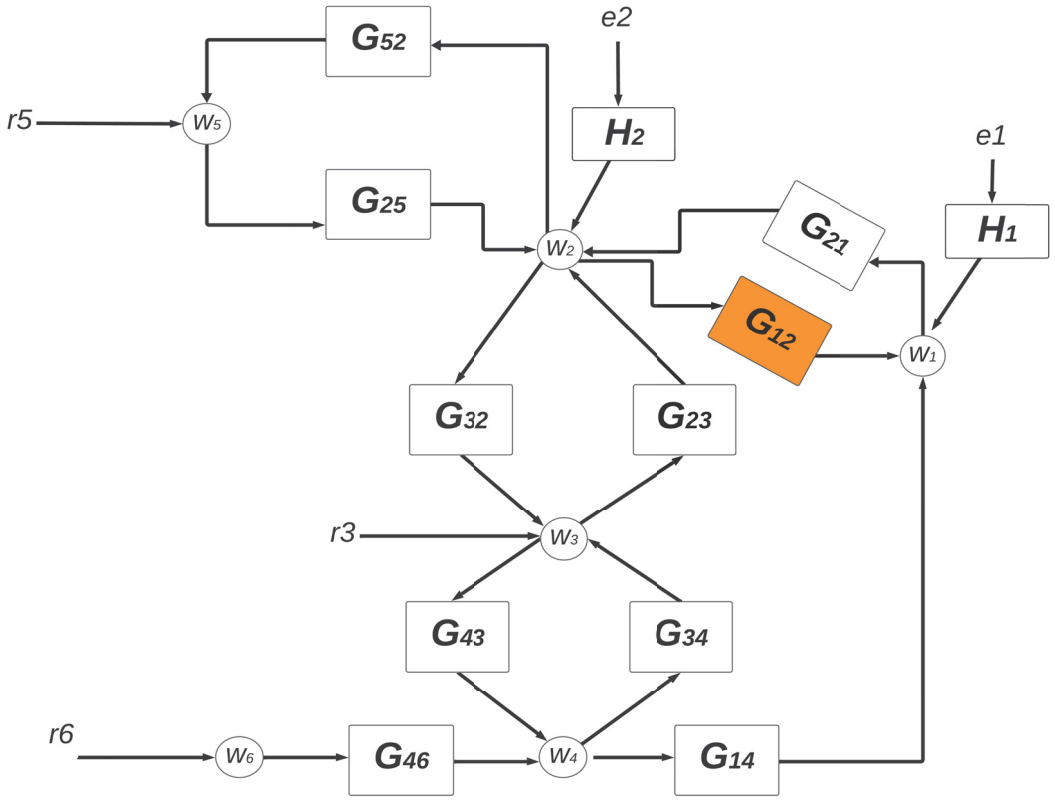

Figure 27 – 6-node example with target module G_{12}.

$$G_{25}^0 = \frac{1 - 0.505q^{-1} + 0.155q^{-2} - 0.01q^{-3}}{1 - 0.729q^{-1} + 0.236q^{-2} - 0.019q^{-3}};$$

$$G_{46}^0 = 1.$$

We aim to estimate the following target module:

$$G_{12}^0(z) = \frac{0.1717z^2 + 0.0202z - 0.1515}{z^2 - 1.771z + 0.8857} = G_{12}(z, \theta_{12}). \tag{5.16}$$

We conducted 100 independent Monte-Carlo experiments in Simulink, each comprising 1300 samples. For each experiment, the data is generated using known reference signals $r_3(t)$, $r_5(t)$ and $r_6(t)$ that are realizations of independent white noise with variance of 0.1, also the noise sources $e_1(t)$ and $e_2(t)$ have variance 0.05 and 0.1 respectively. Each experiment yielded a parametric state-space model for G_{12}^0.

Non-parametric Estimation Results: The first stage of the identification process involves estimating the Frequency Response Function (FRF) for selected target modules using the indirect Local Polynomial Method (iLPM). The input-output pairs for

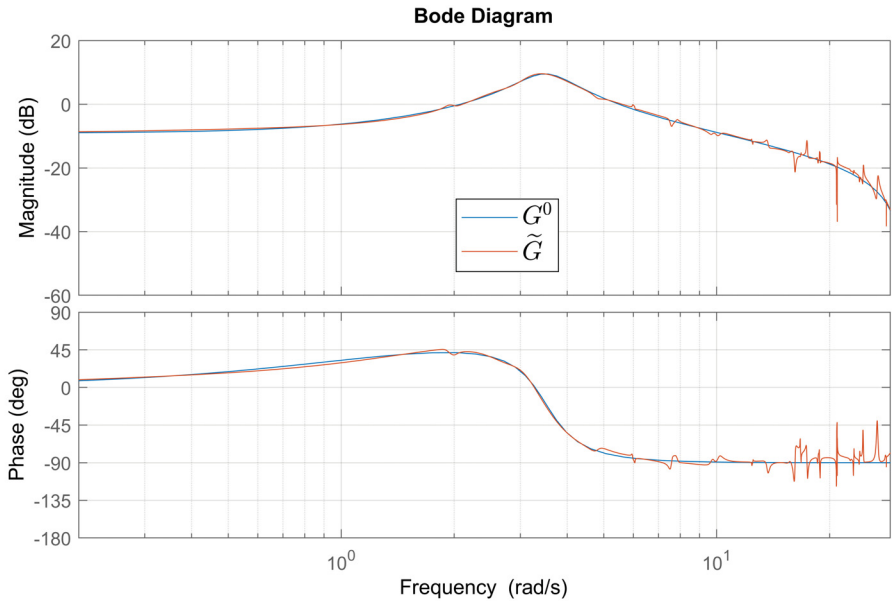

Figure 28 – Frequency response diagram of data and estimated target module G_{12}.

the FRF estimation were carefully chosen based on the network topology to minimize the influence of feedback and adjacent modules.

Figure 28 illustrates the FRF estimates for the target module G_{12}. The results show excellent agreement with the theoretical FRFs, demonstrating the accuracy of the iLPM in handling non-periodic input signals and noisy environments. The method effectively mitigated leakage errors, with a second-order polynomial approximation providing an optimal balance between bias and variance. For this first step, we employ the same parameters for the iLPM as described in Section 5.4.1.

Parametric Modeling with Passive Vector Fitting: Using the estimated FRFs as input, the Passive Vector Fitting (PVF) algorithm was employed to derive passive parametric models for the target modules. The Sanathanan-Koerner iterations ensured that passivity constraints were satisfied throughout the fitting process.

Given that the target module is G_{12}, the predictor model is constructed with input w_2 and output w_1. Due to the presence of a parallel path connecting w_2 to w_1 via w_3, w_3 is included as an additional predictor input. Consequently, the predictor model is defined as $(w_2, w_3) \rightarrow w_1$, which satisfies the necessary conditions for the consistent estimation of G_{12}.

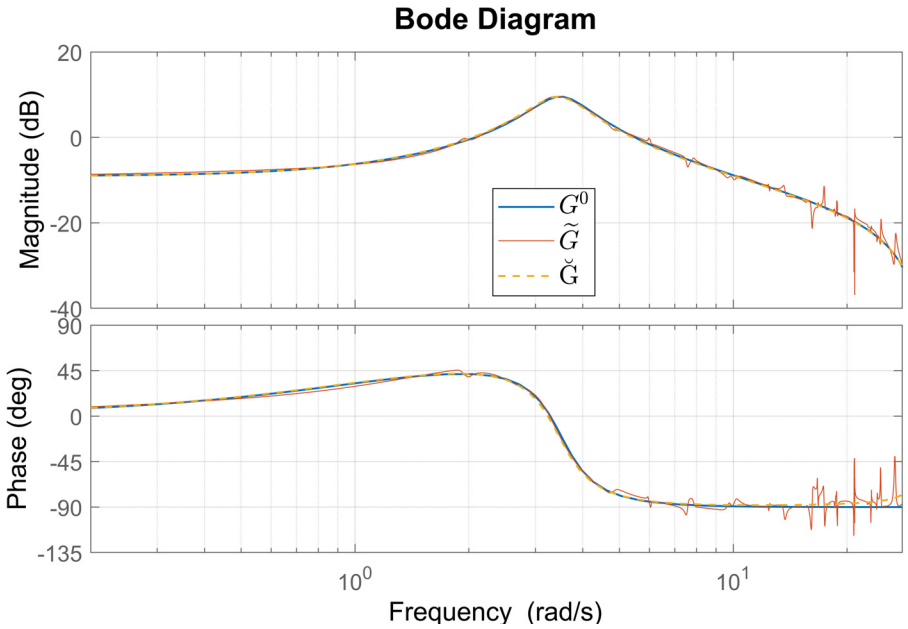

Figure 29 – Frequency response comparison of data and estimated passive target module G_{12}.

Figure 29 illustrates the comparison between the generated modules, namely the FRF estimate and the passive model for G_{12}. The average RMSE between the estimated 2nd order passive model $\breve{G}_{12}$ and the true 2nd order G^0_{12} across the 100 experiments was 0.000984, with a variance of 0.000390. In Figure 29, the frequency response curves for the data and the estimated models and, for that instance, the RMSE is 0.000892.

The combined pole and residue estimates for G^0_{12} across all experiments are summarized in Figures 30 and 31. The experiment reveals $\mathbf{c} = [c_1\, c_2] = [0.3401\ -0.3102]$ suggesting dominant real and imaginary components of the poles at $a = 0.8801$ and $b = 0.3203$.

This case study highlights the strengths of the proposed methodology in identifying passive models within a complex dynamic network. The integration of the iLPM and PVF ensured accurate FRF estimation and robust parametric modeling, even in the presence of feedback, delays, and noise.

The results validate the scalability of the approach, as the computational complexity remained manageable despite the increased number of nodes and connections. Furthermore, the ability to guarantee passivity makes the method particularly suitable for real-world applications where stability is critical.

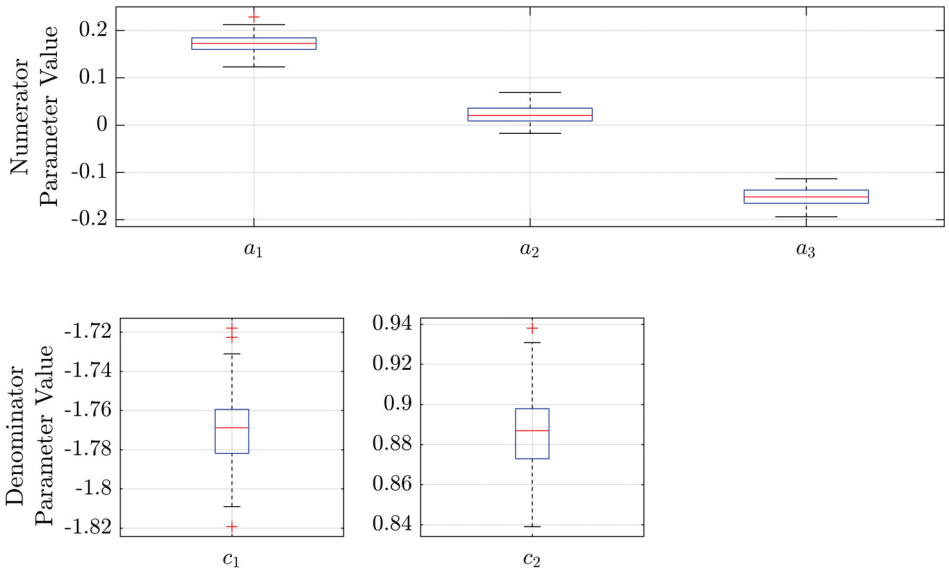

Figure 30 – Boxplot of the parameters of $\hat{G}_{12}$, estimated via 'iLPM+IVVF'.

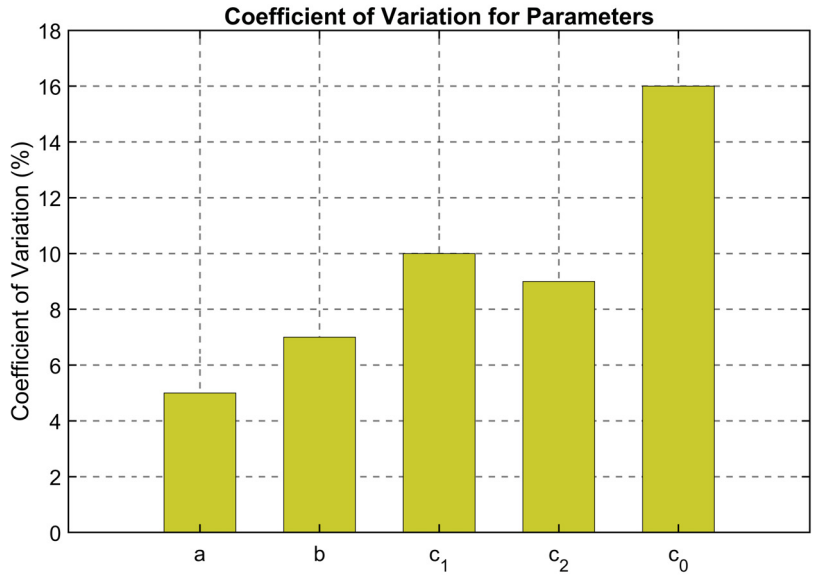

Figure 31 – Coefficient of Variation of the parameters of $\hat{G}_{12}$, estimated via 'iLPM+IVVF'.

In conclusion, the 6-node example demonstrates the practical utility of the proposed framework, setting the stage for its application to larger and more intricate networks in future studies.

5.5 Closing Remarks

This chapter introduced a novel frequency-domain approach for identifying passive local modules in dynamic networks, addressing critical challenges in the realm of system identification. By combining non-parametric and parametric estimation techniques, the proposed methodology leverages the strengths of the indirect Local Polynomial Method (iLPM) and the Passive Vector Fitting (PVF) algorithm to deliver accurate, passive models while maintaining computational efficiency.

The key contributions of this chapter are summarized as follows:

- The non-parametric estimation stage, based on iLPM, provides reliable Frequency Response Function (FRF) estimates. By addressing leakage errors inherent in Fourier transform-based techniques, the iLPM ensures high accuracy even with finite data records and non-periodic signals.
- The PVF algorithm introduced a systematic approach to enforce passivity throughout the iterative fitting process, guaranteeing that the final parametric models comply with energy-preservation principles. This advance eliminates the need for post-processing corrections, making the method more robust and consistent.
- The two-stage framework demonstrated scalability by focusing on local module identification, decoupling the complexity of individual module estimation from the overall network structure. This approach simplifies the identification process while ensuring high fidelity in dynamic networks.

The validation results, presented through detailed case studies, highlight the effectiveness of the proposed methodology in handling complex network scenarios with feedback loops, delays, and noise. The identified models not only matched the true dynamics with high accuracy but also adhered to passivity constraints, reinforcing their stability and practical applicability.

6 Conclusion

This thesis has addressed the challenge of passivity enforcement in the identification of dynamic network systems. By integrating a discrete-time formulation within a comprehensive framework, it has significantly advanced the understanding and application of passive system modeling, particularly for dynamic networks governed by internal disturbances and external excitations. The following summarizes the key contributions and findings of this research:

1. **Passivity Enforcement Through Frequency Domain Techniques:** The Frequency Domain Vector Fitting (FD-VF) algorithm was designed and implemented to ensure passivity in identified systems. By leveraging the Kalman-Yakubovich-Popov (KYP) lemma, the proposed approach guarantees passivity at each iteration, providing stable and reliable models for physical systems. This innovation addresses a critical gap in the literature, offering a systematic way to enforce passivity during the modeling process.

2. **Novel Methodology for Local Module Identification:** The thesis presented advancements in the two-stage approach to local module identification, combining the indirect Local Polynomial Method (iLPM) for non-parametric estimation and the Passive Vector Fitting (PVF) for parametric modeling. This approach minimizes the complexity of identification by focusing on the local environment of the target module rather than the entire network. The results demonstrated the effectiveness of this methodology in identifying accurate and passive models from network data.

3. **Validation Through Case Studies:** The methods were validated using comprehensive case studies, which highlighted their applicability and performance in real-world scenarios. These studies demonstrated the robustness of the proposed algorithms in handling various network complexities, including feedback loops, delays, and noise.

6.1 Future Directions

While this thesis has addressed fundamental challenges in dynamic network identification, several avenues for future research remain open:

1. **Extension to Diffusively Coupled Systems:** Investigating the identification and analysis of dynamic networks with diffusively coupled systems represents a promising direction for future research. These systems, characterized by bi-directional interactions between nodes are common in physical, biological, and social networks. The development of tailored methodologies to accurately estimate the coupling dynamics and analyze the passivity of such networks remains an open challenge.

2. **Extension to Unknown Topologies:** Developing methodologies to handle cases where network topology is partially or entirely unknown.

3. **Incorporation of Nonlinear Dynamics:** Expanding the framework to accommodate nonlinear dynamic networks, which are prevalent in biological and chemical systems.

4. **Real-Time Applications:** Adapting the proposed methods for real-time monitoring and control of dynamic networks, particularly in power grids and autonomous systems.

Throughout this research, several key contributions have been made, culminating in publications that reinforce the validity and impact of the proposed methodologies. The following conference papers document some of the primary findings:

- Lucas F. M. Rodrigues; Ihlenfeld, Lucas; Souza, Wagner; and Oliveira, Gustavo. "Sobre o Uso de Metodos de Predicao de Erro para Identificar Modulos em Redes Dinamicas." *Congresso Brasileiro de Automatica*, 2022.

- Lucas F. M. Rodrigues; Souza, Wagner; and Oliveira, Gustavo. "Uma nova abordagem de identificacao por subespacos com imposicao de modelos passivos." *Congresso Brasileiro de Automatica*, 2022.

- Lucas F. M. Rodrigues; Ihlenfeld, Lucas; Schumacher, Ricardo; and Oliveira, Gustavo. "iLPM+IVVF: uma abordagem eficaz para identificar modulos em redes dinamicas." *Simposio Brasileiro de Automacao Inteligente*, 2023.

Further advancements were presented in peer-reviewed journal articles, which consolidate the theoretical foundations and experimental validations of the developed techniques:

- Rodrigues, Lucas; Oliveira, Gustavo; Ihlenfeld, Lucas; Schumacher, Ricardo; and Van den Hof, Paul. "Frequency domain identification of passive local modules in linear dynamic networks." *Systems and Control Letters (Elsevier)*, 2024.
- Schumacher, Ricardo; Oliveira, Gustavo; and Rodrigues, Lucas. "Enhancing rational approximation of wideband resonant MIMO systems with frequency-domain data." *European Journal of Control (Elsevier)*, 2024.

These publications underscore the significance of the proposed methodologies and their potential to impact real-world applications. Future research directions include extending these techniques to nonlinear systems, improving computational efficiency, and applying them to large-scale networked systems.

6.2 Closing Remarks

This thesis has laid a solid foundation for integrating passivity enforcement into the identification of dynamic network systems. By bridging theoretical advancements with practical applications, it offers valuable tools for analyzing and controlling complex interconnected systems. The findings not only contribute to the existing body of knowledge but also open new pathways for future research and innovation in the field of system identification.

References

AGUIRRE, L. *Introdução à Identificação de Sistemas*. [S.l.: s.n.], 2015. ISBN 978-85-423-0079-6. Cited in page 65.

ALAMEER, Z.; FATHALLA, A.; LI, K.; YE, H.; JIANHUA, Z. Multistep-ahead forecasting of coal prices using a hybrid deep learning model. *Resources Policy*, v. 65, p. 101588, 2020. ISSN 0301-4207. Cited in page 17.

ALI, M.; POPOV, A. P.; WERNER, H.; ABBAS, H. S. Identification of distributed systems with identical subsystems. *IFAC Proceedings Volumes*, v. 44, n. 1, p. 5633–5638, 2011. ISSN 1474-6670. 18th IFAC World Congress. Cited in page 26.

BAZANELLA, A.; GEVERS, M.; HENDRICKX, J.; PARRAGA, A. Identifiability of dynamical networks: Which nodes need be measured? In: . [S.l.: s.n.], 2017. p. 5870–5875. Cited 3 times in pages 19, 49, and 53.

BOMBOIS, X.; COLIN, K.; Van den Hof, P. M. J.; HJALMARSSON, H. On the informativity of direct identification experiments in dynamical networks. *Automatica*, v. 148, p. 110742, 2023. ISSN 0005-1098. Cited in page 103.

BONDY, J. A.; MURTY, U. S. R. *Graph Theory with Applications*. [S.l.]: Elsevier Science Publishing, 1982. Cited in page 39.

BOSCH, P. P. J. van den; KLAUW, A. C. van der. *Modeling, Identification and Simulation of Dynamical Systems*. [S.l.]: CRC PR INC, 1994. Cited in page 65.

BRUNE, O. W. H. O. Synthesis of a

nite two-terminal network whose drivingpoint impedance is a prescribed function of frequency. PhD thesis, MIT - Department of Electrical Engineering, 1931. Cited in page 85.

CHEN, B.; HU, G.; HO, D. W.; YU, L. Distributed kalman filtering for time-varying discrete sequential systems. *Automatica*, v. 99, p. 228–236, 2019. ISSN 0005-1098. Cited in page 26.

COELHO, C. P.; PHILLIPS, J.; SILVEIRA, L. M. A convex programming approach for generating guaranteed passive approximations to tabulated frequency-data. *IEEE Transactions on Computer-Aided Design of Integrated Circuits and Systems*, v. 23, n. 2, p. 293–301, 2004. Cited in page 101.

COUTINO, M.; ISUFI, E.; MAEHARA, T.; LEUS, G. State-space network topology identification from partial observations. *IEEE Transactions on Signal and Information Processing over Networks*, v. 6, p. 211–225, 2020. Cited in page 23.

COUTINO, M.; ISUFI, E.; MAEHARA, T.; LEUS, G. State-space based network topology identification. In: *2020 28th European Signal Processing Conference (EUSIPCO)*. [S.l.: s.n.], 2021. p. 1055–1059. Cited in page 23.

CSURCSIA, P. M.; PEETERS, B.; SCHOUKENS, J. Non-parametric estimation of linear and nonlinear frequency response functions by direct calculation. *Mechanical Systems and Signal Processing*, Elsevier, v. 138, p. 106732, 2020. Cited 2 times in pages 95 and 97.

CSURCSIA, P. Z. Lprm: A user-friendly iteration-free combined local polynomial and rational method toolbox for measurements of multiple input systems. *Software Impacts*, v. 12, p. 100238, 2022. ISSN 2665-9638. Cited 3 times in pages 95, 96, and 98.

DANKERS, A.; HOF, P. M. J. Van den; BOMBOIS, X.; HEUBERGER, P. S. C. Identification of dynamic models in complex networks with prediction error methods: Predictor input selection. *IEEE Transactions on Automatic Control*, v. 61, n. 4, p. 937–952, 2016. Cited 3 times in pages 26, 27, and 50.

DANKERS, A.; HOF, P. M. V. den; BOMBOIS, X.; HEUBERGER, P. S. Errors-in-variables identification in dynamic networks by an instrumental variable approach. *IFAC Proceedings Volumes*, v. 47, n. 3, p. 2335–2340, 2014. ISSN 1474-6670. 19th IFAC World Congress. Cited 2 times in pages 27 and 28.

DANKERS, A.; HOF, P. M. Van den. Non-parametric identification in dynamic networks. In: *2015 54th IEEE Conference on Decision and Control (CDC)*. [S.l.: s.n.], 2015. p. 3487–3492. Cited in page 94.

DANKERS, A.; HOF, P. M. Van den; HEUBERGER, P. S.; BOMBOIS, X. Dynamic network identification using the direct prediction-error method. In: *2012 IEEE 51st IEEE Conference on Decision and Control (CDC)*. [S.l.: s.n.], 2012. p. 901–906. Cited 3 times in pages 20, 26, and 68.

DANKERS, A. G. *System Identification in Dynamic Networks*. Tese (Doutorado) — Dutch Institute of Systems and Control (disc), 2014. Cited 3 times in pages 16, 35, and 67.

DANKERS, A. G.; HOF, P. M. J. Van den; BOMBOIS, X. Direct and indirect continuous-time identification in dynamic networks. In: *53rd IEEE Conference on Decision and Control*. [S.l.: s.n.], 2014. p. 3334–3339. Cited 3 times in pages 20, 29, and 52.

DESOER, C. A.; KUH, E. S. *Basic Circuit Theory*. [S.l.]: McGraw-Hill Book Company, 1969. Cited in page 43.

DIESTEL, R. *Graph Theory*. [S.l.]: Springer, Berlin, Heidelberg, 2017. Cited in page 39.

DORFLER, F.; BULLO, F. Kron reduction of graphs with applications to electrical networks. *IEEE Transactions on Circuits and Systems I: Regular Papers*, v. 60, n. 1, p. 150–163, 2013. Cited in page 47.

ETESAMI, J.; KIYAVASH, N. Directed information graphs: A generalization of linear dynamical graphs. *2014 American Control Conference*, p. 2563–2568, 2014. Cited in page 18.

EVERITT, N.; BOTTEGAL, G.; HJALMARSSON, H. An empirical bayes approach to identification of modules in dynamic networks. *Automatica*, v. 91, p. 144–151, 2018. ISSN 0005-1098. Cited in page 28.

FONKEN, S.; FERIZBEGOVIC, M.; HJALMARSSON, H. Consistent identification of dynamic networks subject to white noise using weighted null-space fitting. *IFAC-PapersOnLine*, v. 53, n. 2, p. 46–51, 2020. ISSN 2405-8963. 21th IFAC World Congress. Cited in page 28.

FORSSELL, U.; LJUNG, L. Closed-loop identification revisited. *Automatica*, v. 35, n. 7, p. 1215–1241, 1999. ISSN 0005-1098. Disponível em: <https://www.sciencedirect.com/science/article/pii/S0005109899000229>. Cited 2 times in pages 68 and 70.

GAO, R.; MEKONNEN, Y. S.; BEYENE, W. T.; SCHUTT-AINE, J. E. Black-box modeling of passive systems by rational function approximation. *IEEE Transactions on Advanced Packaging*, v. 28, n. 2, p. 209–215, 2005. Cited in page 85.

GAWTHROP, P. J.; BEVAN, G. P. Bond-graph modeling. *IEEE Control Systems Magazine*, v. 27, n. 2, p. 24–45, 2007. Cited in page 82.

GEVERS, M.; BAZANELLA, A. S.; SILVA, G. V. da. A practical method for the consistent identification of a module in a dynamical network. *IFAC-PapersOnLine*, v. 51, n. 15, p. 862–867, 2018. ISSN 2405-8963. 18th IFAC Symposium on System Identification SYSID 2018. Cited 2 times in pages 19 and 27.

GEVERS, M.; BOMBOIS, X.; CODRONS, B.; SCORLETTI, G.; ANDERSON, B. D. Model validation for control and controller validation in a prediction error identification framework—part i: theory. *Automatica*, v. 39, n. 3, p. 403–415, 2003. ISSN 0005-1098. Disponível em: <https://www.sciencedirect.com/science/article/pii/S0005109802002340>. Cited in page 64.

GHALEBI, E.; MIRZASOLEIMAN, B.; GROSU, R.; LESKOVEC, J. Dynamic network model from partial observations. 05 2018. Cited in page 35.

GONCALVES, J.; HOWES, R.; WARNICK, S. Dynamical structure functions for the reverse engineering of lti networks. In: *2007 46th IEEE Conference on Decision and Control*. [S.l.: s.n.], 2007. p. 1516–1522. Cited 3 times in pages 23, 49, and 50.

GONCALVES, J.; WARNICK, S. Necessary and sufficient conditions for dynamical structure reconstruction of lti networks. *IEEE Transactions on Automatic Control*, v. 53, n. 7, p. 1670–1674, 2008. Cited in page 55.

GRIVET-TALOCIA, S.; GUSTAVSEN, B. *Passive Macromodeling: Theory and Applications*. [S.l.: s.n.], 2016. ISBN 978-1-118-09491-4. Cited 4 times in pages 34, 84, 85, and 101.

GRIVET-TALOCIA, S.; UBOLLI, A. A comparative study of passivity enforcement schemes for linear lumped macromodels. *IEEE Transactions on Advanced Packaging*, v. 31, n. 4, p. 673–683, 2008. Cited in page 85.

HABER, A.; VERHAEGEN, M. Moving horizon estimation for large-scale interconnected systems. *IEEE Transactions on Automatic Control*, v. 58, n. 11, p. 2834–2847, 2013. Cited in page 26.

HABER, A.; VERHAEGEN, M. Subspace identification of large-scale interconnected systems. *IEEE Transactions on Automatic Control*, v. 59, n. 10, p. 2754–2759, 2014. Cited in page 28.

HAYDEN, D.; CHANG, Y. H.; GONCALVES, J.; TOMLIN, C. J. Sparse network identifiability via compressed sensing. *Automatica*, v. 68, p. 9–17, 2016. ISSN 0005-1098. Cited in page 54.

HENDRICKX, J. M.; GEVERS, M.; BAZANELLA, A. S. Identifiability of dynamical networks with partial node measurements. *IEEE Transactions on Automatic Control*, v. 64, n. 6, p. 2240–2253, 2019. Cited 3 times in pages 19, 35, and 103.

HOF, P. M. V. den; DANKERS, A.; HEUBERGER, P. S.; BOMBOIS, X. Identification of dynamic models in complex networks with prediction error methods—basic methods for consistent module estimates. *Automatica*, v. 49, n. 10, p. 2994–3006, 2013. ISSN 0005-1098. Cited 12 times in pages 9, 20, 26, 27, 29, 50, 56, 70, 71, 78, 93, and 98.

HOF, P. M. Van den; DANKERS, A. G.; HEUBERGER, P. S.; BOMBOIS, X. Identification in dynamic networks with known interconnection topology. In: *2012 IEEE 51st IEEE Conference on Decision and Control (CDC)*. [S.l.: s.n.], 2012. p. 895–900. Cited in page 68.

HOF, P. V. den. *System Identification*. [S.l.]: Delft University of Technology, 2006. Cited in page 20.

IHLENFELD, L. P. R. K. Power transformer passivity enforcement: pre and post-processing approaches. Masters Dissertation, 2015. Cited in page 85.

KALMAN, R. E. On a new characterization of linear passive systems- technical report 64. *Research Institute for Advanced Studies - RIAS*, 1964. Cited in page 87.

KIVITS, E.; HOF, P. M. V. den. On representations of linear dynamic networks. *IFAC-PapersOnLine*, v. 51, n. 15, p. 838–843, 2018. ISSN 2405-8963. 18th IFAC Symposium on System Identification SYSID 2018. Cited in page 50.

KIVITS, E. L.; HOF, P. M. Van den. A dynamic network approach to identification of physical systems. In: *2019 IEEE 58th Conference on Decision and Control (CDC)*. [S.l.: s.n.], 2019. p. 4533–4538. Cited in page 30.

KIVITS, E. L.; Van den Hof, P. M. Identifiability of diffusively coupled linear networks with partial instrumentation*. *IFAC-PapersOnLine*, v. 56, n. 2, p. 2395–2400, 2023. ISSN 2405-8963. 22nd IFAC World Congress. Cited 2 times in pages 30 and 33.

KIVITS, E. M. M. L.; HOF, P. M. J. Van den. Local identification in diffusively coupled linear networks. In: *2022 IEEE 61st Conference on Decision and Control (CDC)*. [S.l.: s.n.], 2022. p. 874–879. Cited in page 30.

KOTTENSTETTE, N.; MCCOURT, M. J.; XIA, M.; GUPTA, V.; ANTSAKLIS, P. J. On relationships among passivity, positive realness, and dissipativity in linear systems. *Automatica*, v. 50, n. 4, p. 1003–1016, 2014. ISSN 0005-1098. Cited in page 82.

KUO, F. F. Network analysis and synthesis. *Wiley International Edition edn*, 1966. Cited in page 87.

KUO, Y. A note on the n-port passivity criterion. *IEEE Transactions on Circuit Theory*, v. 15, n. 1, p. 74–74, March 1968. ISSN 0018-9324. Cited 2 times in pages 85 and 87.

LJUNG, L. Analysis of a general recursive prediction error identification algorithm. *Automatica*, v. 17, n. 1, p. 89–99, 1981. ISSN 0005-1098. Disponível em: <https://www.sciencedirect.com/science/article/pii/0005109881900868>. Cited in page 64.

LJUNG, L. *System Identification: Theory for the User*. [S.l.]: Prentice Hall PTR, 1999. Cited 6 times in pages 61, 62, 65, 66, 69, and 70.

MAHANTA, P.; YAMIN, N.; ZADEHGOL, A. Passivity verification and enforcement - a review paper. *International Journal of Numerical Modelling Electronic Networks Devices and Fields*, v. 31, 07 2017. Cited in page 85.

MAPURUNGA, E.; BAZANELLA, A. S. Identifiability of dynamic networks from structure. *IFAC-PapersOnLine*, v. 54, n. 7, p. 55–60, 2021. ISSN 2405-8963. 19th IFAC Symposium on System Identification SYSID 2021. Disponível em: <https://www.sciencedirect.com/science/article/pii/S2405896321011083>. Cited 2 times in pages 58 and 59.

MAPURUNGA, E.; BAZANELLA, A. S. Optimal allocation of excitation and measurement for identification of dynamic networks. *ArXiv*, abs/2007.09263, 2021. Cited 3 times in pages 35, 36, and 59.

MASSIONI, P.; VERHAEGEN, M. Subspace identification of distributed, decomposable systems. In: *Proceedings of the 48h IEEE Conference on Decision and Control (CDC) held jointly with 2009 28th Chinese Control Conference*. [S.l.: s.n.], 2009. p. 3364–3369. Cited in page 26.

MELO, F. E. M. de. *Identifiability and Accuracy of Dynamic Networks*. Tese (Doutorado) — Universidade Federal do Rio Grande do Sul, 2022. Cited 3 times in pages 9, 46, and 47.

MICHAIL, O.; SPIRAKIS, P. G. Elements of the theory of dynamic netwokrs. *Communications of the ACM*, v. 61, 2018. Cited in page 17.

MORBIDI, F.; KIBANGOU, A. Y. A distributed solution to the network reconstruction problem. *Systems and Control Letters*, v. 70, p. 85–91, 2014. ISSN 0167-6911. Cited in page 24.

RAISBECK, G. A definition of passive linear networks in terms of time and energy. *Journal of Applied Physics*, v. 25, 1954. Cited in page 85.

RAJAGOPAL, V. C.; RAMASWAMY, K. R.; HOF, P. M. V. D. A regularized kernel-based method for learning a module in a dynamic network with correlated noise. In: . [S.l.: s.n.], 2020. Cited in page 28.

RAMASWAMY, K. R.; BOTTEGAL, G.; HOF, P. M. V. den. Learning linear modules in a dynamic network using regularized kernel-based methods. *Automatica*, v. 129, p. 109591, 2021. ISSN 0005-1098. Disponível em: <https://www.sciencedirect.com/science/article/pii/S0005109821001114>. Cited in page 28.

RAMASWAMY, K. R.; BOTTEGAL, G.; HOF, P. M. Van den. Local module identification in dynamic networks using regularized kernel-based methods. In: *2018 IEEE Conference on Decision and Control (CDC)*. [S.l.: s.n.], 2018. p. 4713–4718. Cited in page 20.

RAMASWAMY, K. R.; CSURCSIA, P. Z.; SCHOUKENS, J.; Van den Hof, P. M. A frequency domain approach for local module identification in dynamic networks. *Automatica*, v. 142, p. 110370, 2022. ISSN 0005-1098. Cited 7 times in pages 9, 31, 92, 94, 102, 103, and 104.

RISTEVSKI, S.; YUCELEN, T.; MUSE, J. A. An event-triggered distributed control architecture for scheduling information exchange in networked multiagent systems. *IEEE Transactions on Control Systems Technology*, p. 1–12, 2021. Cited in page 17.

RODRIGUES, L. F.; OLIVEIRA, G. H.; IHLENFELD, L. P.; SCHUMACHER, R.; Van den Hof, P. M. Frequency domain identification of passive local modules in linear dynamic networks. *Systems and Control Letters*, v. 193, p. 105937, 2024. ISSN 0167-6911. Disponível em: <https://www.sciencedirect.com/science/article/pii/S0167691124002251>. Cited 2 times in pages 32 and 92.

RODRIGUES, L. F. M.; IHLENFELD, L. P. R. K.; OLIVEIRA, G. H. da C. A novel subspace identification approach with passivity enforcement. *Automatica*, v. 132, p. 109798, 2021. ISSN 0005-1098. Cited in page 90.

RODRIGUES, L. F. M.; IHLENFELD, L. P. R. K.; SCHUMACHER, R.; OLIVEIRA, G. H. C. 'ilpm+ivvf': uma abordagem eficaz para identificar módulos em redes dinâmicas. *Simposio de Automacao Inteligente (SBAI)*, 2023. Cited in page 32.

RODRIGUES, L. F. M.; IHLENFELD, L. P. R. K.; SOUZA, W. F. S.; OLIVEIRA, G. H. C. Sobre o uso de métodos de predição de erro para identificar módulos em redes dinâmicas. *XXIV Congresso Brasileiro de Automática*, 2022. Cited 2 times in pages 74 and 76.

SANATHANAN, C. K.; KOERNER, J. Transfer function synthesis as a ratio of two complex polynomials. *IEEE Transactions on Automatic Control*, v. 8, n. 1, p. 56–58, 1963. Cited in page 99.

SARWAR, A.; VOULGARIS, P. G.; SALAPAKA, S. M. System identification of spatiotemporally invariant systems. In: *Proceedings of the 2010 American Control Conference*. [S.l.: s.n.], 2010. p. 2947–2952. Cited in page 19.

SCHUMACHER, R.; OLIVEIRA, G. H. An optimal and unifying vector fitting method for frequency-domain system identification. *International Journal of Electrical Power & Energy Systems*, v. 104, p. 326–334, 2019. ISSN 0142-0615. Cited 2 times in pages 100 and 104.

SHAHRAMPOUR, S.; PRECIADO, V. M. Topology identification of directed dynamical networks via power spectral analysis. *IEEE Transactions on Automatic Control*, v. 60, n. 8, p. 2260–2265, 2015. Cited 2 times in pages 23 and 24.

SHEN, Y.; BAINGANA, B.; GIANNAKIS, G. B. Kernel-based structural equation models for topology identification of directed networks. *IEEE Transactions on Signal Processing*, v. 65, n. 10, p. 2503–2516, 2017. Cited in page 24.

SHI, S.; BOTTEGAL, G.; HOF, P. M. J. Van den. Bayesian topology identification of linear dynamic networks. In: *2019 18th European Control Conference (ECC)*. [S.l.: s.n.], 2019. p. 2814–2819. Cited in page 24.

SHI, S.; CHENG, X.; HOF, P. M. Van den. Single module identifiability in linear dynamic networks with partial excitation and measurement. *IEEE Transactions on Automatic Control*, p. 1–1, 2021. Cited 4 times in pages 33, 35, 36, and 58.

STEIGLITZ, K.; MCBRIDE, L. E. A technique for the identification of linear systems. *IEEE Transactions on Automatic Control*, v. 10, n. 4, p. 461–464, 1965. Cited in page 99.

SUZUKI, M.; TAKATSUKI, N.; IMURA, J.-i.; AIHARA, K. Node knock-out based structure identification in networks of identical multi-dimensional subsystems. In: . [S.l.]: 2013 European Control Conference (ECC), 2013. p. 2280–2285. Cited in page 23.

SöDERSTRöM, T.; STOICA, P. *System Identification*. [S.l.]: Prentice Hall, 1989. Cited in page 69.

TELESFORD, Q. K.; SIMPSON, S. L.; BURDETTE, J. H.; HAYASAKA, S.; LAURIENTI, P. J. The brain as a complex system: Using network science as a tool for understanding the brain. *Brain Connectivity*, v. 1, 2011. Cited in page 17.

TORRES, P.; WINGERDEN, J.-W. van; VERHAEGEN, M. Output-error identification of large scale 1d-spatially varying interconnected systems. *IEEE Transactions on Automatic Control*, v. 60, n. 1, p. 130–142, 2015. Cited in page 19.

TRIVERIO, P.; GRIVET-TALOCIA, S.; NAKHLA, M. S.; CANAVERO, F. G.; ACHAR, R. Stability, causality, and passivity in electrical interconnect models. *IEEE Transactions on Advanced Packaging*, v. 30, n. 4, p. 795–808, 2007. Cited 3 times in pages 84, 85, and 86.

Van Den Hof, P. M.; SCHRAMA, R. J. An indirect method for transfer function estimation from closed loop data. *Automatica*, v. 29, n. 6, p. 1523–1527, 1993. ISSN 0005-1098. Disponível em: <https://www.sciencedirect.com/science/article/pii/000510989390015L>. Cited 2 times in pages 20 and 70.

Van den Hof, P. M. J. *MATLAB App/Toolbox for Dynamic Network Identification*. Eindhoven, The Netherlands: [s.n.], www.sysdynet.net, 2023. Eindhoven University of Technology (TUe). Disponível em: <www.sysdynet.net>. Cited 2 times in pages 57 and 103.

WAARDE, H. J. van; TESI, P.; CAMLIBEL, M. K. Topology identification of heterogeneous networks: Identifiability and reconstruction. *Automatica*, v. 123, p. 109331, 2021. ISSN 0005-1098. Cited 2 times in pages 23 and 33.

WANG, W.-X.; LAI, Y.-C.; GREBOGI, C.; YE, J. Network reconstruction based on evolutionary-game data via compressive sensing. *Phys. Rev. X*, American Physical Society, v. 1, p. 021021, Dec 2011. Cited in page 24.

WEERTS, H. H.; DANKERS, A. G.; HOF, P. M. V. den. Identifiability in dynamic network identification. *IFAC-PapersOnLine*, v. 48, n. 28, p. 1409–1414, 2015. ISSN 2405-8963. 17th IFAC Symposium on System Identification SYSID 2015. Disponível em: <https://www.sciencedirect.com/science/article/pii/S2405896315029547>. Cited 3 times in pages 56, 57, and 59.

WEERTS, H. H.; DANKERS, A. G.; Van den Hof, P. M. Identifiability in dynamic network identification. *IFAC-PapersOnLine*, v. 48, n. 28, p. 1409–1414, 2015. ISSN 2405-8963. 17th IFAC Symposium on System Identification SYSID 2015. Cited 3 times in pages 53, 54, and 55.

WEERTS, H. H.; HOF, P. M. V. den; DANKERS, A. G. Identifiability of linear dynamic networks. *Automatica*, v. 89, p. 247–258, 2018. ISSN 0005-1098. Cited 2 times in pages 53 and 59.

WEERTS, H. H.; HOF, P. M. V. den; DANKERS, A. G. Prediction error identification of linear dynamic networks with rank-reduced noise. *Automatica*, v. 98, p. 256–268, 2018. ISSN 0005-1098. Cited 4 times in pages 19, 20, 26, and 64.

WILLEMS, J. C. Dissipative dynamical systems : Part I general theory. *Archive for Rational Mechanics and Analysis*, v. 45, p. 321–351, 1972. Cited 3 times in pages 82, 83, and 85.

WILLEMS, J. C. Modeling interconnected systems. In: *2008 3rd International Symposium on Communications, Control and Signal Processing*. [S.l.: s.n.], 2008. p. 421–424. Cited in page 18.

WILLEMS, J. C. Modeling interconnected systems. *International Symposium on Communications Control and Signal Processing*, p. 421–424, 2008. Cited in page 18.

YEUNG, E.; GONçALVES, J.; SANDBERG, H.; WARNICK, S. Mathematical relationships between representations of structure in linear interconnected dynamical systems. In: *Proceedings of the 2011 American Control Conference*. [S.l.: s.n.], 2011. p. 4348–4353. Cited in page 48.

ZHANG, X.; MOORE, C.; NEWMAN, M. Random graph models for dynamic networks. *The European Physical Journal B*, v. 90, 07 2016. Cited in page 19.

ZHENG, J.; OKAMURA, H.; PANG, T.; DOHI, T. Availability importance measures of components in smart electric power grid systems. *Reliability Engineering System Safety*, v. 205, p. 107164, 2021. ISSN 0951-8320. Cited in page 17.

ZHENG, K.; ZHENG, Q.; YANG, H.; ZHAO, L.; HOU, L.; CHATZIMISIOS, P. Reliable and efficient autonomous driving: the need for heterogeneous vehicular networks. *IEEE Communications Magazine*, v. 53, n. 12, p. 72–79, 2015. Cited in page 17.

ZHU, S.; ZHOU, J.; CHEN, G.; LU, J.-A. A new method for topology identification of complex dynamical networks. *IEEE Transactions on Cybernetics*, v. 51, n. 4, p. 2224–2231, 2021. Cited in page 25.

ZORZI, M.; CHIUSO, A. Sparse plus low rank network identification: A nonparametric approach. *Automatica*, v. 76, p. 355–366, 2017. ISSN 0005-1098. Cited in page 26.